A measurement of soft-drop jet observables in pp collisions with the ATLAS detector at $\sqrt{s}$ = 13 TeV

The ATLAS Collaboration

Jet substructure quantities are measured using jets groomed with the soft-drop grooming procedure in dijet events from 32.9 fb^{-1} of pp collisions collected with the ATLAS detector at $\sqrt{s}$ = 13 TeV. These observables are sensitive to a wide range of QCD phenomena. Some observables, such as the jet mass and opening angle between the two subjets which pass the soft-drop condition, can be described by a high-order (resummed) series in the strong coupling constant α_S. Other observables, such as the momentum sharing between the two subjets, are nearly independent of α_S. These observables can be constructed using all interacting particles or using only charged particles reconstructed in the inner tracking detectors. Track-based versions of these observables are not collinear safe, but are measured more precisely, and universal non-perturbative functions can absorb the collinear singularities. The unfolded data are directly compared with QCD calculations and hadron-level Monte Carlo simulations. The measurements are performed in different pseudorapidity regions, which are then used to extract quark and gluon jet shapes using the predicted quark and gluon fractions in each region. All of the parton shower and analytical calculations provide an excellent description of the data in most regions of phase space.

Contents

1 Introduction

Jets are collimated sprays of particles that are initiated by high-energy quarks and gluons. Grooming techniques systematically remove soft and wide-angle radiation, making the structure of the jet robust against contamination from multiple simultaneous proton–proton interactions (pileup) as well as against final-state radiation and the underlying event. This internal structure of a jet has been successfully used to tag the origin of jets in precision measurements and searches at the Large Hadron Collider (LHC) [1, 2]. While grooming has been a powerful tool for applications of jet substructure techniques, it also provides a unique opportunity for the study of the strong force itself. If groomed in a suitable way, the radiation pattern inside the resulting jet can be predicted from first principles in QCD. The differential cross sections as a function of key observables such as the groomed jet mass have been computed beyond leading-logarithmic accuracy [3–8] as an expansion in the strong coupling constant α_S along with logarithms of ratios of physical scales. New 'Sudakov safe' observables [9] that are the ratio of attributes that are both infrared-safe and collinear-safe cannot be expressed as an expansion in α_S, but can be described with a series in fractional

powers of α_S. For particular grooming configurations, observables such as the ratio of subjet energies can be *independent* of α_S [9]. These nonstandard and universal behaviors are now being tested with precision at the LHC and the Relativistic Heavy Ion Collider (RHIC).

While many grooming procedures suppress difficult-to-model soft and wide-angle radiation, only one grooming algorithm has been successfully used for calculations beyond the formal precision of the parton shower (leading logarithm). This *soft-drop* grooming procedure [10] is a generalization of the modified mass drop procedure [11] and is formally insensitive to *nonglobal logarithmic corrections* [12]: resummation terms resulting from radiation which leaves the jet cone and then produces radiation that reenters the jet. Soft-drop jet observables have been calculated to next-to-leading-logarithm (NLL) and next-to-next-to-leading-logarithm (NNLL) accuracy. The soft-drop jet mass has recently been measured in dijet events [13, 14]. In the region where the calculations are expected to be accurate, the agreement with the data is excellent, and nonperturbative effects [15] have become the most important theoretical source of uncertainty instead of higher-order effects.

This analysis goes beyond the jet mass by adding other soft-drop jet observables that are connected with the grooming procedure. Furthermore, in addition to measuring observables reconstructed using all interacting particles, charged-particle observables are measured using tracks. These track-based observables can be probed with better experimental precision compared to the calorimeter-based observables. Charged-particle observables are not formally collinear-safe, but universal nonperturbative functions, like parton distribution functions, can absorb the relevant singularities and allow for precise predictions [16–19]. Finally, the differences between these distributions in regions with different quark/gluon composition is used to understand how the behavior and sensitivity of the different observables depends on the origin of the jet. Previous measurements of groomed jet observables have been conducted at the LHC by CMS [14, 20], ATLAS [13, 21], and ALICE [22], and at RHIC by the STAR Collaboration [23] and additional studies at detector level have been performed using CMS data [24–27].

2 Soft-drop procedure

The soft-drop grooming algorithm proceeds as follows. After a jet is clustered using any algorithm, its constituents are then reclustered using the Cambridge/Aachen (C/A) algorithm [28, 29], which iteratively clusters the closest constituents in rapidity and azimuth. This typically produces a jet with the same constituents as the original jet, but with a modified jet clustering history, which is sensitive to the angle-ordered nature of parton shower evolution. Then, the last step of the C/A clustering algorithm is undone, breaking the jet j into the last two subjets, j_1 and j_2, which were clustered together. These two subjets are then used to evaluate the soft-drop condition:

$$\frac{\min(p_{\mathrm{T},j_1}, p_{\mathrm{T},j_2})}{p_{\mathrm{T},j_1} + p_{\mathrm{T},j_2}} > z_{\mathrm{cut}} \left(\frac{\Delta R_{12}}{R} \right)^{\beta},$$

where p_{T,j_i} is the transverse momentum of subjet j_i, and ΔR_{12} is the distance between the two subjets in y–ϕ space.[1] The parameters z_{cut} and β are algorithm parameters explained in greater detail below, and R

---

[1] ATLAS uses a right-handed coordinate system with its origin at the nominal interaction point (IP) in the center of the detector and the z-axis along the beam pipe. The x-axis points from the IP to the center of the LHC ring, and the y-axis points upwards. Cylindrical coordinates (r, ϕ) are used in the transverse plane, ϕ being the azimuthal angle around the z-axis. Rapidity is defined as $y = \frac{1}{2} \ln[(E + p_z)/(E - p_z)]$. The pseudorapidity is defined in terms of the polar angle θ as $\eta = -\ln\tan(\theta/2)$. Angular distance is measured in units of $\Delta R \equiv \sqrt{(\Delta\eta)^2 + (\Delta\phi)^2}$.

is the jet radius parameter. If j_1 and j_2 fail the soft-drop condition, then the subjet with the lower p_T is removed, and the one with the higher p_T is relabeled as j and the procedure is iterated. If the soft-drop condition is satisfied, then the algorithm is stopped, and the resulting jet j is the soft-dropped jet. If no pairs of subjets in the declustering satisfy the soft-drop condition, then the resulting jet is the zero vector.

The parameters z_{cut} and β determine the sensitivity of the algorithm to soft and wide-angle radiation. As $\beta \to \infty$ (and $z_{cut} < 1$), the soft-drop condition is always satisfied, and no grooming is applied. Decreasing β preferentially removes wide-angle radiation and increasing z_{cut} preferentially removes soft radiation. The theoretical calculations are performed for a range in β and assume z_{cut} is small enough so that it does not introduce large logarithms (which was explicitly checked in Refs. [5, 6]). This measurement adopts the same choice as the available theoretical calculations: $z_{cut} = 0.1$ and $\beta \geq 0$. Several β values are tested to probe different scales of angular strulcture inside the jets.

This paper measures three closely related substructure observables, which are calculated from jets after they have been groomed with the soft-drop algorithm. These are the jet mass, the p_T balance z_g (which is the left-hand side of Eq.(1)) of the splitting which passes the soft-drop condition, and r_g, which is the opening angle R_{12} of this splitting in Eq.(1). These three observables – the jet mass, z_g and r_g – are described in greater detail in Section 5.2. These observables are approximately related by $m^2/p_T^2 \sim z_g r_g^2$, and each probes different aspects of the structure of the jet.

3 ATLAS detector

The ATLAS detector [30] at the LHC covers nearly the entire solid angle around the collision point. It consists of an inner tracking detector surrounded by a thin superconducting solenoid, electromagnetic and hadronic calorimeters, and a muon spectrometer incorporating three large superconducting toroidal magnets.

The inner-detector system (ID) is immersed in a 2 T axial magnetic field and provides charged-particle tracking in the range $|\eta| < 2.5$. The high-granularity silicon pixel detector, the innermost layer of the tracking detector, covers the vertex region and typically provides four measurements per track, the first hit being typically recorded in the insertable B-layer that was installed before Run 2 [31, 32]. It is followed by the silicon microstrip tracker, which usually provides eight measurements per track. These silicon detectors are complemented by the transition radiation tracker, which enables radially extended track reconstruction up to $|\eta| = 2.0$.

The calorimeter system covers the pseudorapidity range $|\eta| < 4.9$. Within the region $|\eta| < 3.2$, electromagnetic calorimetry is provided by barrel and endcap high-granularity lead/liquid-argon (LAr) detectors, with an additional thin LAr presampler covering $|\eta| < 1.8$, to correct for energy loss in material upstream of the detectors. Hadronic calorimetry is provided by the steel/scintillator-tile detector, segmented into three barrel structures within $|\eta| < 1.7$, and two copper/LAr hadronic endcap calorimeters which cover $1.5 < |\eta| < 3.2$. The solid angle coverage is completed with forward copper/LAr and tungsten/LAr calorimeter modules covering $3.1 < |\eta| < 4.9$, which are optimized for electromagnetic and hadronic measurements respectively.

Interesting events are selected for recording by the first-level trigger system implemented in custom hardware, followed by selections made by algorithms implemented in software in the high-level trigger [33]. The first-level trigger makes decisions at the 40 MHz bunch crossing rate to keep the accepted-event rate

below 100 kHz, which the high-level trigger further reduces in order to record events to disk at about 1 kHz.

4 Datasets

These measurements use the dataset of pp collisions recorded by the ATLAS detector in 2016, corresponding to an integrated luminosity of 32.9 fb^{-1} [34, 35] at a center-of-mass energy of $\sqrt{s} = 13$ TeV. Events are only considered if they were collected during stable beam conditions and satisfy all data quality requirements [36]. Due to the high instantaneous luminosity and the large total inelastic proton–proton (pp) cross section, on average there are about 25 simultaneous (pileup) collisions in each bunch crossing.

The measurements presented in this paper use a variety of Monte Carlo (MC) event generator samples to estimate the impact of detector efficiency and resolution as well as for comparison with the unfolded data. Dijet events were generated at leading order (LO) with PYTHIA 8.186 [37, 38], with the $2 \rightarrow 2$ matrix element convolved with the NNPDF2.3LO parton distribution function (PDF) set [39] and using the A14 set of multiple-parton-interaction and parton-shower parameters [40]. PYTHIA 8 uses a p_T-ordered parton shower model. Additional dijet events were generated using different generators, in order to study the impact of modeling uncertainties. SHERPA 2.1 [41, 42] was used to generate events using multileg $2 \rightarrow 2$ and $2 \rightarrow 3$ matrix elements, which were matched to parton showers following the CKKW prescription [43]. These SHERPA events were generated using the CT10nlo PDF set [44] and the default SHERPA set of tuned parameters. Herwig++ 2.7 [45, 46] was used to provide a sample of events with an angle-ordered parton shower model. These events were generated with the $2 \rightarrow 2$ matrix element, convolved with the CTEQ6L1 PDF set [47] and configured with the UE-EE-5 set of tuned parameters [48].

All generator events were passed through a full simulation of the ATLAS detector [49] implemented in GEANT 4 [50], which describes the interactions of particles with the detector and the subsequent digitization of analog signals. The effects of pileup were simulated with unbiased pp collisions using the PYTHIA 8.186 generator with the A2 [51] set of tuned parameters and the MSTW2008LO [52] PDF set; these events were overlaid on the nominal dijet events. These events are then reweighted such that the distribution of the average number of interactions per bunch crossing matches that seen in data.

5 Event selection and object reconstruction

Since the data are unfolded to particle level, it is necessary to define both the particle-level and detector-level objects used in the measurement. The former are chosen to be as close as possible to the latter in order to minimize the model dependence caused by an extrapolation from the phase space measured at detector level to the phase space measured at particle level. Section 5.1 describes the particle-level and detector-level event selection criteria. Following this, Section 5.2 describes the particle-level and detector-level jet reconstruction procedure for both the calorimeter-based (all-particle) observables and the track-based (charged-particle) observables.

5.1 Jet and event selection

Detector-level events are required to have at least one primary vertex reconstructed from at least two tracks with p_T greater than 400 MeV. The primary hard-scattering vertex of the event is chosen to be the one with the highest $\sum_{\text{tracks}} p_T^2$. The inputs to the jet clustering algorithm are locally calibrated topological calorimeter-cell clusters [53].

Jets are clustered with FastJet [54] using the anti-k_t [55] algorithm with radius parameter $R = 0.8$. A series of simulation-based calibration factors are applied to ensure that the detector-level jet p_T is the same as the particle-level value on average [56]. Each event is required to have at least two reconstructed jets, where the transverse momentum of the leading jet, p_T^{lead}, is greater than 300 GeV. The jet selection is applied to ungroomed jets, which ensures that the same jets are studied for all grooming configurations. In order to enhance the dijet topology and allow an interpretation of quark or gluon origin of the jets in the event, the leading two jets are required to be well-balanced: $p_T^{\text{lead}}/p_T^{\text{sublead}} < 1.5$. Both jets are required to have $|\eta| < 1.5$, and only jets with a nonzero mass are retained.

Events are selected using single-jet triggers. Due to the large cross section for jet production, most of the jet triggers are prescaled. Therefore events which pass these triggers are randomly discarded with some fixed probability. The lowest-p_T-threshold unprescaled $R = 0.4$ single-jet trigger in 2016 is fully efficient for $R = 0.8$ dijet events where the leading-jet p_T is greater than 600 GeV. In events where the leading jet has 300 GeV $< p_T < 600$ GeV, a prescaled trigger is used with an average prescale value of 1000 (the inverse of the probability to be recorded). While this results in a lower effective luminosity, it provides access to the lower p_T region.

The inputs to particle-level jets are stable particles ($c\tau > 10$ mm) excluding muons and neutrinos. These jets are clustered using the same radius parameter as the detector-level jets and have the same η and p_T cuts as for the detector-level selection.

5.2 Inputs for jet substructure

Two types of jet substructure observables are measured: calorimeter-based observables, which correspond to observables reconstructed from all particles inside the jet at particle level, and track-based observables, which correspond to observables reconstructed from charged particles. Track-based observables are theoretically more complicated to describe, but are experimentally cleaner to measure due to the precise angular measurement from the ID. For both the calorimeter-based and track-based measurements, the jet selection is performed on the calorimeter-based jets, while the soft-drop grooming is applied to the cluster inputs and the track inputs respectively (Section 2). The jets after the application of this algorithm are often referred to as groomed, and the constituents of these jets are used to compute the jet substructure observables. It is noted that since the event selection is applied to un-groomed jets, some selected jets are left with one constituent after grooming, resulting in jets with a mass of zero.

For the calorimeter-based observables, the same constituents are used to calculate the observables as are used to create the jets described in Section 5.1 for both detector level and particle level. For detector-level track-based observables, the soft-drop procedure is applied to tracks matched to the ungroomed jet via ghost association [57], and jet substructure observables are calculated using the groomed tracks. These tracks are selected with a $p_T > 500$ MeV requirement and assigned to the primary vertex in accord with the track-to-vertex matching. Tracks not included in vertex reconstruction are assigned to the primary vertex if it has the smallest $|\Delta z_0 \sin\theta|$ compared to any other reconstructed vertex, up to a maximum distance of 3.0

mm. Tracks not matched to the primary vertex are not considered. At particle level, these track-based observables are built using the charged-particle constituents of the particle-level jets, excluding muons.

Both the leading and subleading jet are used in this measurement. In order to expose differences between quark and gluon jets, the more forward and more central of the two jets are distinguished and measured separately. Between the leading and subleading jets, the one with the smaller $|\eta|$ will be referred to as the "central" jet, and the other one as the "forward" jet. For a fixed jet p_T at high rapidity where the high-x contribution is more important, jets are more often quark-initiated due to the large contribution of valence quarks.

6 Observables

Three substructure observables are calculated from the two jets groomed with the soft-drop algorithm (using the C/A algorithm with $R = 0.8$ to recluster the jets), including the jet mass, z_g, and r_g. These three observables completely characterize the splitting from the soft-drop condition, and they are all measured using both the calorimeter and tracker inputs.

Jet mass: One of the most basic and important jet substructure observables is the jet mass:

$$m^2 = \left(\sum_{i \in \text{jet}} E_i \right)^2 - \left(\sum_{i \in \text{jet}} \vec{p}_i \right)^2 , \tag{1}$$

where i refers to the constituents of the jet. The measurement is performed for a dimensionless version of the jet mass: the relative mass $\rho \equiv \log(m^2/p_T^2)$, where m is groomed and p_T is ungroomed (groomed jet p_T is not infrared- and collinear-safe [5]). The calorimeter-cluster inputs are treated as massless and tracks are assigned the pion mass. Since the probability distribution of ρ is approximately linear in the resummation regime ($\Lambda_{\text{QCD}}/p_T \lesssim m/p_T \lesssim z_{\text{cut}}$, where Λ_{QCD} is the energy scale of hadronization) [3–8], the binning for ρ is evenly spaced. For ρ, the distributions are normalized to the integrated cross section, σ_{resum}, measured in the resummation region, $-3.7 < \rho < -1.7$. By changing β, the distribution shifts to higher values as fewer constituents are removed from the jets during grooming.

An example of the distribution of ρ in simulation at detector level (particle level) for the calorimeter-based (all particles) definition is shown in Figure 1(a) for the more central of the two jets and for $\beta = 0$. For this observable, particularly in the lower-relative-mass region, there are nontrivial detector effects which occur due to the calorimeter granularity, resulting in a distribution with different shapes at particle and detector levels. As expected, the distribution of $\log(m^2/p_T^2)$ is approximately linear for $\beta = 0$ in the resummation regime.

One way to reduce the impact of these detector corrections is to consider track-based (charged-particle) observables. An example of the track-based (charged-particle-based) ρ is shown in Figure 1(b), where tracks (charged particles) are used for both the mass and the p_T. As in the calorimeter case, the mass is calculated using the groomed jet, while the p_T is calculated using the ungroomed constituents, but no calibration is applied to the ungroomed jet since no such calibration exists for track-based inputs. Although the particle-level distributions only include charged particles, the distributions are similar to those shown in Figure 1(a), but in this case the impact of the detector corrections is significantly smaller.

(a) ρ distribution, $\beta = 0$, calorimeter-based

(b) ρ distribution, $\beta = 0$, track-based
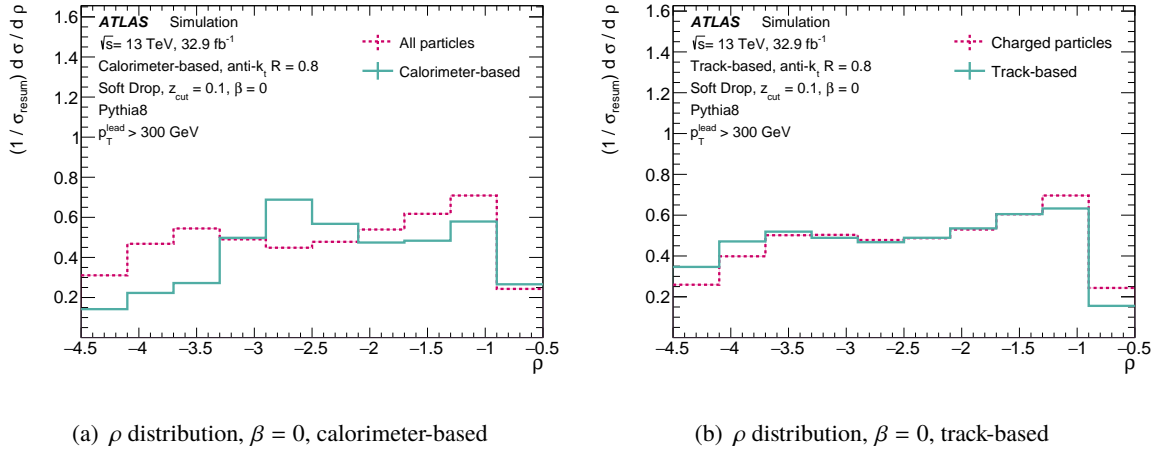
Figure 1: The distribution in simulation of ρ at detector level and particle level for the more central of the two jets for $\beta = 0$ for (a) calorimeter-based (all particles), and (b) track-based (charged particles). The statistical uncertainties are drawn, but are too small to be visible.

z_g: An important quantity when describing the hard splitting scale that defines the mass is z_g, which is $\min(p_{T,j_1}, p_{T,j_2})/(p_{T,j_1} + p_{T,j_2})$ for the splitting that satisfies the soft-drop condition. If no such splitting occurs, then the jet is not included in the measurement. Symmetric splittings are characterized by $z_g \sim 0.5$. Figure 2 shows an example of the normalized distribution in simulation of z_g at detector level (particle level) with $\beta = 0$ for both the calorimeter-based (all particles) and track-based (charged particles) definitions. For $\beta = 0$ and $z_{cut} = 0.1$, z_g must be greater than 0.1 in order to pass the soft-drop condition, and therefore bins with z_g values less than 0.1 are not shown (this is not the case for $\beta > 0$). As in the case with the mass, the distributions of the charged-particles and all-particles versions of z_g are similar. Detector effects for the calorimeter-based z_g are smaller than for the relative mass, because z_g is less sensitive to the angular distribution of energy within the jet.

The binning is evenly spaced in z_g and the distributions are normalized to the integrated cross section σ.

r_g: The opening angle ΔR_{12} between the two subjets that pass the soft-drop condition is r_g. This angle is smaller than the jet radius by definition. Although r_g is highly correlated with the relative mass and z_g, it is useful for explicitly exposing the angular distribution. Figure 3 shows an example of the normalized calorimeter-based (all particles) and track-based (charged particles) r_g distributions. As expected, there are large detector effects for the calorimeter-based case, especially at low angles. Due to the correlation between mass and r_g, the distribution shapes and detector effects look similar to the ones shown in Figure 1.

The binning for r_g is logarithmically spaced. The distributions are normalized to the integrated cross section σ. Similar to ρ, increasing β shifts the distribution to higher values as there is less grooming.

8
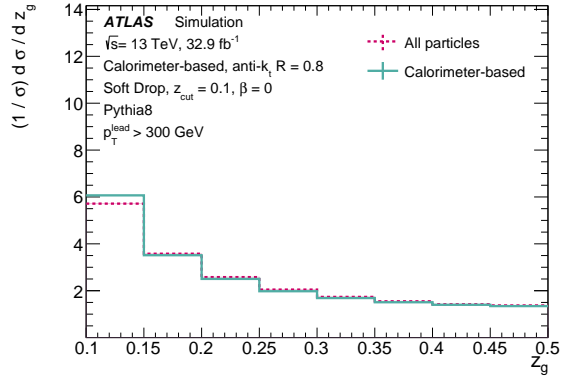
(a) z_g distribution, $\beta = 0$, calorimeter-based
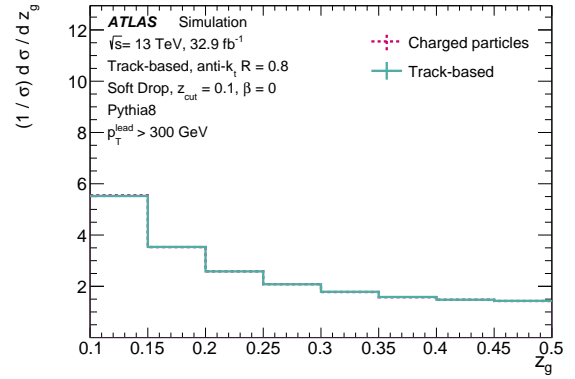
(b) z_g distribution, $\beta = 0$, track-based

Figure 2: The distribution in simulation of z_g at detector level and particle level for $\beta = 0$ for (a) calorimeter-based (all particles), and (b) track-based (charged particles). The statistical uncertainties are drawn, but are too small to be visible.
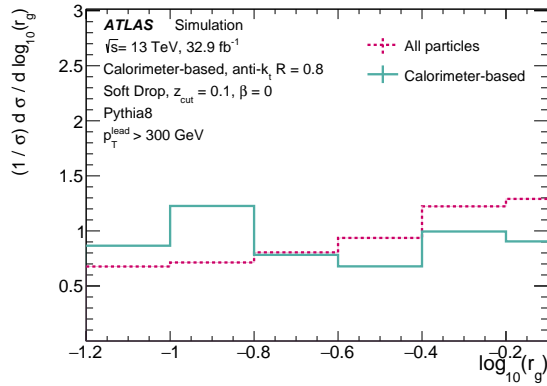
(a) r_g distribution, $\beta = 0$, calorimeter-based
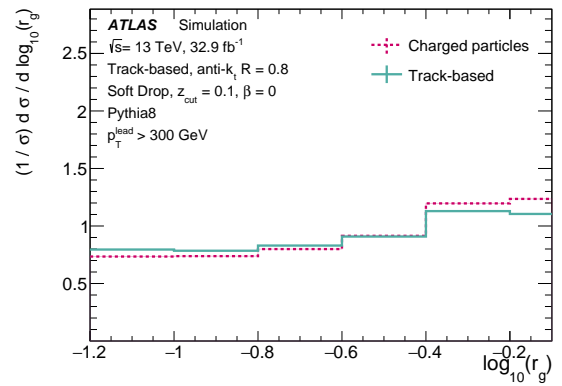
(b) r_g distribution, $\beta = 0$, track-based

Figure 3: The distribution in simulation of r_g at detector level and particle level for the more central of the dijet system for $\beta = 0$ for (a) calorimeter-based (all particles), and (b) track-based (charged particles). The statistical uncertainties are drawn, but are too small to be visible.

7 Unfolding

The substructure observables are reconstructed in bins of the transverse momentum of the jet, and the double-differential distributions are unfolded using PYTHIA 8.186. An iterative Bayesian technique [58] is used with one (four) iterations for track-based (calorimeter-based) observables. These values were chosen to minimize the total uncertainty, and are implemented in the RooUnfold framework [59].

The probability distributions of obtaining a particle-level value given a detector-level observation, Pr(particle-level|detector-level), in PYTHIA 8 for $\beta = 0$ are presented for all three observables for the

calorimeter-based and track-based definitions in Figure 4. While the unfolding is done simultaneously in p_T and the jet observable, the unfolding matrices are shown inclusively in p_T for simplicity. As anticipated, the unfolding matrices for the track-based observables have significantly smaller off-diagonal elements than their calorimeter-based analogs.

8 Uncertainties

Several sources of statistical and systematic uncertainties are considered for this analysis. The data and simulation statistical uncertainties are evaluated from pseudo-experiments using the bootstrap method [60]. The uncertainties from the calorimeter-cell reconstruction, track reconstruction, and MC modeling are determined by applying variations to the simulation, as detailed in Sections 8.1, 8.2, and 8.3, respectively. The impact of the calorimeter-cell cluster uncertainties on the jets is taken into account for both the calorimeter-based measurement as well as the track-based measurement since it impacts the selection of jets. The varied simulation is then used to repeat the unfolding procedure and the deviation from the nominal result is used to estimate the uncertainty. The uncertainty in the pileup modeling is determined by reweighting the pileup profile up by 10% in MC simulation. The uncertainty in the unfolding procedure (unfolding nonclosure) is computed using a data-driven reweighting procedure [61]. In this method, the particle-level spectrum is reweighted such that the reconstructed spectrum better matches the data distribution, while the response matrix is left unchanged. The difference between the reweighted detector-level simulation after unfolding and the generator-level simulation from the same generator is then taken as an uncertainty. All uncertainties are symmetrized unless stated otherwise.

A summary of all the uncertainties considered is given in Section 8.4.

8.1 Calorimeter-cell cluster uncertainties

Uncertainties on the reconstruction of calorimeter cell clusters are estimated using comparisons between tracks with momentum p and clusters with energy E in data and in simulation.

Calorimeter cell clusters require seed cells that exceed the noise threshold; if a particle interacts with the material in front of the calorimeter and produces many spread-out low-energy secondary particles, there may not be sufficient localized energy to seed a cluster. The rate at which particles do not seed a cluster is studied with tracks that do not match a calorimeter cell cluster within $\Delta R < 0.2$, where tracks are extrapolated to the calorimeter layer corresponding to the energy-weighted position of the calorimeter cell cluster. This rate is studied at 13 TeV pp collisions using tracks isolated from all other track candidates by at least $\Delta R = 0.4$. The data/MC difference is then used to derive the cluster reconstruction efficiency uncertainty, which is evaluated in bins of pseudorapidity and energy [62]. To assess the impact of this uncertainty on the unfolded results, clusters are randomly removed at a rate determined by the measured difference between data and simulation – less than 5% for low-momentum clusters and negligible beyond 10 GeV.

The cluster energy scale and resolution uncertainties are determined in three separate regions. For $E < 30$ GeV, there are enough events to derive these uncertainties using the full E/p distribution in data [62]. For any clusters with $30 < E < 350$ GeV, the uncertainties are derived from the combined testbeam data [63]. Finally, for regions outside of the testbeam and E/p coverage, a p_T- and η-independent 10% uncertainty is assigned as a conservative estimate of the uncertainty, as done in previous studies [62].

For the regions where the uncertainty is derived using E/p, the mean and standard deviation of the distributions are extracted in bins of E and $|\eta|$. Only tracks with at least one associated cluster are included, using the same matching criteria as for the cluster efficiency. Depending on the fit quality, either the mean and σ of a Gaussian fit to the data, or the distribution mean and RMS values are used. For example, for $p \approx 25$ GeV and $\eta \approx 0$, the data and simulation are consistent with $\langle E/p \rangle = 1$ and $\sigma(E/p) = 0.22$ within 1% for the mean and 5% for the standard deviation.

To evaluate the cluster energy scale uncertainty, the cluster energy in simulation is shifted according to the difference of the E/p mean value between data and MC simulation. Similarly, to evaluate the cluster energy resolution uncertainty, cluster energies are smeared according to data/MC differences in the E/p distribution by one standard deviation. The effect of the energy scale and resolution uncertainties is defined as the relative difference between the nominal and modified jet substructure observable. A series of validation studies which probe the jet energy scale, jet mass scale, and jet mass resolution were performed to ensure that this prescription is also valid for nonisolated clusters within jets.

The cluster angular resolution is estimated using a similar method by studying the modeling of the ΔR distribution between tracks and calorimeter-cell clusters.

8.2 Tracking uncertainties

Systematic uncertainties are evaluated for the track reconstruction efficiency, fake rate, and momentum scale. The efficiency is decomposed into two components: one from the uncertainty in the inner detector material ('inclusive efficiency') and one from the modeling of pixel cluster merging inside dense environments, such as inside the core of high-energy jets ('efficiency within jets').

The inclusive efficiency uncertainty is due to the material uncertainty, which is constrained by detector construction knowledge and photon conversions as well as hadronic interactions [64]. The total relative uncertainty on the efficiency is 0.5% for $|\eta| < 0.1$ and grows to 2.7% for the $2.3 < |\eta| < 2.5$ region. The impact of this uncertainty in the measured distributions is evaluated by randomly removing tracks in simulation with a p_{T}- and $|\eta|$-dependent probability.

The uncertainty in the tracking efficiency in dense environments is due to the modeling of pixel cluster merging. This is studied using the dE/dx method [65, 66]: the rate of pixel clusters assigned to single tracks with a large charge (comparable to twice a minimum ionizing particle charge) in the core of jets is measured in data and in simulation. The comparison between data and simulation results in an additional 0.4% (absolute) uncertainty that is only applied to tracks within a $\Delta R = 0.1$ of a jet.

Fake tracks result from random combinations of hits mostly from charged particles that happen to overlap in space. Outside of jets, the fake rate is highly pileup dependent, as the chances for many low-p_{T} particles to be close increases with the number of particles in the event. However, inside jets, the density from primary charged particles is also high and can result in an increased fake rate. The fake rate itself is much less than 1%, but fake tracks can have a large p_{T}. The modeling of the fake rate is studied with a dedicated measurement that enriches the rate of fake tracks by inverting various track quality criteria [67]. The simulation reproduces the fake rate to within about 30% of the observed rate in data. The fake-rate uncertainty is estimated by randomly removing 30% of fake tracks.

The leading source of uncertainty in the track parameters is in the q/p_{T} (q is the electric charge) from a potential sagitta distortion due to detector-misalignment weak modes [68]. This bias is corrected for, once per data-taking period, and the correction is about 0.1/TeV except at $\phi \approx 0$ and $|\eta| \approx 2.5$ where

the correction can reach 1/TeV. The impact on the measurement is smaller than that of the other tracking uncertainties.

8.3 Modeling uncertainty

Since the detector response depends on the energy and angular distribution of particles inside jets, it is sensitive to the fragmentation model used for the unfolding. An uncertainty is estimated by repeating the unfolding procedure using SHERPA and comparing that with the nominal unfolding that uses PYTHIA 8, and taking the full difference as the uncertainty. The result of performing this procedure with Herwig++ instead of SHERPA produces a similar uncertainty. In addition to the direct sensitivity to the fragmentation modeling, there is also an indirect sensitivity to the quark/gluon fractions and the jet momentum distribution. An uncertainty due to the PDFs is evaluated as the spread in the unfolded distributions from 100 NNPDF2.3LO eigenvector variations.

8.4 Summary of uncertainties

Figure 5 presents a summary of the total and individual uncertainties for all observables and $\beta = 0$ for both the calorimeter-based and track-based measurements, where all of the uncertainties are summed in quadrature to obtain the total uncertainty. The uncertainties change with β, due to the differing angular sensitivity, but the overall conclusions are similar. For the calorimeter-based ρ, the fragmentation modeling is the dominant uncertainty for most of the mass range, while the pileup modeling and cluster energy scale uncertainties dominate at high relative mass. A similar description is true for the track-based ρ, where the fragmentation modeling is the dominant uncertainty across the entire ρ range and the effects from the unfolding nonclosure are subdominant, while the tracking uncertainties are typically negligible. Analogous results hold for the calorimeter-based r_g observable, while for the track-based r_g measurement, subdominant effects are seen from the cluster energy scale, fake rate, and data statistical uncertainty. For calorimeter-based z_g, the cluster energy scale and modeling uncertainties are most important, and the uncertainties are generally smaller than for ρ and r_g. A similar description holds for the track-based z_g, whose uncertainty is dominated by the modeling and unfolding nonclosure uncertainties.

9 Results

The unfolded data are presented in several different ways, in order to highlight various aspects of the measurement. Since these distributions change slowly as a function of p_T, most of the results are shown inclusively in p_T. Section 9.1 provides a comparison between the unfolded data and several MC predictions, highlighting the various regions of each measurement which are well-modeled by simulation. This is followed by a comparison between the unfolded data and state-of-the-art analytical predictions in Section 9.2. Section 9.3 directly compares the results of the measurements of the calorimeter- and track-based observables. While these observables are unfolded to different particle-level definitions, this comparison highlights the similarities between the different definitions, as well as demonstrating the improved precision in track-based measurements of observables sensitive to the angular structure of the jet. The forward and central measurements are compared in Section 9.4, and these measurements are used as input to the extraction of the quark- and gluon-jet distributions of these observables, which are shown in Section 9.5.

9.1 Comparison with MC predictions

Figures 6– 8 compare the unfolded data from both jets with the particle-level distributions from MC generators described in Section 4. Several trends are visible in these results. For ρ, the MC predictions are mostly accurate within 10% except for the lowest relative masses, which are dominated by nonperturbative physical effects. This becomes more visible for larger values of β, where more soft radiation is included within the jet, increasing the size of the nonperturbative effects. In addition, in the high-relative-mass region, where the effects of the fixed-order calculation are relevant, some differences between MC generators are seen. A similar trend may be seen for r_g, where the small-angle region shows more pronounced differences between MC generators, since this corresponds to the region where nonperturbative effects are largest. Overall, these effects are smaller than for the relative mass. Unlike the other two observables, z_g is modeled well within about 10% across most of the spectrum. However, there is some tension between the predictions and the unfolded data, which is visible particularly for the track-based observables, which have better precision.

In general, the MC predictions show similar behavior for the calorimeter-based and track-based definitions, both in their overall distributions and in their agreement with the unfolded data distribution. However, as the tracking measurement is more precise, the disagreement between data and MC simulation in the nonperturbative regions is more significant. For instance, in Figure 7(e)– 7(f), the Herwig++ prediction does not agree with the unfolded distribution at high values of z_g for the track-based case, but it does agree in the calorimeter-based case.

(a) ρ distribution, $\beta = 0$, calorimeter-based

(b) ρ distribution, $\beta = 0$, track-based

(c) z_g distribution, $\beta = 0$, calorimeter-based

(d) z_g distribution, $\beta = 0$, track-based

(e) r_g distribution, $\beta = 0$, calorimeter-based

(f) r_g distribution, $\beta = 0$, track-based
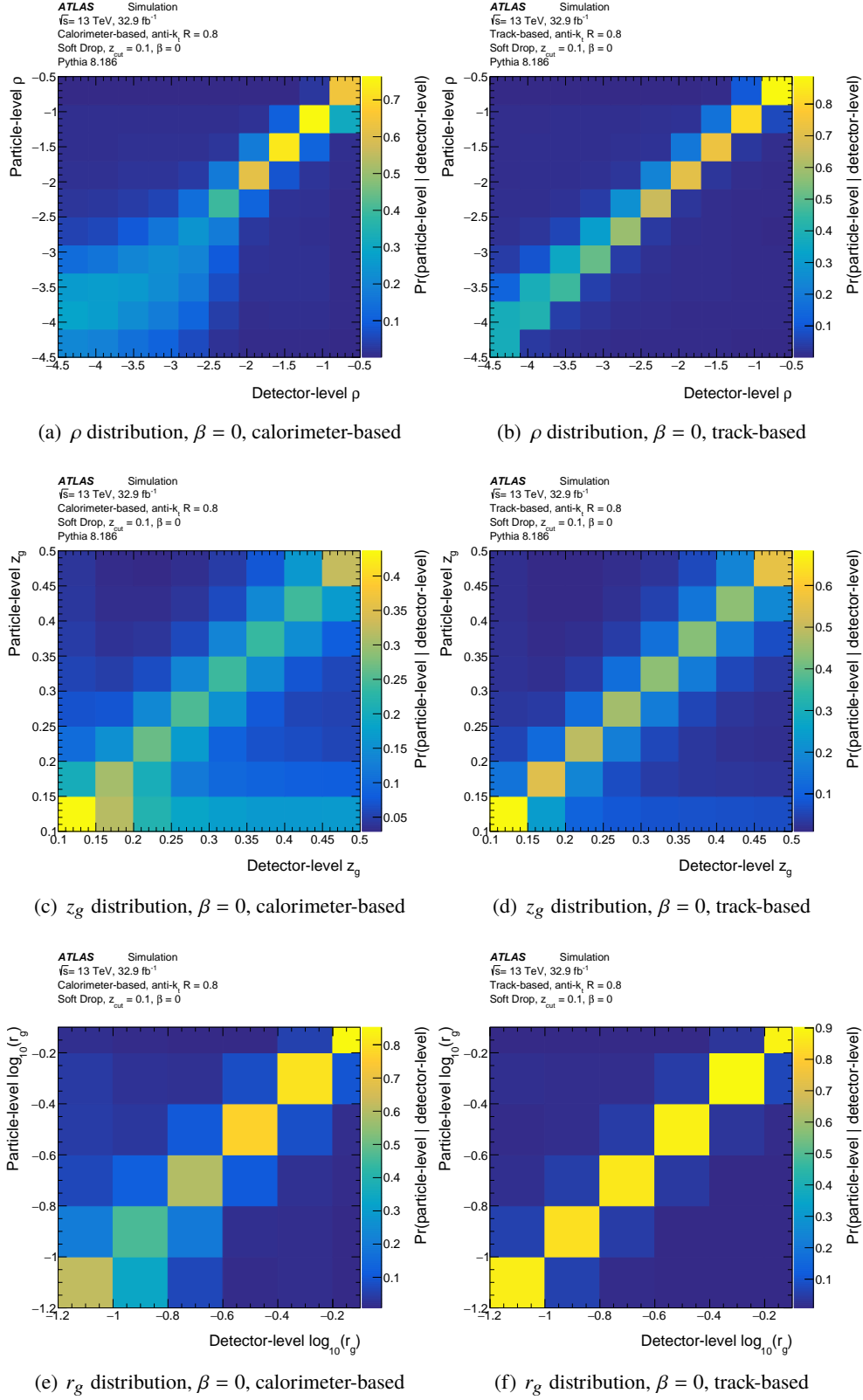
Figure 4: The distribution of Pr(particle-level|detector-level) for the more central jet for (top) ρ, (middle) z_g, and (bottom) r_g with $\beta = 0$ for Pythia 8 for (left) calorimeter-based definition, and (right) track-based definition.
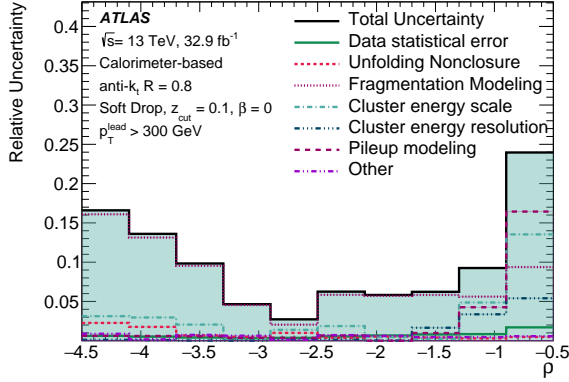
(a) ρ, $\beta = 0$, calorimeter-based
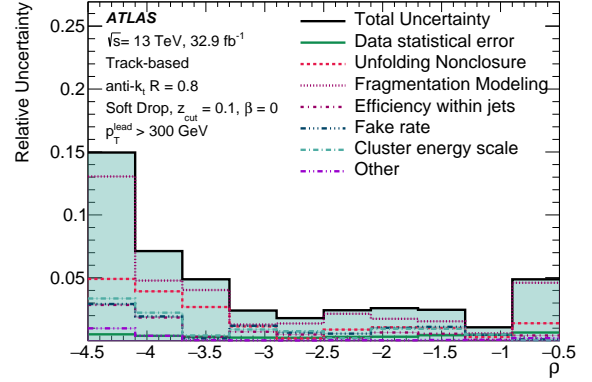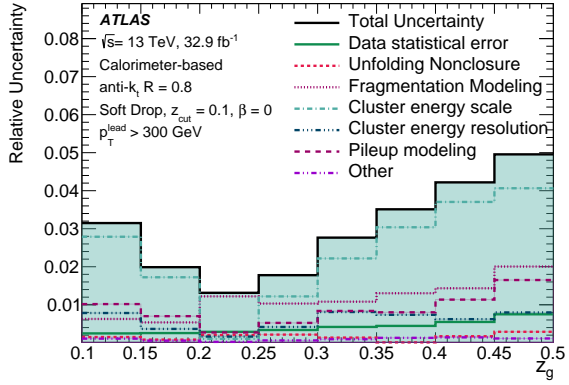
(b) ρ, $\beta = 0$, track-based

(c) z_g, $\beta = 0$, calorimeter-based
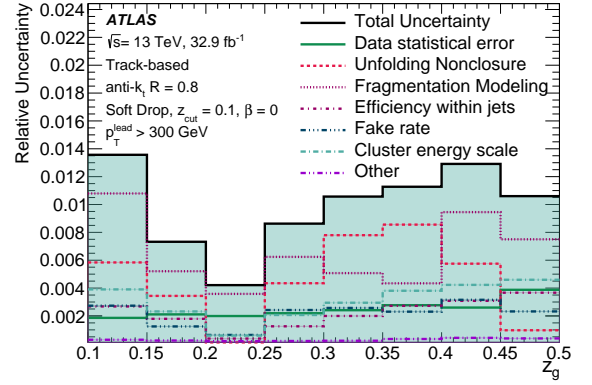
(d) z_g, $\beta = 0$, track-based
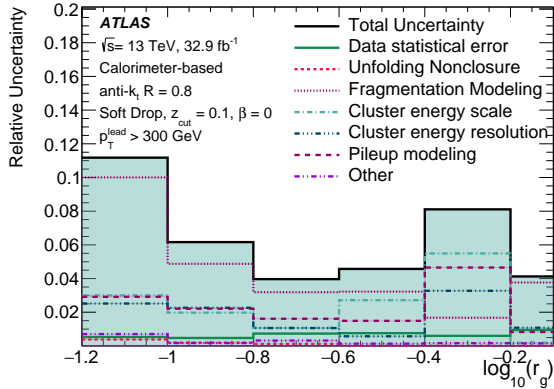
(e) r_g, $\beta = 0$, calorimeter-based
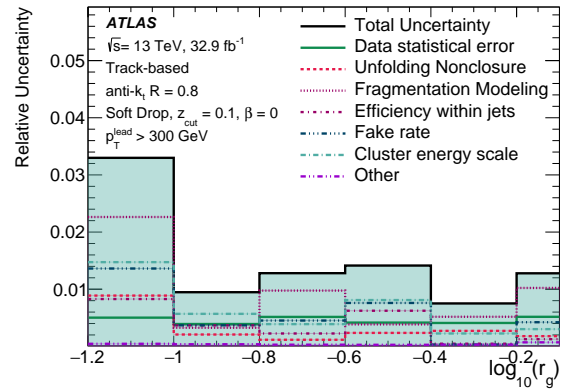
(f) r_g, $\beta = 0$, track-based

Figure 5: Total and individual uncertainties inclusive in p_T for $\beta = 0$ for calorimeter-based observables (left) and track-based observables (right) for ρ (top), z_g (middle), and r_g (bottom).

(a) $\beta = 0$, calorimeter-based

(b) $\beta = 0$, track-based

(c) $\beta = 1$, calorimeter-based

(d) $\beta = 1$, track-based

(e) $\beta = 2$, calorimeter-based

(f) $\beta = 2$, track-based
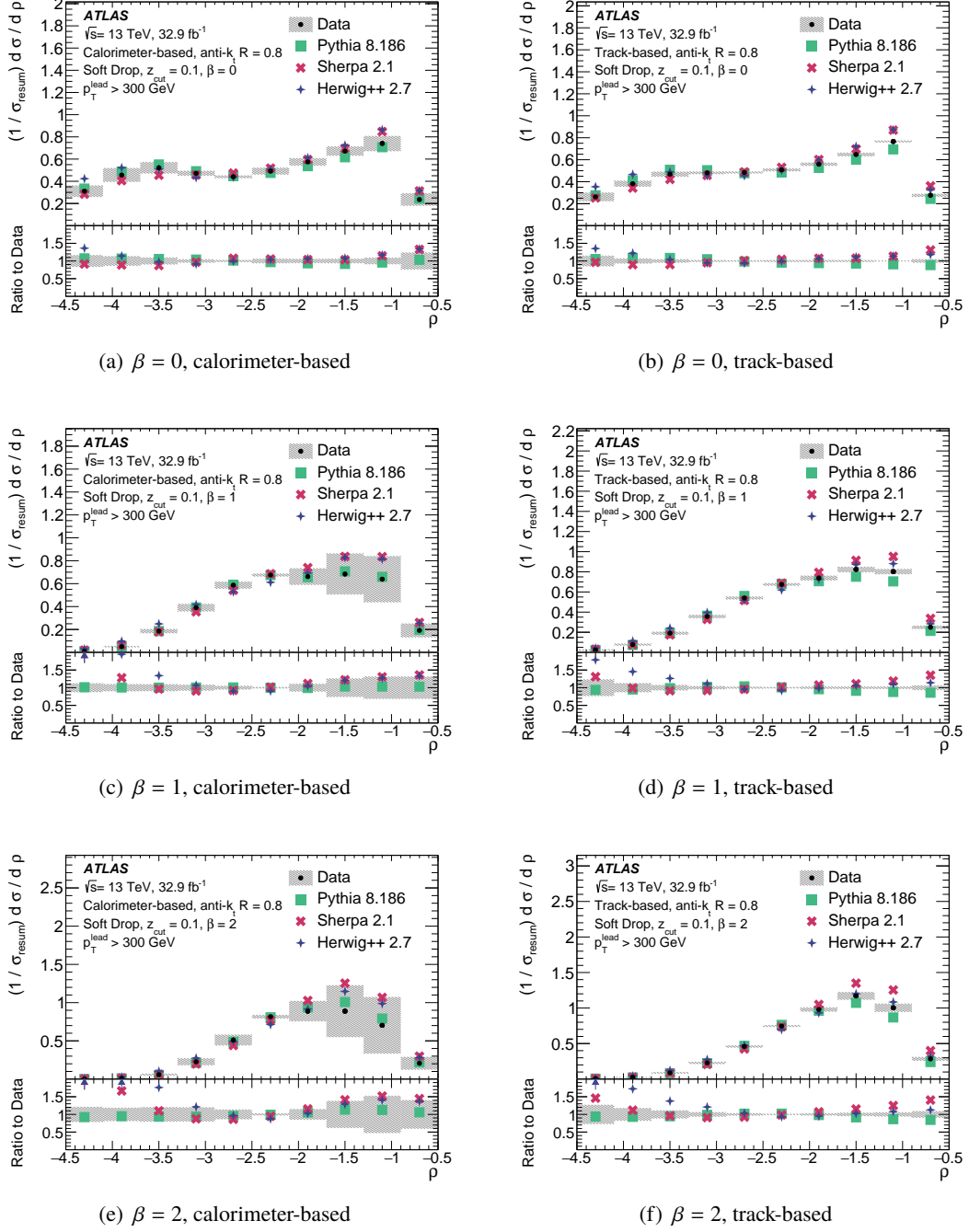
Figure 6: Comparison of the unfolded ρ distribution with MC predictions. The uncertainty bands include all sources: data and MC statistical uncertainties, nonclosure, modeling, and cluster or tracking uncertainties where relevant.

(a) $\beta = 0$, calorimeter-based

(b) $\beta = 0$, track-based

(c) $\beta = 1$, calorimeter-based

(d) $\beta = 1$, track-based

(e) $\beta = 2$, calorimeter-based

(f) $\beta = 2$, track-based
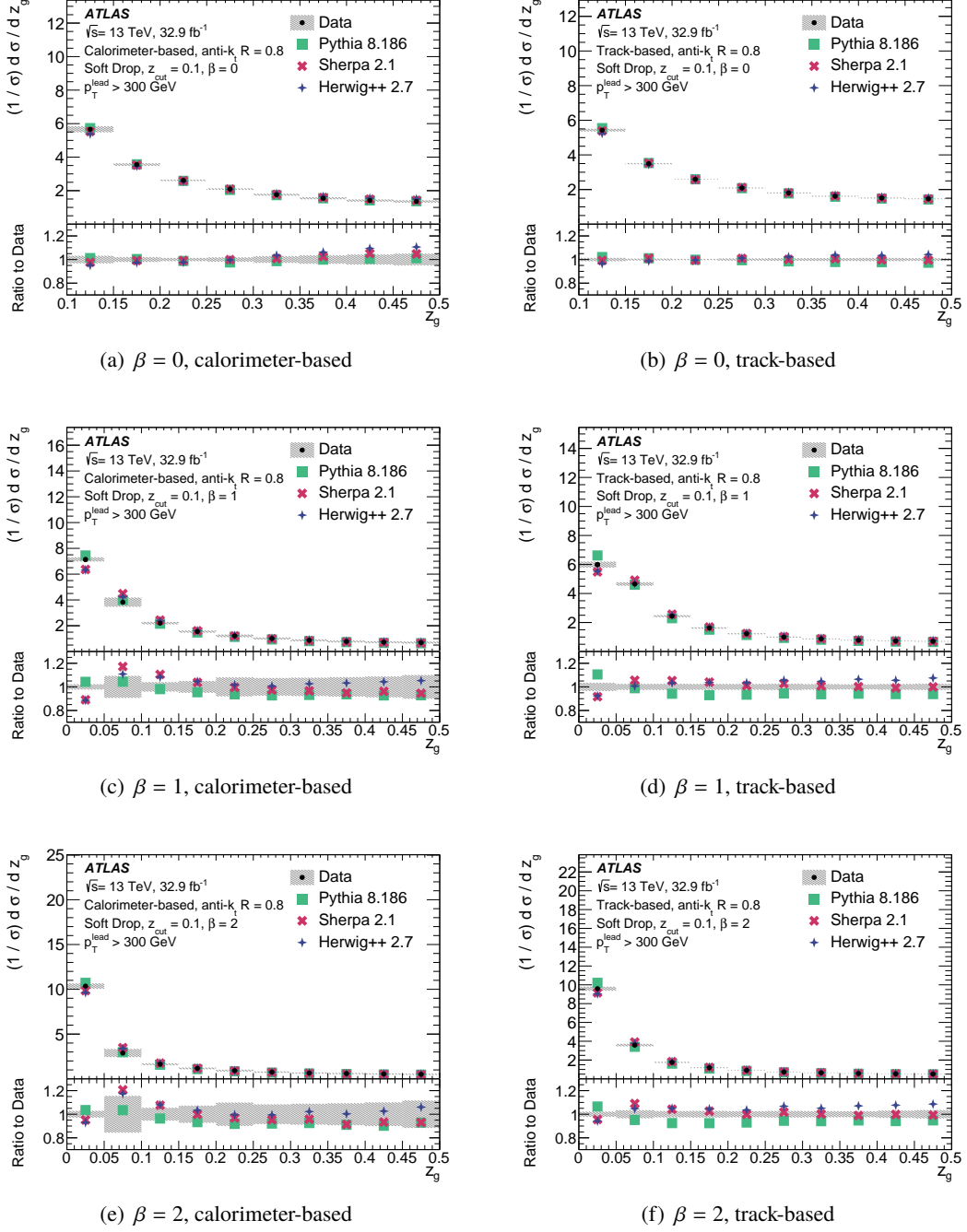
Figure 7: Comparison of the unfolded z_g distribution with MC predictions. The uncertainty bands include all sources: data and MC statistical uncertainties, nonclosure, modeling, and cluster or tracking uncertainties where relevant.
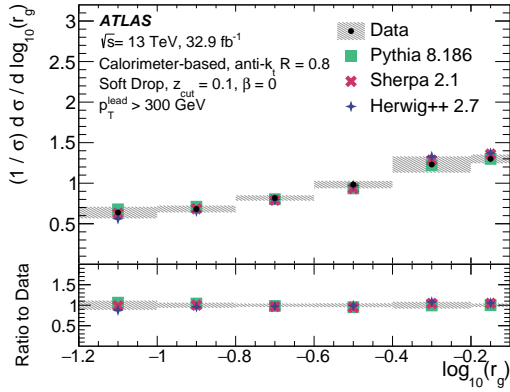
(a) $\beta = 0$, calorimeter-based
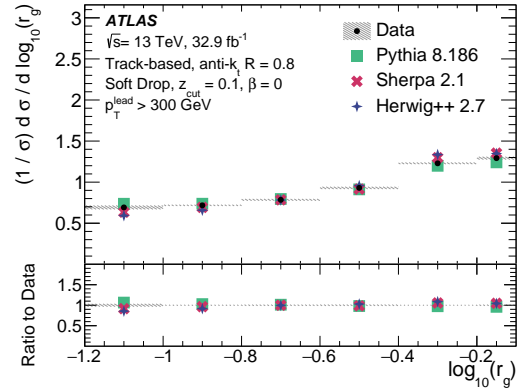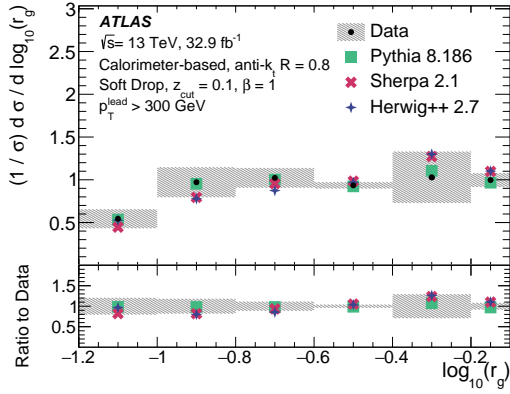
(b) $\beta = 0$, track-based

(c) $\beta = 1$, calorimeter-based
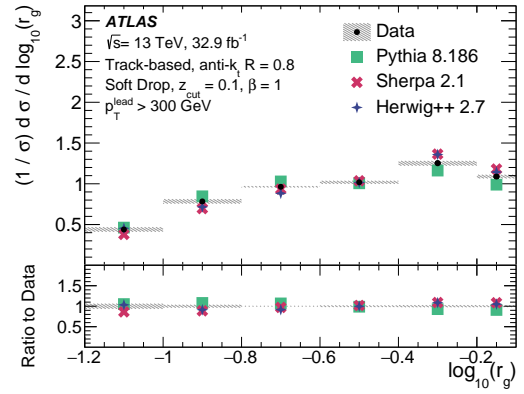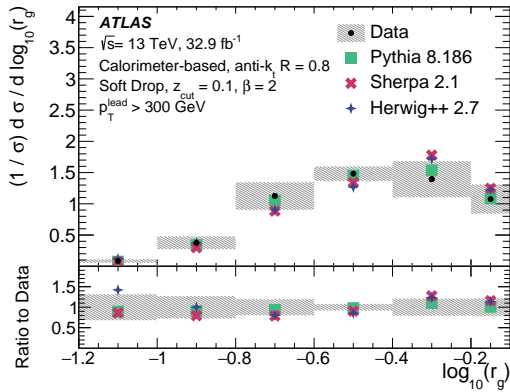
(d) $\beta = 1$, track-based

(e) $\beta = 2$, calorimeter-based
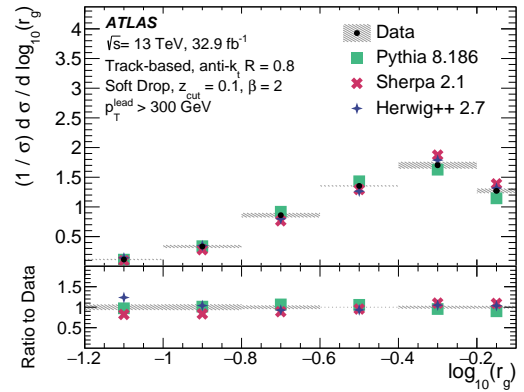
(f) $\beta = 2$, track-based

Figure 8: Comparison of the unfolded r_g distribution with MC predictions. The uncertainty bands include all sources: data and MC statistical uncertainties, nonclosure, modeling, and cluster or tracking uncertainties where relevant.

9.2 Comparison with analytical predictions

Currently, it is only possible to perform analytical predictions when including both charged and neutral particles, and therefore results in this section are only compared with the calorimeter-based results. Subleading logarithms have been computed for ρ and r_g, as described below. Several calculations have been performed to predict the ρ distribution, and these predictions are compared with the unfolded data. In addition, only ρ and r_g are studied, since no predictions exist for z_g beyond leading-logarithmic accuracy. In particular, these include the NLO+NLL prediction from Refs. [5, 6], the LO+NNLL prediction from Refs. [3, 4], and the NNLL prediction from Refs. [7, 8].

The LO+NNLL and NNLL calculations are based on soft collinear effective theory (SCET) [69, 70]. The former is matched to leading order using MadGraph5_aMC@NLO [71] with the MSTW2008LO PDF. The latter uses the CT14nlo [72] PDF set and includes finite z_{cut} resummation as well as nonperturbative corrections based on an analytic shape function with one free parameter that is chosen based on comparisons with PYTHIA 8. While strictly for inclusive jets, the NNLL calculation is also applicable here because at high jet p_T, the difference between inclusive jets and dijets is negligible. The NLO+NLL calculation is matched to fixed order using NLOJet++ [73, 74] with the CT14nlo PDF and includes finite z_{cut} resummation as well as nonperturbative corrections from the envelope of parton shower MC predictions from HERWIG 6.521 [75] AUET2 [76], PYTHIA 6.428 [37] Perugia 2011 [77], PYTHIA 6.428 Z2 [78], PYTHIA 8.223 [37, 38, 79] 4C [80], and PYTHIA 8.223 Monash 13 [81].

These predictions are compared with the unfolded data in Figure 9. Because the LO+NNLL and NLO+NLL calculations for ρ are only available for $p_T > 600$ GeV, the unfolded data are shown for both a low-p_T jet selection ($p_T > 300$ GeV) and a high-p_T jet selection (($p_T > 600$ GeV). The calculations are able to model the data in the resummation region (approximately $-3 \lesssim \rho \lesssim -1$) at the level of a 10% difference. The NLO+NLL calculation also provides an accurate model of the data at the high values of ρ, while the LO+NNLL and NNLL calculations do not model this region as accurately. This is the region where the fixed-order effects are dominant, and so this behavior is expected.

At lower values of relative mass, the nonperturbative corrections are needed to describe the data. This can be seen particularly from the low-p_T results, which show the NNLL prediction with and without the inclusion of nonperturbative effects. As expected, the inclusion of these effects brings the prediction much closer to the unfolded data distribution, although the level of agreement is still not as good as in the resummation region. The region where nonperturbative corrections are relevant shifts to higher relative mass with increased values of β, since more soft radiation is included within the jet. In general, similar levels of agreement are seen in the low-p_T and high-p_T cases, although it is noted that the nonperturbative region shifts to slightly lower relative mass in the high-p_T case.

An NLL calculation of r_g has been performed recently [82], and the results of this calculation are compared with the unfolded data distribution in Figure 10. Unlike the jet mass case, nonglobal logarithms are not absent ($\beta = 0$) or power suppressed ($\beta > 0$). The calculation includes both the nonglobal and clustering logarithms to achieve full NLL accuracy. In general, in the region where nonperturbative effects are expected to be small, the prediction agrees with the data within uncertainties, while in the regions where nonperturbative effects are large, the prediction is systematically higher than the data.
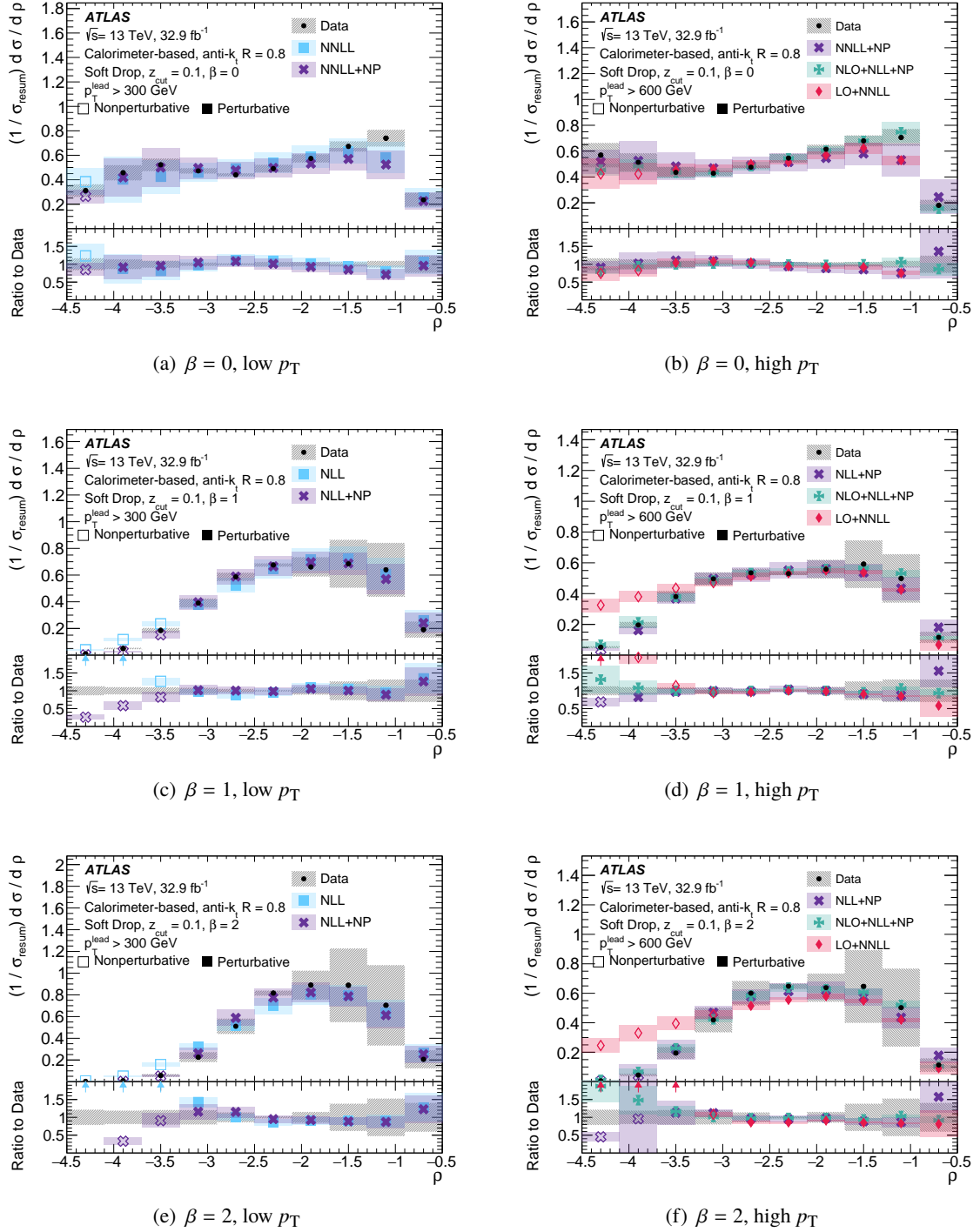
Figure 9: Comparison of the unfolded ρ distribution with the theory predictions. For the (N)NLL, (N)NLL+NP, and LO+NNLL predictions, the open marker style indicates that nonperturbative effects on the calculation are expected to be large. 'NP' indicates that nonperturbative corrections have been applied. The experimental uncertainty bands include all sources: data and MC statistical uncertainties, nonclosure, modeling, and cluster or tracking uncertainties where relevant. The theory error bands include perturbative scale variations as well as nonperturbative model variations (NLO+NLL only).

(a) $\beta = 0$, low p_T

(b) $\beta = 0$, high p_T

(c) $\beta = 1$, low p_T

(d) $\beta = 1$, high p_T

(e) $\beta = 2$, low p_T

(f) $\beta = 2$, high p_T
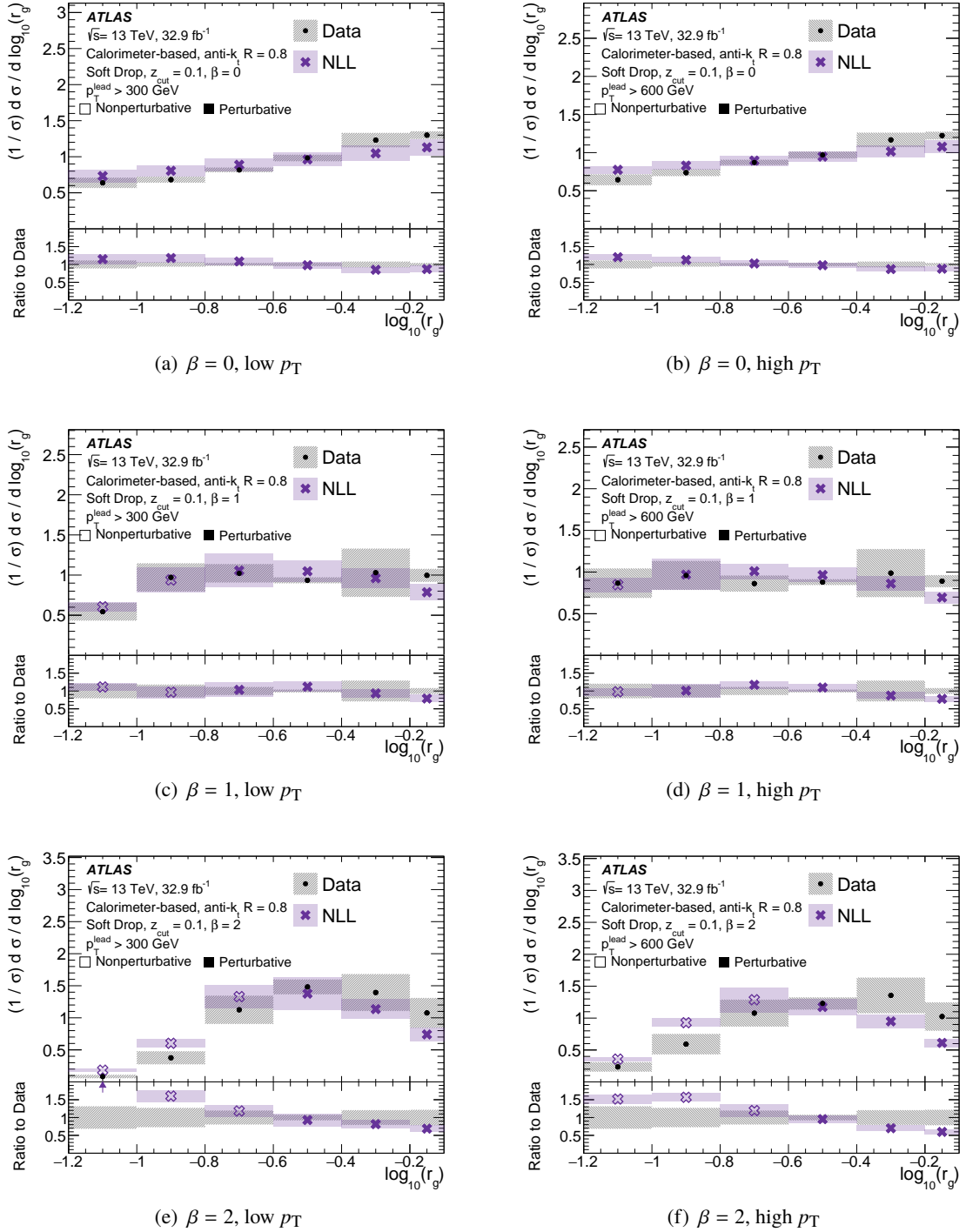
Figure 10: Comparison of the unfolded r_g distribution with the theory predictions. For the NLL predictions, the open marker style indicates that nonperturbative effects on the calculation are expected to be large. The experimental uncertainty bands include all sources: data and MC statistical uncertainties, nonclosure, modeling, and cluster or tracking uncertainties where relevant. The theory error bands include perturbative scale variations.

9.3 Comparison of track-based and calorimeter-based measurements

On a jet-by-jet basis, the value of the all-particles and charged-particles jet substructure observables are largely uncorrelated. However, due to isospin symmetry, the probability distributions for all-particles and charged-particles distributions are nearly identical. This is studied by comparing the unfolded distributions for the cluster-based and track-based measurements, which are shown in Figures 11–13 for the region which includes both jets in the dijet system. The results generally agree in the perturbative regions at high values of ρ and r_g, and there is disagreement in the low-relative-mass regions. There is also some disagreement for low values of z_g for $\beta > 0$.

These studies also enable a comparison of the sizes of the uncertainties for calorimeter-based and track-based observables. For all of these observables, the uncertainties for the track-based observables are significantly smaller than those for the calorimeter-based observables, particularly for higher values of β, where more soft radiation is included within the jet. However, since no track-based calculations exist at the present time, calorimeter-based measurements are still useful for precision QCD studies.
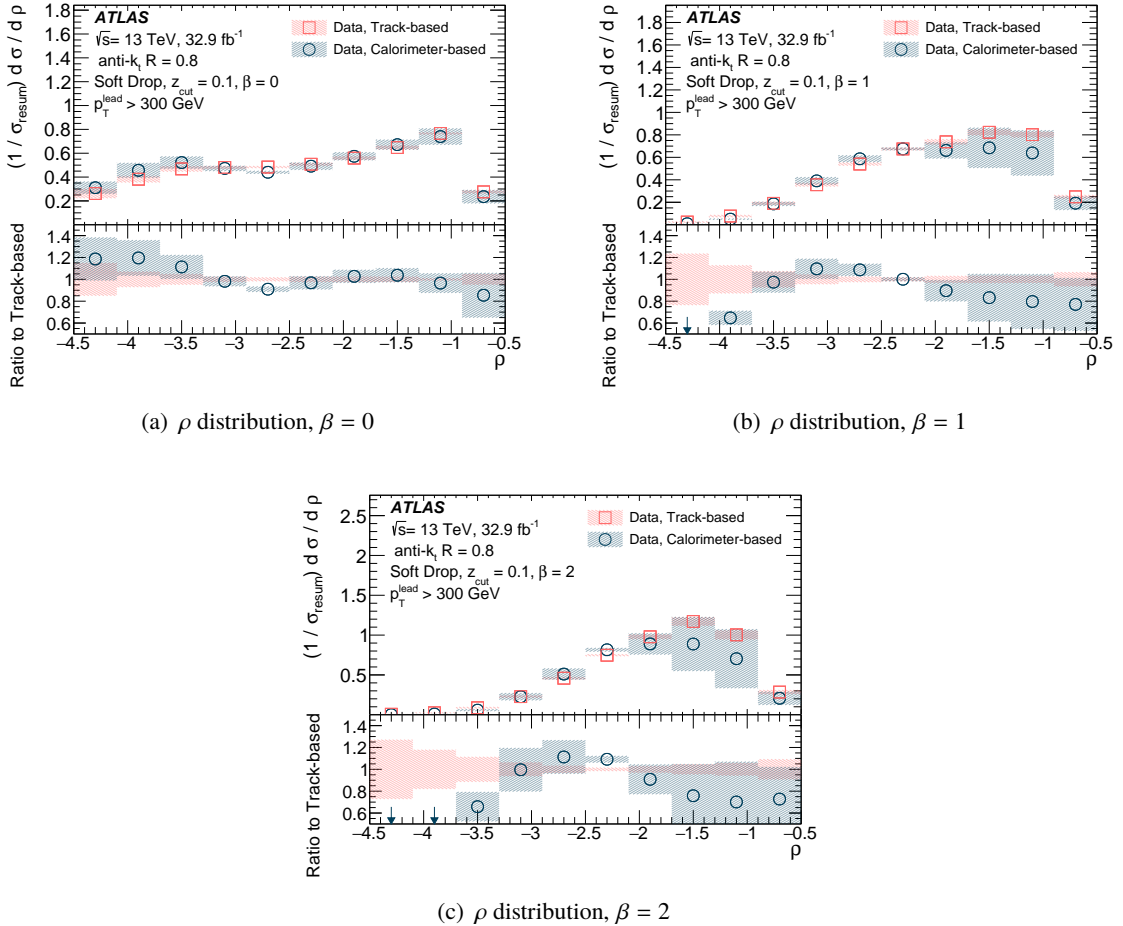
(a) ρ distribution, $\beta = 0$

(b) ρ distribution, $\beta = 1$

(c) ρ distribution, $\beta = 2$

Figure 11: Unfolded ρ distribution, for calorimeter- and track-based jets. The uncertainty bands include all sources: data and MC statistical uncertainties, nonclosure, modeling, and cluster or tracking uncertainties where relevant.

(a) z_g distribution, $\beta = 0$

(b) z_g distribution, $\beta = 1$
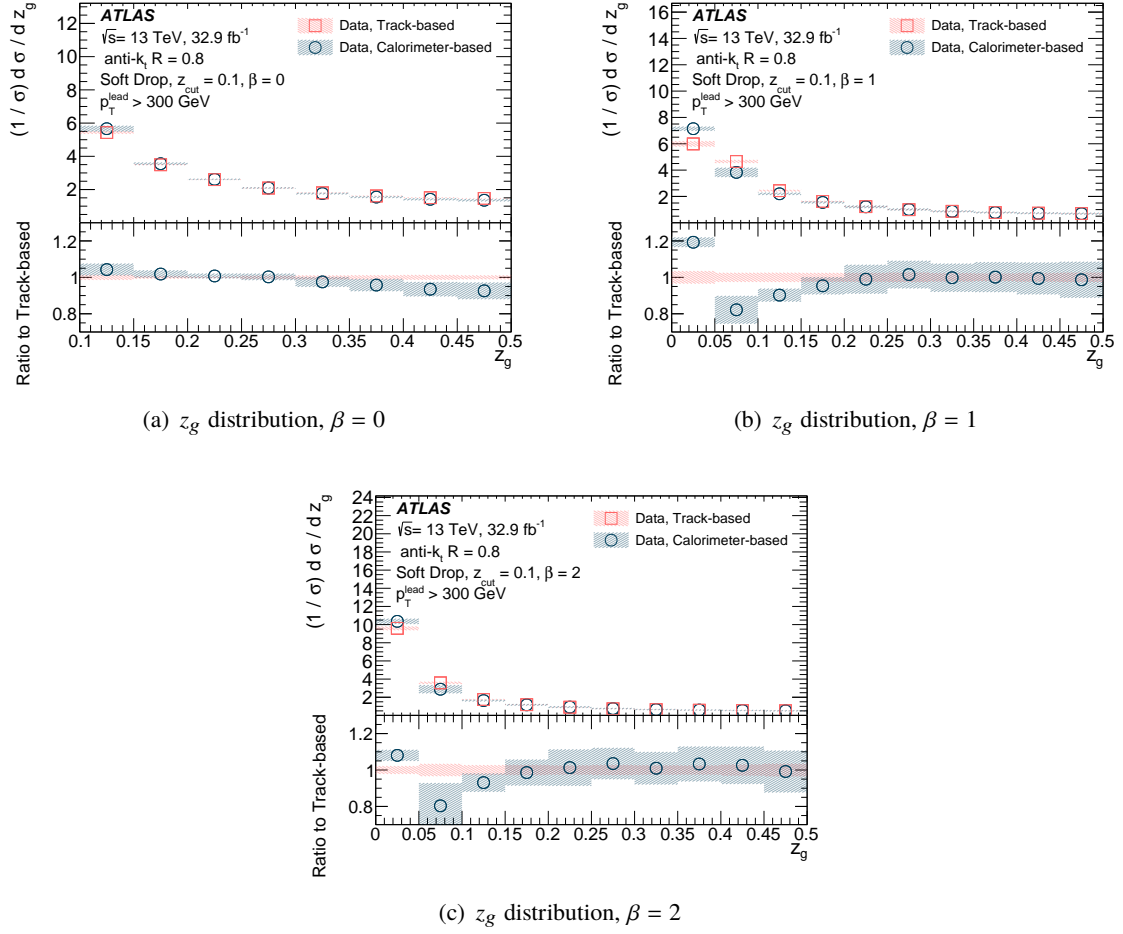
(c) z_g distribution, $\beta = 2$

Figure 12: Unfolded z_g distribution, for calorimeter- and track-based jets. The uncertainty bands include all sources: data and MC statistical uncertainties, nonclosure, modeling, and cluster or tracking uncertainties where relevant.

9.4 Comparison of forward and central measurements

The distribution of the substructure observables at a given p_T is a function of the composition of the initiating parton type, and should not be affected by where the jet is produced within the detector. Therefore, any differences seen between the distribution of the observable in different regions of the detector are related to the quark–gluon composition of the events produced there. Since this measurement was done separately for the more forward and more central jet in the dijet samples, it is possible to compare these distributions to see if these effects are visible. The fraction of central and forward jets originating from gluons, f_G, in PYTHIA 8 multijet events is shown in Table 1, where the jet flavor is determined by the highest-energy parton inside the jet cone.[2] This shows that the gluon fractions in the forward and central regions differ by about 5–10%. For each of the three observables, Figure 14 compares the unfolded distributions for the jets in the forward region with those for jets in the central region. As expected, since the forward region is

---

[2] Various definitions were studied in Ref. [83] and found to have a small effect on quark/gluon extractions. Furthermore, the universality of this definition was studied in Ref. [84].

(a) r_g distribution, $\beta = 0$

(b) r_g distribution, $\beta = 1$
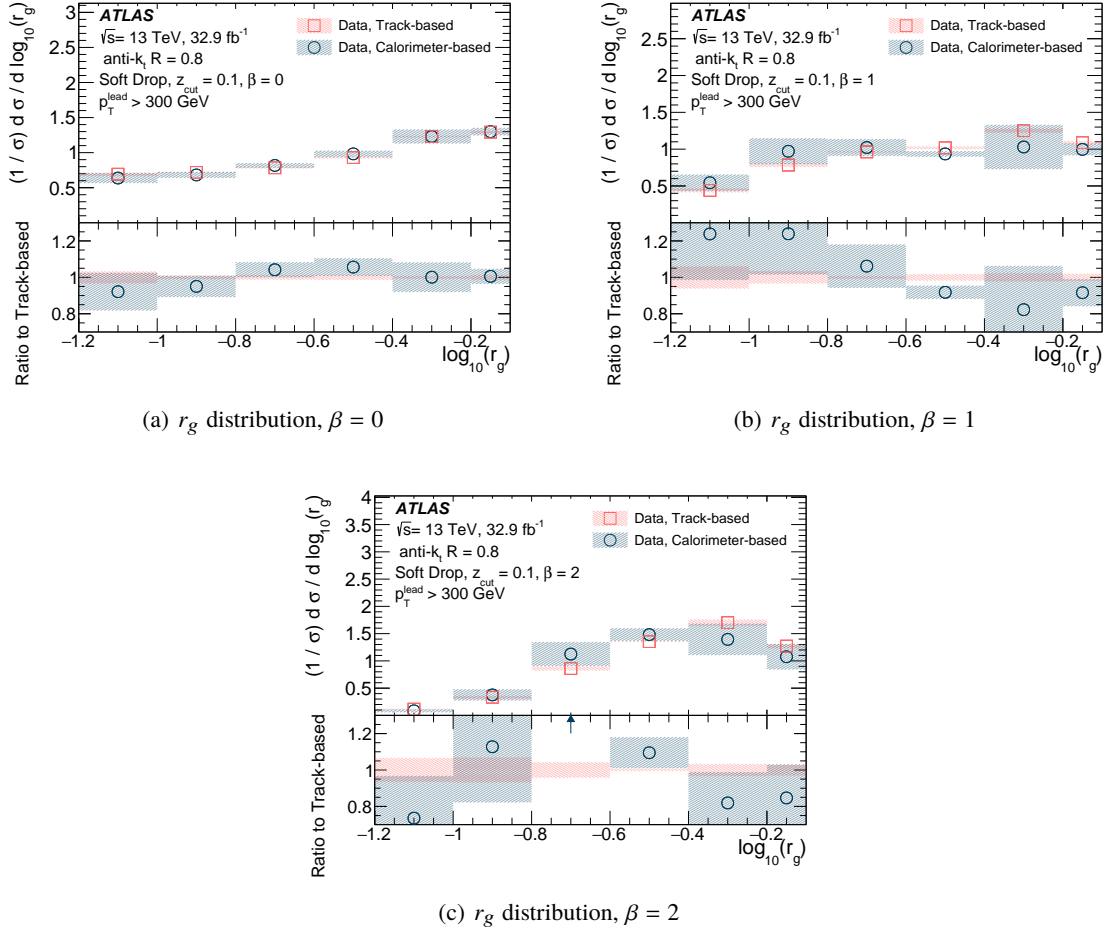
(c) r_g distribution, $\beta = 2$

Figure 13: Unfolded r_g distribution, for calorimeter- and track-based jets. The uncertainty bands include all sources: data and MC statistical uncertainties, nonclosure, modeling, and cluster or tracking uncertainties where relevant.

quark-enhanced, it has more jets at lower relative masses. These differences are numerically small because the gluon fractions are similar for the forward and central jets.

Table 1: The gluon fractions predicted by the PYTHIA 8 multijet simulation.

	Gluon Fraction [%]	
	Central Region	Forward Region
300 GeV$< p_T <$ 400 GeV	75.1	69.5
400 GeV$< p_T <$ 600 GeV	71.7	64.4
600 GeV$< p_T <$ 800 GeV	66.2	56.9
800 GeV$< p_T <$ 1000 GeV	61.0	50.5
1000 GeV$< p_T <$ 2000 GeV	54.4	43.3
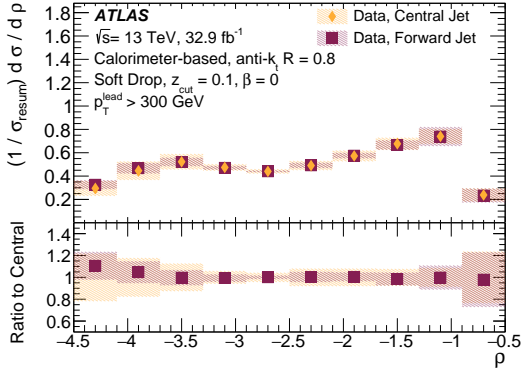
(a) ρ distribution, $\beta = 0$, calorimeter-based
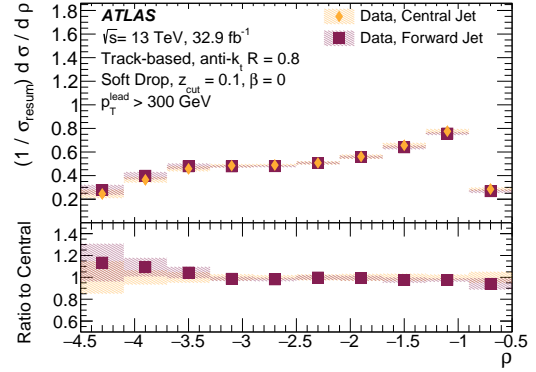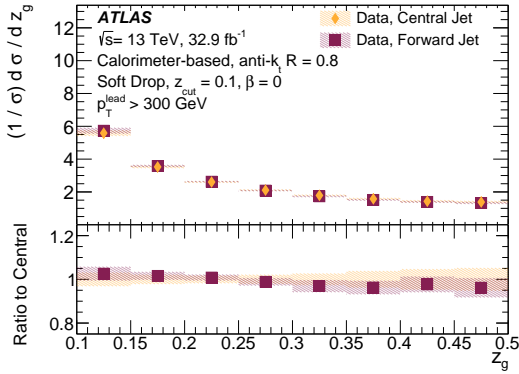
(b) ρ distribution, $\beta = 0$, track-based

(c) z_g distribution, $\beta = 0$, calorimeter-based
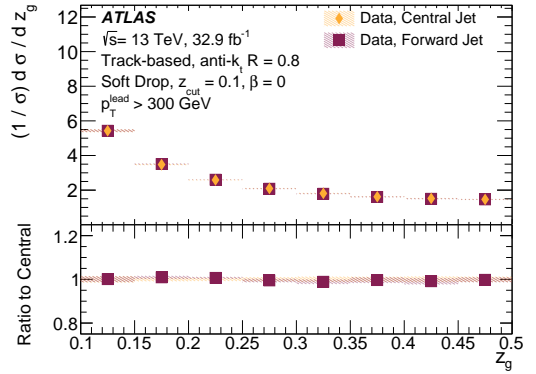
(d) z_g distribution, $\beta = 0$, track-based
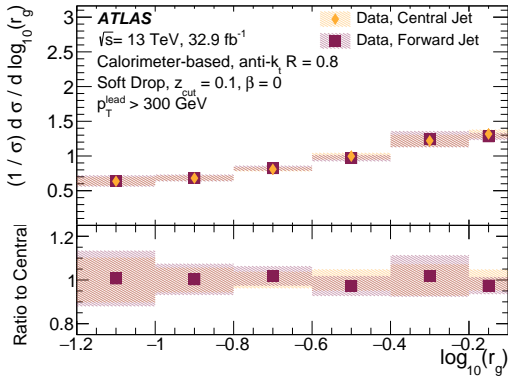
(e) r_g distribution, $\beta = 0$, calorimeter-based
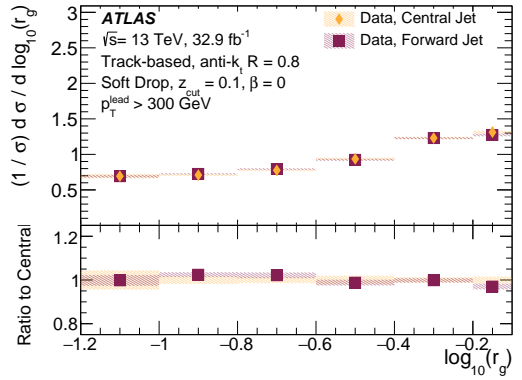
(f) r_g distribution, $\beta = 0$, track-based

Figure 14: Comparison of the forward and central unfolded distributions for $\beta = 0$. The uncertainty bands include all sources: data and MC statistical uncertainties, cluster uncertainties, nonclosure, and modeling. See Section 8 for details.

9.5 Quark–gluon Extraction of the observables

Since the shape of the ρ, r_g, and z_g distributions at a given jet p_T only depends on the flavor of the initiating parton and not on the rapidity, the quark and gluon distributions may be extracted from the measurements of the central and forward distributions if the quark–gluon fraction is known for each region. In particular, the central and forward distributions for these observables may be described as the sum of the quark and gluon distributions, weighted by the quark and gluon composition of the sample:

$$
\begin{aligned}
h_i^F &= f_Q^F h_i^Q + f_G^F h_i^G, \\
h_i^C &= f_Q^C h_i^Q + f_G^C h_i^G,
\end{aligned}
\tag{2}
$$

where h_i is a bin of a histogram for an observable, F and C represent the forward and central regions, and Q and G represent quark or gluon. The quark and gluon fractions (f_Q and f_G) for the more forward and more central jets are determined from the nominal Pythia 8 MC event sample, where the quark fraction f_Q is given by $1 - f_G$. This extraction is model-dependent, but the more forward and more central distributions are made public for reinterpretation using any model. Table 1 shows these values for each p_T bin. Equations (2) may then be solved for h_i^G and h_i^Q to extract these distributions from the forward and central distributions.

The extracted quark and gluon distributions are shown in Figures 15– 17 for track-based observables. Cluster-based observables are not shown, but exhibit similar behavior overall. For these results, the PDF uncertainties and the uncertainties in the jet inputs are taken to be fully correlated between the more forward and more central jets, while all other uncertainties are considered fully uncorrelated. In addition, to account for the uncertainty in the composition of the sample, the difference between the extracted distributions using the Pythia 8 and Sherpa compositions is taken as an uncertainty. A few observations can be made about the differences between the quark and gluon distributions. For the jet mass, the gluon distribution tends towards higher values of the mass, which is expected due to the larger color factor associated with gluons. These differences become more apparent at larger values of β. For $\beta = 0$, z_g is independent of α_S to leading order, and the distributions are very similar, while for $\beta > 0$, some differences begin to appear. Finally, for r_g, the gluon distribution tends towards a larger splitting, which is similarly more apparent at larger values of β.
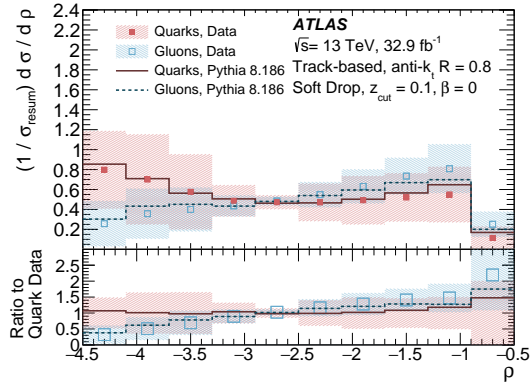
(a) ρ distribution, $\beta = 0$, track-based
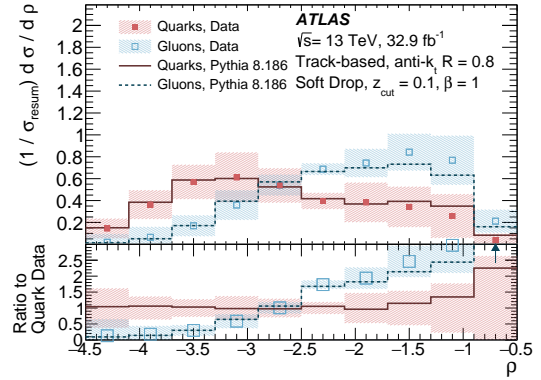
(b) ρ distribution, $\beta = 1$, track-based
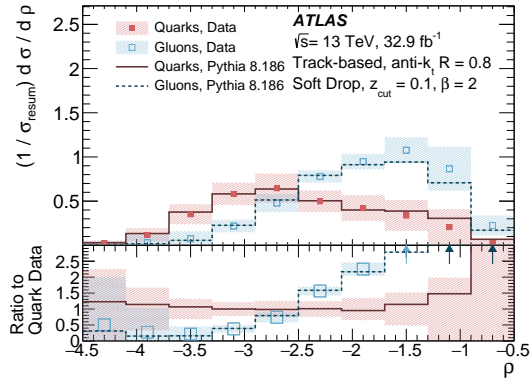
(c) ρ distribution, $\beta = 2$, track-based

Figure 15: Comparison of the quark and gluon unfolded ρ distributions for the track-based measurement. The uncertainty bands include all sources: data and MC statistical uncertainties, tracking uncertainties, nonclosure, and modeling.
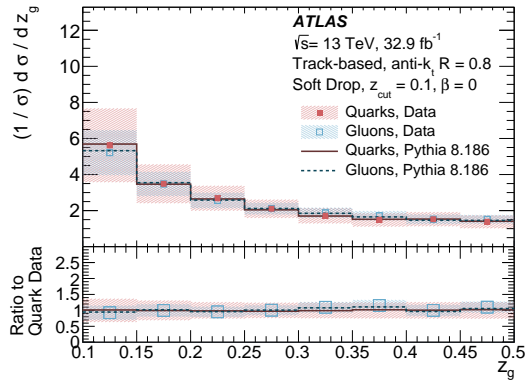
(a) z_g distribution, $\beta = 0$, track-based
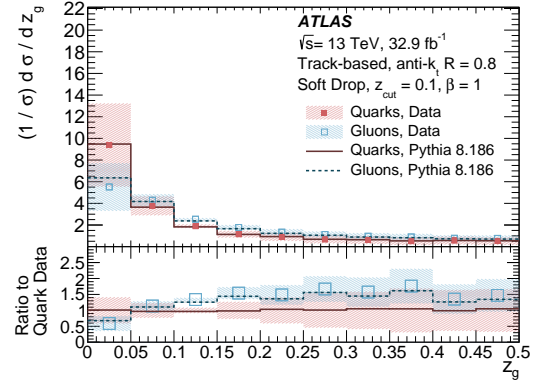
(b) z_g distribution, $\beta = 1$, track-based
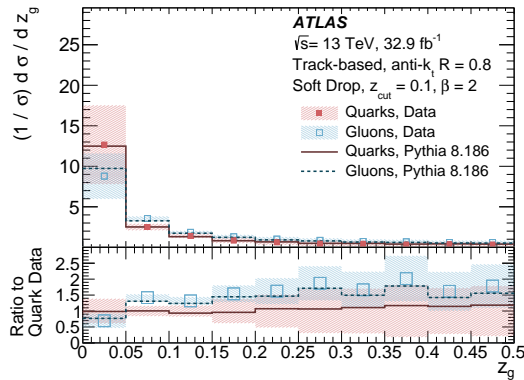
(c) z_g distribution, $\beta = 2$, track-based

Figure 16: Comparison of the quark and gluon unfolded z_g distribution for the track-based measurement. The uncertainty bands include all sources: data and MC statistical uncertainties, nonclosure, modeling, and tracking uncertainties where relevant.
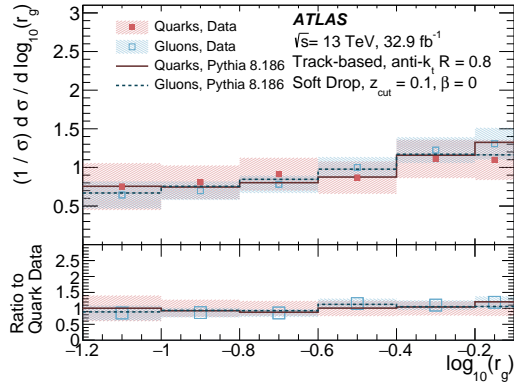
(a) r_g distribution, $\beta = 0$, track-based
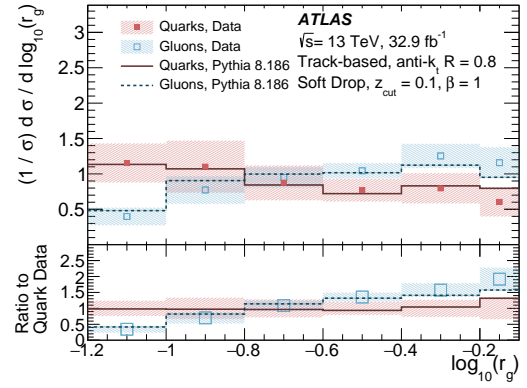
(b) r_g distribution, $\beta = 1$, track-based
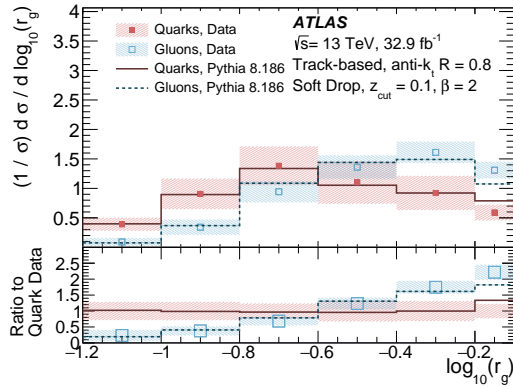
(c) r_g distribution, $\beta = 2$, track-based

Figure 17: Comparison of the quark and gluon unfolded r_g distribution for the track-based measurement. The uncertainty bands include all sources: data and MC statistical uncertainties, nonclosure, modeling, and tracking uncertainties where relevant.

10 Conclusion

This paper presents a measurement of soft-drop jet substructure observables in dijet events in pp collisions at $\sqrt{s} = 13$ TeV using a dataset corresponding to an integrated luminosity of 32.9 fb^{-1} collected with the ATLAS detector at the LHC. Unfolded measurements of three substructure observables are shown for both the calorimeter-based observables unfolded to the all-particle level and track-based observables unfolded to the charged-particles level. These two types of measurements allow a direct comparison of how the different object definitions affect on the measured observables. The calorimeter-based measurements for the relative jet mass and r_g are compared with analytical predictions and are shown to be in good agreement in the perturbative region. In particular, this provides the first comparison between an analytical prediction and an unfolded measurement of r_g. Particularly for observables which are sensitive to the angular distribution of radiation within a jet, track-based observables are shown to be more precise than calorimeter-based observables, due to the better angular resolution of tracks. Since analytical predictions of track-based observables are not currently available, cluster-based observables are still relevant for probing the perturbative region. The forward and central jets are measured separately, which enables an extraction of the quark- and gluon-jet distributions using input from simulation. The extractions demonstrate differences between the observables in their sensitivity to the quark and gluon composition of the sample, which are most pronounced for the least amount of grooming.

(Taiwan), RAL (UK) and BNL (USA), the Tier-2 facilities worldwide and large non-WLCG resource providers. Major contributors of computing resources are listed in Ref. [85].

References

[1] R. Kogler et al., *Jet Substructure at the Large Hadron Collider*, Rev. Mod. Phys. **91** (2019) 045003, arXiv: 1803.06991 [hep-ex].

[2] A. J. Larkoski, I. Moult and B. Nachman, *Jet Substructure at the Large Hadron Collider: A Review of Recent Advances in Theory and Machine Learning*, (2017), arXiv: 1709.04464 [hep-ph].

[3] C. Frye, A. J. Larkoski, M. D. Schwartz and K. Yan, *Factorization for groomed jet substructure beyond the next-to-leading logarithm*, JHEP **07** (2016) 064, arXiv: 1603.09338 [hep-ph].

[4] C. Frye, A. J. Larkoski, M. D. Schwartz and K. Yan, *Precision physics with pile-up insensitive observables*, (2016), arXiv: 1603.06375 [hep-ph].

[5] S. Marzani, L. Schunk and G. Soyez, *A study of jet mass distributions with grooming*, JHEP **07** (2017) 132, arXiv: 1704.02210 [hep-ph].

[6] S. Marzani, L. Schunk and G. Soyez, *The jet mass distribution after Soft Drop*, Eur. Phys. J. C **78** (2018) 96, arXiv: 1712.05105 [hep-ph].

[7] Z.-B. Kang, K. Lee, X. Liu and F. Ringer, *Soft drop groomed jet angularities at the LHC*, Phys. Lett. B **793** (2019) 41, arXiv: 1811.06983 [hep-ph].

[8] Z.-B. Kang, K. Lee, X. Liu and F. Ringer, *The groomed and ungroomed jet mass distribution for inclusive jet production at the LHC*, JHEP **10** (2018) 137, arXiv: 1803.03645 [hep-ph].

[9] A. J. Larkoski, S. Marzani and J. Thaler, *Sudakov safety in perturbative QCD*, Phys. Rev. D **91** (2015) 111501, arXiv: 1502.01719 [hep-ph].

[10] A. J. Larkoski, S. Marzani, G. Soyez and J. Thaler, *Soft drop*, JHEP **05** (2014) 146, arXiv: 1402.2657 [hep-ph].

[11] M. Dasgupta, A. Fregoso, S. Marzani and G. P. Salam, *Towards an understanding of jet substructure*, JHEP **09** (2013) 029, arXiv: 1307.0007 [hep-ph].

[12] M. Dasgupta and G. P. Salam, *Resummation of non-global QCD observables*, Phys. Lett. B **512** (2001) 323, arXiv: hep-ph/0104277 [hep-ph].

[13] ATLAS Collaboration, *Measurement of the Soft-Drop Jet Mass in pp Collisions at $\sqrt{s}$ = 13 TeV with the ATLAS detector*, Phys. Rev. Lett. **121** (2018) 092001, arXiv: 1711.08341 [hep-ex].

[14] CMS Collaboration, *Measurements of the differential jet cross section as a function of the jet mass in dijet events from proton-proton collisions at $\sqrt{s}$ = 13 TeV*, JHEP **11** (2018) 113, arXiv: 1807.05974 [hep-ex].

[15] A. H. Hoang, S. Mantry, A. Pathak and I. W. Stewart, *Nonperturbative Corrections to Soft Drop Jet Mass*, JHEP **12** (2019) 002, arXiv: 1906.11843 [hep-ph].

[16] D. Krohn, M. D. Schwartz, T. Lin and W. J. Waalewijn, *Jet Charge at the LHC*, Phys. Rev. Lett. **110** (2013) 212001, arXiv: 1209.2421 [hep-ph].

[17] W. J. Waalewijn, *Calculating the charge of a jet*, Phys. Rev. D **86** (2012) 094030, arXiv: 1209.3019 [hep-ph].

[18] H.-M. Chang, M. Procura, J. Thaler and W. J. Waalewijn, *Calculating Track-Based Observables for the LHC*, Phys. Rev. Lett. **111** (2013) 102002, arXiv: 1303.6637 [hep-ph].

[19] B. T. Elder, M. Procura, J. Thaler, W. J. Waalewijn and K. Zhou, *Generalized fragmentation functions for fractal jet observables*, JHEP **06** (2017) 085, arXiv: 1704.05456 [hep-ph].

[20] CMS Collaboration, *Measurement of jet substructure observables in $t\bar{t}$ events from proton–proton collisions at $\sqrt{s}$ = 13 TeV*, Phys. Rev. D **98** (2018) 092014, arXiv: `1808.07340 [hep-ex]`.

[21] ATLAS Collaboration, *Measurement of jet-substructure observables in top quark, W boson and light jet production in proton–proton collisions at $\sqrt{s}$ = 13 TeV with the ATLAS detector*, JHEP **08** (2019) 033, arXiv: `1903.02942 [hep-ex]`.

[22] ALICE Collaboration, *Exploration of jet substructure using iterative declustering in pp and Pb-Pb collisions at LHC energies*, (2019), arXiv: `1905.02512 [nucl-ex]`.

[23] STAR Collaboration, *Measurements of the jet internal sub-structure and its relevance to parton shower evolution in p+p and Au+Au collisions at STAR*, PoS **345** (2019) 90, arXiv: `1903.12115 [hep-ex]`.

[24] CMS Collaboration, *Measurement of the groomed jet mass in PbPb and pp collisions at $\sqrt{s_{\mathrm{NN}}}$ = 5.02 TeV*, JHEP **10** (2018) 161, arXiv: `1805.05145 [hep-ex]`.

[25] CMS Collaboration, *Measurement of the Splitting Function in pp and Pb-Pb Collisions at $\sqrt{s_{\mathrm{NN}}}$ = 5.02 TeV*, Phys. Rev. Lett. **120** (2018) 142302, arXiv: `1708.09429 [nucl-ex]`.

[26] A. Larkoski, S. Marzani, J. Thaler, A. Tripathee and W. Xue, *Exposing the QCD Splitting Function with CMS Open Data*, Phys. Rev. Lett. **119** (2017) 132003, arXiv: `1704.05066 [hep-ph]`.

[27] A. Tripathee, W. Xue, A. Larkoski, S. Marzani and J. Thaler, *Jet substructure studies with CMS open data*, Phys. Rev. D **96** (2017) 074003, arXiv: `1704.05842 [hep-ph]`.

[28] Y. L. Dokshitzer, G. D. Leder, S. Moretti and B. R. Webber, *Better jet clustering algorithms*, JHEP **08** (1997) 001, arXiv: `hep-ph/9707323`.

[29] M. Wobisch and T. Wengler, *Hadronization Corrections to Jet Cross-Sections in Deep-Inelastic Scattering*, Monte Carlo generators for HERA physics (1999) 270, arXiv: `hep-ph/9907280 [hep-ph]`.

[30] ATLAS Collaboration, *The ATLAS Experiment at the CERN Large Hadron Collider*, JINST **3** (2008) S08003.

[31] ATLAS Collaboration, *ATLAS Insertable B-Layer Technical Design Report*, ATLAS-TDR-19, 2010, URL: `https://cds.cern.ch/record/1291633`, Addendum: ATLAS-TDR-19-ADD-1, 2012, URL: `https://cds.cern.ch/record/1451888`.

[32] B. Abbott et al., *Production and integration of the ATLAS Insertable B-Layer*, JINST **13** (2018) T05008, arXiv: `1803.00844 [physics.ins-det]`.

[33] ATLAS Collaboration, *Performance of the ATLAS trigger system in 2015*, Eur. Phys. J. C **77** (2017) 317, arXiv: `1611.09661 [hep-ex]`.

[34] ATLAS Collaboration, *Luminosity determination in pp collisions at $\sqrt{s}$ = 13 TeV using the ATLAS detector at the LHC*, ATLAS-CONF-2019-021 (2019), URL: `https://cds.cern.ch/record/2677054`.

[35] G. Avoni et al., *The new LUCID-2 detector for luminosity measurement and monitoring in ATLAS*, Journal of Instrumentation **13** (2018) P07017.

[36] ATLAS Collaboration, *ATLAS data quality operations and performance for 2015-2018 data-taking*, (2019), arXiv: `1911.04632 [physics.ins-det]`.

[37] T. Sjöstrand, S. Mrenna and P. Z. Skands, *PYTHIA 6.4 Physics and Manual*, JHEP **05** (2006) 026, arXiv: `hep-ph/0603175`.

[38] T. Sjöstrand, S. Mrenna and P. Z. Skands, *A brief introduction to PYTHIA 8.1*, Comput. Phys. Commun. **178** (2008) 852, arXiv: 0710.3820 [hep-ph].

[39] R. D. Ball et al., *Parton distributions with LHC data*, Nucl. Phys. B **867** (2013) 244, arXiv: 1207.1303 [hep-ph].

[40] ATLAS Collaboration, *ATLAS Pythia 8 tunes to 7 TeV data*, ATL-PHYS-PUB-2014-021, 2014, URL: https://cds.cern.ch/record/1966419.

[41] T. Gleisberg et al., *Event generation with SHERPA 1.1*, JHEP **02** (2009) 007, arXiv: 0811.4622 [hep-ph].

[42] E. Bothmann et al., *Event Generation with Sherpa 2.2*, SciPost Phys. **7** (2019) 034, arXiv: 1905.09127 [hep-ph].

[43] S. Catani, F. Krauss, B. R. Webber and R. Kuhn, *QCD Matrix Elements + Parton Showers*, JHEP **11** (2001) 063, arXiv: hep-ph/0109231.

[44] H.-L. Lai et al., *New parton distributions for collider physics*, Phys. Rev. D **82** (2010) 074024, arXiv: 1007.2241 [hep-ph].

[45] M. Bähr et al., *Herwig++ physics and manual*, Eur. Phys. J. C **58** (2008) 639, arXiv: 0803.0883 [hep-ph].

[46] G. Corcella et al., *HERWIG 6: An event generator for hadron emission reactions with interfering gluons (including supersymmetric processes)*, JHEP **01** (2001) 010.

[47] J. Pumplin et al., *New Generation of Parton Distributions with Uncertainties from Global QCD Analysis*, JHEP **07** (2002) 012, arXiv: hep-ph/0201195.

[48] M. H. Seymour and A. Siodmok, *Constraining MPI models using σ_{eff} and recent Tevatron and LHC Underlying Event data*, JHEP **10** (2013) 113, arXiv: 1307.5015 [hep-ph].

[49] ATLAS Collaboration, *The ATLAS Simulation Infrastructure*, Eur. Phys. J. C **70** (2010) 823, arXiv: 1005.4568 [physics.ins-det].

[50] S. Agostinelli et al., *GEANT4 – a simulation toolkit*, Nucl. Instrum. Meth. A **506** (2003) 250.

[51] ATLAS Collaboration, *Summary of ATLAS Pythia 8 tunes*, ATL-PHYS-PUB-2012-003, 2012, URL: https://cds.cern.ch/record/1474107.

[52] A. D. Martin, W. J. Stirling, R. S. Thorne and G. Watt, *Parton distributions for the LHC*, Eur. Phys. J. C **63** (2009) 189, arXiv: 0901.0002 [hep-ph].

[53] ATLAS Collaboration, *Topological cell clustering in the ATLAS calorimeters and its performance in LHC Run 1*, Eur. Phys. J. C **77** (2017) 490, arXiv: 1603.02934 [hep-ex].

[54] M. Cacciari, G. P. Salam and G. Soyez, *FastJet user manual*, Eur. Phys. J. C **72** (2012) 1896, arXiv: 1111.6097 [hep-ph].

[55] M. Cacciari, G. P. Salam and G. Soyez, *The anti-k_t jet clustering algorithm*, JHEP **04** (2008) 063, arXiv: 0802.1189 [hep-ph].

[56] ATLAS Collaboration, *Jet energy scale measurements and their systematic uncertainties in proton–proton collisions at $\sqrt{s}$ = 13 TeV with the ATLAS detector*, Phys. Rev. D **96** (2017) 072002, arXiv: 1703.09665 [hep-ex].

[57] M. Cacciari, G. P. Salam and G. Soyez, *The catchment area of jets*, JHEP **04** (2008) 005, arXiv: 0802.1188 [hep-ph].

[58] G. D'Agostini, *A multidimensional unfolding method based on Bayes' theorem*, Nucl. Instrum. Meth. A **362** (1995) 487.

[59] T. Adye, *Unfolding algorithms and tests using RooUnfold*, (2011), arXiv: `1105.1160 [physics.data-an]`.

[60] B. Efron, *Bootstrap Methods: Another Look at the Jackknife*, Ann. Statist. **7** (1979) 1.

[61] B. Malaescu, *An iterative, dynamically stabilized method of data unfolding*, LAL-09-107 (2009), arXiv: `0907.3791 [physics.data-an]`.

[62] ATLAS Collaboration, *A measurement of the calorimeter response to single hadrons and determination of the jet energy scale uncertainty using LHC Run-1 pp-collision data with the ATLAS detector*, Eur. Phys. J. C **77** (2017) 26, arXiv: `1607.08842 [hep-ex]`.

[63] E. Abat et al., *Study of energy response and resolution of the ATLAS barrel calorimeter to hadrons of energies from 20 to 350 GeV*, Nucl. Instrum. Meth. A **621** (2010) 134.

[64] ATLAS Collaboration, *Study of the material of the ATLAS inner detector for Run 2 of the LHC*, JINST **12** (2017) P12009, arXiv: `1707.02826 [hep-ex]`.

[65] ATLAS Collaboration, *Performance of the ATLAS track reconstruction algorithms in dense environments in LHC Run 2*, Eur. Phys. J. C **77** (2017) 673, arXiv: `1704.07983 [hep-ex]`.

[66] ATLAS Collaboration, *Measurement of track reconstruction inefficiencies in the core of jets via pixel dE/dx with the ATLAS experiment using $\sqrt{s}$ = 13 TeV pp collision data*, ATL-PHYS-PUB-2016-007, 2016, URL: `https://cds.cern.ch/record/2140460`.

[67] ATLAS Collaboration, *Modelling of Track Reconstruction Inside Jets with the 2016 ATLAS $\sqrt{s}$ = 13 TeV pp Dataset*, ATL-PHYS-PUB-2017-016, 2017, URL: `https://cds.cern.ch/record/2275639`.

[68] ATLAS Collaboration, *Early Inner Detector Tracking Performance in the 2015 Data at $\sqrt{s}$ = 13 TeV*, ATL-PHYS-PUB-2015-051, 2015, URL: `https://cds.cern.ch/record/2110140`.

[69] C. W. Bauer, S. Fleming, D. Pirjol and I. W. Stewart, *An effective field theory for collinear and soft gluons: Heavy to light decays*, Phys. Rev. D **63** (2001) 114020, arXiv: `hep-ph/0011336 [hep-ph]`.

[70] C. W. Bauer, D. Pirjol and I. W. Stewart, *Soft collinear factorization in effective field theory*, Phys. Rev. D **65** (2002) 054022, arXiv: `hep-ph/0109045 [hep-ph]`.

[71] J. Alwall et al., *The automated computation of tree-level and next-to-leading order differential cross sections, and their matching to parton shower simulations*, JHEP **07** (2014) 079, arXiv: `1405.0301 [hep-ph]`.

[72] S. Dulat et al., *New parton distribution functions from a global analysis of quantum chromodynamics*, Phys. Rev. D **93** (2016) 033006, arXiv: `1506.07443 [hep-ph]`.

[73] S. Catani and M. H. Seymour, *A general algorithm for calculating jet cross sections in NLO QCD*, Nucl. Phys. B **485** (1997) 291, arXiv: `hep-ph/9605323 [hep-ph]`, Erratum: Nucl. Phys. B 510 (1998) 503.

[74] Z. Nagy, *Next-to-leading order calculation of three-jet observables in hadron-hadron collision*, Phys. Rev. D **68** (2003) 094002, arXiv: `hep-ph/0307268 [hep-ph]`.

[75] G. Corcella et al., *HERWIG 6.5 Release Note*, (2002), arXiv: `hep-ph/0210213 [hep-ph]`.

[76] ATLAS Collaboration, *New ATLAS event generator tunes to 2010 data*, ATL-PHYS-PUB-2011-008, 2011, URL: `https://cds.cern.ch/record/1345343`.

[77] P. Z. Skands, *Tuning Monte Carlo generators: The Perugia tunes*, Phys. Rev. D **82** (2010) 074018, arXiv: 1005.3457 [hep-ph].

[78] R. Field, 'Early LHC Underlying Event Data - Findings and Surprises', *Hadron collider physics. Proceedings, 22nd Conference, HCP 2010, Toronto, Canada, August 23-27, 2010*, 2010, arXiv: 1010.3558 [hep-ph].

[79] T. Sjöstrand et al., *An introduction to PYTHIA 8.2*, Comput. Phys. Commun. **191** (2015) 159, arXiv: 1410.3012 [hep-ph].

[80] R. Corke and T. Sjöstrand, *Interleaved parton showers and tuning prospects*, JHEP **03** (2011) 032, arXiv: 1011.1759 [hep-ph].

[81] P. Skands, S. Carrazza and J. Rojo, *Tuning PYTHIA 8.1: the Monash 2013 Tune*, Eur. Phys. J. C **74** (2014) 3024, arXiv: 1404.5630 [hep-ph].

[82] Z.-B. Kang, K. Lee, X. Liu, D. Neill and F. Ringer, *The soft drop groomed jet radius at NLL*, (2019), arXiv: 1908.01783 [hep-ph].

[83] ATLAS Collaboration, *Measurement of the charged-particle multiplicity inside jets from $\sqrt{s} = 8\,TeV$ pp collisions with the ATLAS detector*, Eur. Phys. J. C **76** (2016) 322, arXiv: 1602.00988 [hep-ex].

[84] S. Bright-Thonney and B. Nachman, *Investigating the topology dependence of quark and gluon jets*, JHEP **03** (2019) 098, arXiv: 1810.05653 [hep-ph].

[85] ATLAS Collaboration, *ATLAS Computing Acknowledgements*, ATL-GEN-PUB-2016-002, URL: https://cds.cern.ch/record/2202407.

The ATLAS Collaboration

G. Aad[102], B. Abbott[129], D.C. Abbott[103], A. Abed Abud[36], K. Abeling[53], D.K. Abhayasinghe[94], S.H. Abidi[167], O.S. AbouZeid[40], N.L. Abraham[156], H. Abramowicz[161], H. Abreu[160], Y. Abulaiti[6], B.S. Acharya[67a,67b,n], B. Achkar[53], S. Adachi[163], L. Adam[100], C. Adam Bourdarios[5], L. Adamczyk[84a], L. Adamek[167], J. Adelman[121], M. Adersberger[114], A. Adiguzel[12c], S. Adorni[54], T. Adye[144], A.A. Affolder[146], Y. Afik[160], C. Agapopoulou[65], M.N. Agaras[38], A. Aggarwal[119], C. Agheorghiesei[27c], J.A. Aguilar-Saavedra[140f,140a,ag], F. Ahmadov[80], W.S. Ahmed[104], X. Ai[18], G. Aielli[74a,74b], S. Akatsuka[86], T.P.A. Åkesson[97], E. Akilli[54], A.V. Akimov[111], K. Al Khoury[65], G.L. Alberghi[23b,23a], J. Albert[176], M.J. Alconada Verzini[161], S. Alderweireldt[36], M. Aleksa[36], I.N. Aleksandrov[80], C. Alexa[27b], T. Alexopoulos[10], A. Alfonsi[120], F. Alfonsi[23b,23a], M. Alhroob[129], B. Ali[142], M. Aliev[166], G. Alimonti[69a], S.P. Alkire[148], C. Allaire[65], B.M.M. Allbrooke[156], B.W. Allen[132], P.P. Allport[21], A. Aloisio[70a,70b], F. Alonso[89], C. Alpigiani[148], A.A. Alshehri[57], M. Alvarez Estevez[99], M.G. Alviggi[70a,70b], Y. Amaral Coutinho[81b], A. Ambler[104], L. Ambroz[135], C. Amelung[26], D. Amidei[106], S.P. Amor Dos Santos[140a], S. Amoroso[46], C.S. Amrouche[54], F. An[79], C. Anastopoulos[149], N. Andari[145], T. Andeen[11], C.F. Anders[61b], J.K. Anders[20], A. Andreazza[69a,69b], V. Andrei[61a], C.R. Anelli[176], S. Angelidakis[38], A. Angerami[39], A.V. Anisenkov[122b,122a], A. Annovi[72a], C. Antel[54], M.T. Anthony[149], E. Antipov[130], M. Antonelli[51], D.J.A. Antrim[171], F. Anulli[73a], M. Aoki[82], J.A. Aparisi Pozo[174], L. Aperio Bella[15a], J.P. Araque[140a], V. Araujo Ferraz[81b], R. Araujo Pereira[81b], C. Arcangeletti[51], A.T.H. Arce[49], F.A. Arduh[89], J-F. Arguin[110], S. Argyropoulos[78], J.-H. Arling[46], A.J. Armbruster[36], A. Armstrong[171], O. Arnaez[167], H. Arnold[120], Z.P. Arrubarrena Tame[114], G. Artoni[135], S. Artz[100], S. Asai[163], T. Asawatavonvanich[165], N. Asbah[59], E.M. Asimakopoulou[172], L. Asquith[156], J. Assahsah[35d], K. Assamagan[29], R. Astalos[28a], R.J. Atkin[33a], M. Atkinson[173], N.B. Atlay[19], H. Atmani[65], K. Augsten[142], G. Avolio[36], R. Avramidou[60a], M.K. Ayoub[15a], A.M. Azoulay[168b], G. Azuelos[110,ar], H. Bachacou[145], K. Bachas[68a,68b], M. Backes[135], F. Backman[45a,45b], P. Bagnaia[73a,73b], M. Bahmani[85], H. Bahrasemani[152], A.J. Bailey[174], V.R. Bailey[173], J.T. Baines[144], C. Bakalis[10], O.K. Baker[183], P.J. Bakker[120], D. Bakshi Gupta[8], S. Balaji[157], E.M. Baldin[122b,122a], P. Balek[180], F. Balli[145], W.K. Balunas[135], J. Balz[100], E. Banas[85], A. Bandyopadhyay[24], Sw. Banerjee[181,i], A.A.E. Bannoura[182], L. Barak[161], W.M. Barbe[38], E.L. Barberio[105], D. Barberis[55b,55a], M. Barbero[102], G. Barbour[95], T. Barillari[115], M-S. Barisits[36], J. Barkeloo[132], T. Barklow[153], R. Barnea[160], S.L. Barnes[60c], B.M. Barnett[144], R.M. Barnett[18], Z. Barnovska-Blenessy[60a], A. Baroncelli[60a], G. Barone[29], A.J. Barr[135], L. Barranco Navarro[45a,45b], F. Barreiro[99], J. Barreiro Guimarães da Costa[15a], S. Barsov[138], R. Bartoldus[153], G. Bartolini[102], A.E. Barton[90], P. Bartos[28a], A. Basalaev[46], A. Basan[100], A. Bassalat[65,am], M.J. Basso[167], R.L. Bates[57], S. Batlamous[35e], J.R. Batley[32], B. Batool[151], M. Battaglia[146], M. Bauce[73a,73b], F. Bauer[145], K.T. Bauer[171], H.S. Bawa[31], J.B. Beacham[49], T. Beau[136], P.H. Beauchemin[170], F. Becherer[52], P. Bechtle[24], H.C. Beck[53], H.P. Beck[20,r], K. Becker[178], C. Becot[46], A. Beddall[12d], A.J. Beddall[12a], V.A. Bednyakov[80], M. Bedognetti[120], C.P. Bee[155], T.A. Beermann[182], M. Begalli[81b], M. Begel[29], A. Behera[155], J.K. Behr[46], F. Beisiegel[24], A.S. Bell[95], G. Bella[161], L. Bellagamba[23b], A. Bellerive[34], P. Bellos[9], K. Beloborodov[122b,122a], K. Belotskiy[112], N.L. Belyaev[112], D. Benchekroun[35a], N. Benekos[10], Y. Benhammou[161], D.P. Benjamin[6], M. Benoit[54], J.R. Bensinger[26], S. Bentvelsen[120], L. Beresford[135], M. Beretta[51], D. Berge[46], E. Bergeaas Kuutmann[172], N. Berger[5], B. Bergmann[142], L.J. Bergsten[26], J. Beringer[18], S. Berlendis[7], G. Bernardi[136], C. Bernius[153], F.U. Bernlochner[24], T. Berry[94], P. Berta[100], C. Bertella[15a], I.A. Bertram[90], O. Bessidskaia Bylund[182], N. Besson[145], A. Bethani[101], S. Bethke[115], A. Betti[42], A.J. Bevan[93], J. Beyer[115], D.S. Bhattacharya[177], P. Bhattarai[26], R. Bi[139], R.M. Bianchi[139], O. Biebel[114], D. Biedermann[19], R. Bielski[36], K. Bierwagen[100], N.V. Biesuz[72a,72b], M. Biglietti[75a], T.R.V. Billoud[110], M. Bindi[53], A. Bingul[12d], C. Bini[73a,73b], S. Biondi[23b,23a], M. Birman[180], T. Bisanz[53],

J.P. Biswal[161], D. Biswas[181,i], A. Bitadze[101], C. Bittrich[48], K. Bjørke[134], T. Blazek[28a], I. Bloch[46],
C. Blocker[26], A. Blue[57], U. Blumenschein[93], G.J. Bobbink[120], V.S. Bobrovnikov[122b,122a], S.S. Bocchetta[97],
A. Bocci[49], D. Boerner[46], D. Bogavac[14], A.G. Bogdanchikov[122b,122a], C. Bohm[45a], V. Boisvert[94],
P. Bokan[53,172], T. Bold[84a], A.S. Boldyrev[113], A.E. Bolz[61b], M. Bomben[136], M. Bona[93], J.S. Bonilla[132],
M. Boonekamp[145], C.D. Booth[94], H.M. Borecka-Bielska[91], A. Borisov[123], G. Borissov[90], J. Bortfeldt[36],
D. Bortoletto[135], D. Boscherini[23b], M. Bosman[14], J.D. Bossio Sola[104], K. Bouaouda[35a], J. Boudreau[139],
E.V. Bouhova-Thacker[90], D. Boumediene[38], S.K. Boutle[57], A. Boveia[127], J. Boyd[36], D. Boye[33b,an],
I.R. Boyko[80], A.J. Bozson[94], J. Bracinik[21], N. Brahimi[102], G. Brandt[182], O. Brandt[32], F. Braren[46],
B. Brau[103], J.E. Brau[132], W.D. Breaden Madden[57], K. Brendlinger[46], L. Brenner[46], R. Brenner[172],
S. Bressler[180], B. Brickwedde[100], D.L. Briglin[21], D. Britton[57], D. Britzger[115], I. Brock[24], R. Brock[107],
G. Brooijmans[39], W.K. Brooks[147c], E. Brost[121], J.H Broughton[21], P.A. Bruckman de Renstrom[85],
D. Bruncko[28b], A. Bruni[23b], G. Bruni[23b], L.S. Bruni[120], S. Bruno[74a,74b], M. Bruschi[23b], N. Bruscino[73a,73b],
P. Bryant[37], L. Bryngemark[97], T. Buanes[17], Q. Buat[36], P. Buchholz[151], A.G. Buckley[57], I.A. Budagov[80],
M.K. Bugge[134], F. Bührer[52], O. Bulekov[112], T.J. Burch[121], S. Burdin[91], C.D. Burgard[120], A.M. Burger[130],
B. Burghgrave[8], J.T.P. Burr[46], C.D. Burton[11], J.C. Burzynski[103], V. Büscher[100], E. Buschmann[53],
P.J. Bussey[57], J.M. Butler[25], C.M. Buttar[57], J.M. Butterworth[95], P. Butti[36], W. Buttinger[36],
C.J. Buxo Vazquez[107], A. Buzatu[158], A.R. Buzykaev[122b,122a], G. Cabras[23b,23a], S. Cabrera Urbán[174],
D. Caforio[56], H. Cai[173], V.M.M. Cairo[153], O. Cakir[4a], N. Calace[36], P. Calafiura[18], A. Calandri[102],
G. Calderini[136], P. Calfayan[66], G. Callea[57], L.P. Caloba[81b], A. Caltabiano[74a,74b], S. Calvente Lopez[99],
D. Calvet[38], S. Calvet[38], T.P. Calvet[155], M. Calvetti[72a,72b], R. Camacho Toro[136], S. Camarda[36],
D. Camarero Munoz[99], P. Camarri[74a,74b], D. Cameron[134], R. Caminal Armadans[103], C. Camincher[36],
S. Campana[36], M. Campanelli[95], A. Camplani[40], A. Campoverde[151], V. Canale[70a,70b], A. Canesse[104],
M. Cano Bret[60c], J. Cantero[130], T. Cao[161], Y. Cao[173], M.D.M. Capeans Garrido[36], M. Capua[41b,41a],
R. Cardarelli[74a], F. Cardillo[149], G. Carducci[41b,41a], I. Carli[143], T. Carli[36], G. Carlino[70a], B.T. Carlson[139],
L. Carminati[69a,69b], R.M.D. Carney[153], S. Caron[119], E. Carquin[147c], S. Carrá[46], J.W.S. Carter[167],
M.P. Casado[14,e], A.F. Casha[167], D.W. Casper[171], R. Castelijn[120], F.L. Castillo[174], L. Castillo Garcia[14],
V. Castillo Gimenez[174], N.F. Castro[140a,140e], A. Catinaccio[36], J.R. Catmore[134], A. Cattai[36], V. Cavaliere[29],
E. Cavallaro[14], M. Cavalli-Sforza[14], V. Cavasinni[72a,72b], E. Celebi[12b], L. Cerda Alberich[174], K. Cerny[131],
A.S. Cerqueira[81a], A. Cerri[156], L. Cerrito[74a,74b], F. Cerutti[18], A. Cervelli[23b,23a], S.A. Cetin[12b], Z. Chadi[35a],
D. Chakraborty[121], J. Chan[181], W.S. Chan[120], W.Y. Chan[91], J.D. Chapman[32], B. Chargeishvili[159b],
D.G. Charlton[21], T.P. Charman[93], C.C. Chau[34], S. Che[127], S. Chekanov[6], S.V. Chekulaev[168a],
G.A. Chelkov[80,aq], M.A. Chelstowska[36], B. Chen[79], C. Chen[60a], C.H. Chen[79], H. Chen[29], J. Chen[60a],
J. Chen[39], J. Chen[26], S. Chen[137], S.J. Chen[15c], X. Chen[15b], Y-H. Chen[46], H.C. Cheng[63a], H.J. Cheng[15a],
A. Cheplakov[80], E. Cheremushkina[123], R. Cherkaoui El Moursli[35e], E. Cheu[7], K. Cheung[64],
T.J.A. Chevalérias[145], L. Chevalier[145], V. Chiarella[51], G. Chiarelli[72a], G. Chiodini[68a], A.S. Chisholm[21],
A. Chitan[27b], I. Chiu[163], Y.H. Chiu[176], M.V. Chizhov[80], K. Choi[11], A.R. Chomont[73a,73b], S. Chouridou[162],
Y.S. Chow[120], M.C. Chu[63a], X. Chu[15a,15d], J. Chudoba[141], A.J. Chuinard[104], J.J. Chwastowski[85],
L. Chytka[131], D. Cieri[115], K.M. Ciesla[85], D. Cinca[47], V. Cindro[92], I.A. Cioară[27b], A. Ciocio[18],
F. Cirotto[70a,70b], Z.H. Citron[180,j], M. Citterio[69a], D.A. Ciubotaru[27b], B.M. Ciungu[167], A. Clark[54],
M.R. Clark[39], P.J. Clark[50], C. Clement[45a,45b], Y. Coadou[102], M. Cobal[67a,67c], A. Coccaro[55b], J. Cochran[79],
H. Cohen[161], A.E.C. Coimbra[36], L. Colasurdo[119], B. Cole[39], A.P. Colijn[120], J. Collot[58],
P. Conde Muiño[140a,140h], S.H. Connell[33b], I.A. Connelly[57], S. Constantinescu[27b], F. Conventi[70a,as],
A.M. Cooper-Sarkar[135], F. Cormier[175], K.J.R. Cormier[167], L.D. Corpe[95], M. Corradi[73a,73b],
E.E. Corrigan[97], F. Corriveau[104,ae], A. Cortes-Gonzalez[36], M.J. Costa[174], F. Costanza[5], D. Costanzo[149],
G. Cowan[94], J.W. Cowley[32], J. Crane[101], K. Cranmer[125], S.J. Crawley[57], R.A. Creager[137],
S. Crépé-Renaudin[58], F. Crescioli[136], M. Cristinziani[24], V. Croft[170], G. Crosetti[41b,41a], A. Cueto[5],
T. Cuhadar Donszelmann[149], A.R. Cukierman[153], W.R. Cunningham[57], S. Czekierda[85], P. Czodrowski[36],

M.J. Da Cunha Sargedas De Sousa[60b], J.V. Da Fonseca Pinto[81b], C. Da Via[101], W. Dabrowski[84a],
F. Dachs[36], T. Dado[28a], S. Dahbi[33d], T. Dai[106], C. Dallapiccola[103], M. Dam[40], G. D'amen[29],
V. D'Amico[75a,75b], J. Damp[100], J.R. Dandoy[137], M.F. Daneri[30], N.P. Dang[181,i], N.S. Dann[101],
M. Danninger[175], V. Dao[36], G. Darbo[55b], O. Dartsi[5], A. Dattagupta[132], T. Daubney[46], S. D'Auria[69a,69b],
C. David[168b], T. Davidek[143], D.R. Davis[49], I. Dawson[149], K. De[8], R. De Asmundis[70a], M. De Beurs[120],
S. De Castro[23b,23a], S. De Cecco[73a,73b], N. De Groot[119], P. de Jong[120], H. De la Torre[107], A. De Maria[15c],
D. De Pedis[73a], A. De Salvo[73a], U. De Sanctis[74a,74b], M. De Santis[74a,74b], A. De Santo[156],
K. De Vasconcelos Corga[102], J.B. De Vivie De Regie[65], C. Debenedetti[146], D.V. Dedovich[80],
A.M. Deiana[42], J. Del Peso[99], Y. Delabat Diaz[46], D. Delgove[65], F. Deliot[145,q], C.M. Delitzsch[7],
M. Della Pietra[70a,70b], D. Della Volpe[54], A. Dell'Acqua[36], L. Dell'Asta[74a,74b], M. Delmastro[5],
C. Delporte[65], P.A. Delsart[58], D.A. DeMarco[167], S. Demers[183], M. Demichev[80], G. Demontigny[110],
S.P. Denisov[123], L. D'Eramo[136], D. Derendarz[85], J.E. Derkaoui[35d], F. Derue[136], P. Dervan[91], K. Desch[24],
C. Deterre[46], K. Dette[167], C. Deutsch[24], M.R. Devesa[30], P.O. Deviveiros[36], A. Dewhurst[144],
F.A. Di Bello[54], A. Di Ciaccio[74a,74b], L. Di Ciaccio[5], W.K. Di Clemente[137], C. Di Donato[70a,70b],
A. Di Girolamo[36], G. Di Gregorio[72a,72b], B. Di Micco[75a,75b], R. Di Nardo[75a,75b], K.F. Di Petrillo[59],
R. Di Sipio[167], D. Di Valentino[34], C. Diaconu[102], F.A. Dias[40], T. Dias Do Vale[140a], M.A. Diaz[147a],
J. Dickinson[18], E.B. Diehl[106], J. Dietrich[19], S. Díez Cornell[46], A. Dimitrievska[18], W. Ding[15b],
J. Dingfelder[24], F. Dittus[36], F. Djama[102], T. Djobava[159b], J.I. Djuvsland[17], M.A.B. Do Vale[81c],
M. Dobre[27b], D. Dodsworth[26], C. Doglioni[97], J. Dolejsi[143], Z. Dolezal[143], M. Donadelli[81d], B. Dong[60c],
J. Donini[38], A. D'onofrio[15c], M. D'Onofrio[91], J. Dopke[144], A. Doria[70a], M.T. Dova[89], A.T. Doyle[57],
E. Drechsler[152], E. Dreyer[152], T. Dreyer[53], A.S. Drobac[170], D. Du[60b], Y. Duan[60b], F. Dubinin[111],
M. Dubovsky[28a], A. Dubreuil[54], E. Duchovni[180], G. Duckeck[114], A. Ducourthial[136], O.A. Ducu[110],
D. Duda[115], A. Dudarev[36], A.C. Dudder[100], E.M. Duffield[18], L. Duflot[65], M. Dührssen[36], C. Dülsen[182],
M. Dumancic[180], A.E. Dumitriu[27b], A.K. Duncan[57], M. Dunford[61a], A. Duperrin[102], H. Duran Yildiz[4a],
M. Düren[56], A. Durglishvili[159b], D. Duschinger[48], B. Dutta[46], D. Duvnjak[1], G.I. Dyckes[137], M. Dyndal[36],
S. Dysch[101], B.S. Dziedzic[85], K.M. Ecker[115], R.C. Edgar[106], M.G. Eggleston[49], T. Eifert[8], G. Eigen[17],
K. Einsweiler[18], T. Ekelof[172], H. El Jarrari[35e], R. El Kosseifi[102], V. Ellajosyula[172], M. Ellert[172],
F. Ellinghaus[182], A.A. Elliot[93], N. Ellis[36], J. Elmsheuser[29], M. Elsing[36], D. Emeliyanov[144], A. Emerman[39],
Y. Enari[163], M.B. Epland[49], J. Erdmann[47], A. Ereditato[20], P.A. Erland[85], M. Errenst[36], M. Escalier[65],
C. Escobar[174], O. Estrada Pastor[174], E. Etzion[161], H. Evans[66], A. Ezhilov[138], F. Fabbri[57], L. Fabbri[23b,23a],
V. Fabiani[119], G. Facini[95], R.M. Faisca Rodrigues Pereira[140a], R.M. Fakhrutdinov[123], S. Falciano[73a],
P.J. Falke[5], S. Falke[5], J. Faltova[143], Y. Fang[15a], Y. Fang[15a], G. Fanourakis[44], M. Fanti[69a,69b],
M. Faraj[67a,67c,t], A. Farbin[8], A. Farilla[75a], E.M. Farina[71a,71b], T. Farooque[107], S. Farrell[18],
S.M. Farrington[50], P. Farthouat[36], F. Fassi[35e], P. Fassnacht[36], D. Fassouliotis[9], M. Faucci Giannelli[50],
W.J. Fawcett[32], L. Fayard[65], O.L. Fedin[138,o], W. Fedorko[175], A. Fehr[20], M. Feickert[173], L. Feligioni[102],
A. Fell[149], C. Feng[60b], M. Feng[49], M.J. Fenton[57], A.B. Fenyuk[123], S.W. Ferguson[43], J. Ferrando[46],
A. Ferrante[173], A. Ferrari[172], P. Ferrari[120], R. Ferrari[71a], D.E. Ferreira de Lima[61b], A. Ferrer[174],
D. Ferrere[54], C. Ferretti[106], F. Fiedler[100], A. Filipčič[92], F. Filthaut[119], K.D. Finelli[25],
M.C.N. Fiolhais[140a,140c,a], L. Fiorini[174], F. Fischer[114], W.C. Fisher[107], I. Fleck[151], P. Fleischmann[106],
R.R.M. Fletcher[137], T. Flick[182], B.M. Flierl[114], L. Flores[137], L.R. Flores Castillo[63a], F.M. Follega[76a,76b],
N. Fomin[17], J.H. Foo[167], G.T. Forcolin[76a,76b], A. Formica[145], F.A. Förster[14], A.C. Forti[101], A.G. Foster[21],
M.G. Foti[135], D. Fournier[65], H. Fox[90], P. Francavilla[72a,72b], S. Francescato[73a,73b], M. Franchini[23b,23a],
S. Franchino[61a], D. Francis[36], L. Franconi[20], M. Franklin[59], A.N. Fray[93], P.M. Freeman[21], B. Freund[110],
W.S. Freund[81b], E.M. Freundlich[47], D.C. Frizzell[129], D. Froidevaux[36], J.A. Frost[135], C. Fukunaga[164],
E. Fullana Torregrosa[174], E. Fumagalli[55b,55a], T. Fusayasu[116], J. Fuster[174], A. Gabrielli[23b,23a],
A. Gabrielli[18], S. Gadatsch[54], P. Gadow[115], G. Gagliardi[55b,55a], L.G. Gagnon[110], C. Galea[27b],
B. Galhardo[140a], G.E. Gallardo[135], E.J. Gallas[135], B.J. Gallop[144], G. Galster[40], R. Gamboa Goni[93],

K.K. Gan[127], S. Ganguly[180], J. Gao[60a], Y. Gao[50], Y.S. Gao[31,l], C. García[174], J.E. García Navarro[174], J.A. García Pascual[15a], C. Garcia-Argos[52], M. Garcia-Sciveres[18], R.W. Gardner[37], N. Garelli[153], S. Gargiulo[52], C.A. Garner[167], V. Garonne[134], S.J. Gasiorowski[148], P. Gaspar[81b], A. Gaudiello[55b,55a], G. Gaudio[71a], I.L. Gavrilenko[111], A. Gavrilyuk[124], C. Gay[175], G. Gaycken[46], E.N. Gazis[10], A.A. Geanta[27b], C.M. Gee[146], C.N.P. Gee[144], J. Geisen[53], M. Geisen[100], C. Gemme[55b], M.H. Genest[58], C. Geng[106], S. Gentile[73a,73b], S. George[94], T. Geralis[44], L.O. Gerlach[53], P. Gessinger-Befurt[100], G. Gessner[47], S. Ghasemi[151], M. Ghasemi Bostanabad[176], M. Ghneimat[151], A. Ghosh[65], A. Ghosh[78], B. Giacobbe[23b], S. Giagu[73a,73b], N. Giangiacomi[23b,23a], P. Giannetti[72a], A. Giannini[70a,70b], G. Giannini[14], S.M. Gibson[94], M. Gignac[146], D. Gillberg[34], G. Gilles[182], D.M. Gingrich[3,ar], M.P. Giordani[67a,67c], P.F. Giraud[145], G. Giugliarelli[67a,67c], D. Giugni[69a], F. Giuli[74a,74b], S. Gkaitatzis[162], I. Gkialas[9,g], E.L. Gkougkousis[14], P. Gkountoumis[10], L.K. Gladilin[113], C. Glasman[99], J. Glatzer[14], P.C.F. Glaysher[46], A. Glazov[46], G.R. Gledhill[132], M. Goblirsch-Kolb[26], D. Godin[110], S. Goldfarb[105], T. Golling[54], D. Golubkov[123], A. Gomes[140a,140b], R. Goncalves Gama[53], R. Gonçalo[140a], G. Gonella[52], L. Gonella[21], A. Gongadze[80], F. Gonnella[21], J.L. Gonski[39], S. González de la Hoz[174], S. Gonzalez-Sevilla[54], G.R. Gonzalvo Rodriguez[174], L. Goossens[36], N.A. Gorasia[21], P.A. Gorbounov[124], H.A. Gordon[29], B. Gorini[36], E. Gorini[68a,68b], A. Gorišek[92], A.T. Goshaw[49], M.I. Gostkin[80], C.A. Gottardo[119], M. Gouighri[35b], A.G. Goussiou[148], N. Govender[33b], C. Goy[5], E. Gozani[160], I. Grabowska-Bold[84a], E.C. Graham[91], J. Gramling[171], E. Gramstad[134], S. Grancagnolo[19], M. Grandi[156], V. Gratchev[138], P.M. Gravila[27f], F.G. Gravili[68a,68b], C. Gray[57], H.M. Gray[18], C. Grefe[24], K. Gregersen[97], I.M. Gregor[46], P. Grenier[153], K. Grevtsov[46], C. Grieco[14], N.A. Grieser[129], A.A. Grillo[146], K. Grimm[31,k], S. Grinstein[14,z], J.-F. Grivaz[65], S. Groh[100], E. Gross[180], J. Grosse-Knetter[53], Z.J. Grout[95], C. Grud[106], A. Grummer[118], L. Guan[106], W. Guan[181], C. Gubbels[175], J. Guenther[36], A. Guerguichon[65], J.G.R. Guerrero Rojas[174], F. Guescini[115], D. Guest[171], R. Gugel[52], T. Guillemin[5], S. Guindon[36], U. Gul[57], J. Guo[60c], W. Guo[106], Y. Guo[60a,s], Z. Guo[102], R. Gupta[46], S. Gurbuz[12c], G. Gustavino[129], M. Guth[52], P. Gutierrez[129], C. Gutschow[95], C. Guyot[145], C. Gwenlan[135], C.B. Gwilliam[91], A. Haas[125], C. Haber[18], H.K. Hadavand[8], A. Hadef[60a], S. Hageböck[36], M. Haleem[177], J. Haley[130], G. Halladjian[107], G.D. Hallewell[102], K. Hamacher[182], P. Hamal[131], K. Hamano[176], H. Hamdaoui[35e], M. Hamer[24], G.N. Hamity[50], K. Han[60a,y], L. Han[60a], S. Han[15a], Y.F. Han[167], K. Hanagaki[82,w], M. Hance[146], D.M. Handl[114], B. Haney[137], R. Hankache[136], E. Hansen[97], J.B. Hansen[40], J.D. Hansen[40], M.C. Hansen[24], P.H. Hansen[40], E.C. Hanson[101], K. Hara[169], T. Harenberg[182], S. Harkusha[108], P.F. Harrison[178], N.M. Hartmann[114], Y. Hasegawa[150], A. Hasib[50], S. Hassani[145], S. Haug[20], R. Hauser[107], L.B. Havener[39], M. Havranek[142], C.M. Hawkes[21], R.J. Hawkings[36], D. Hayden[107], C. Hayes[106], R.L. Hayes[175], C.P. Hays[135], J.M. Hays[93], H.S. Hayward[91], S.J. Haywood[144], F. He[60a], M.P. Heath[50], V. Hedberg[97], S. Heer[24], K.K. Heidegger[52], W.D. Heidorn[79], J. Heilman[34], S. Heim[46], T. Heim[18], B. Heinemann[46,ao], J.J. Heinrich[132], L. Heinrich[36], J. Hejbal[141], L. Helary[61b], A. Held[175], S. Hellesund[134], C.M. Helling[146], S. Hellman[45a,45b], C. Helsens[36], R.C.W. Henderson[90], Y. Heng[181], L. Henkelmann[61a], S. Henkelmann[175], A.M. Henriques Correia[36], H. Herde[26], V. Herget[177], Y. Hernández Jiménez[33d], H. Herr[100], M.G. Herrmann[114], T. Herrmann[48], G. Herten[52], R. Hertenberger[114], L. Hervas[36], T.C. Herwig[137], G.G. Hesketh[95], N.P. Hessey[168a], A. Higashida[163], S. Higashino[82], E. Higón-Rodriguez[174], K. Hildebrand[37], J.C. Hill[32], K.K. Hill[29], K.H. Hiller[46], S.J. Hillier[21], M. Hils[48], I. Hinchliffe[18], F. Hinterkeuser[24], M. Hirose[133], S. Hirose[52], D. Hirschbuehl[182], B. Hiti[92], O. Hladik[141], D.R. Hlaluku[33d], X. Hoad[50], J. Hobbs[155], N. Hod[180], M.C. Hodgkinson[149], A. Hoecker[36], D. Hohn[52], D. Hohov[65], T. Holm[24], T.R. Holmes[37], M. Holzbock[114], L.B.A.H. Hommels[32], S. Honda[169], T.M. Hong[139], J.C. Honig[52], A. Hönle[115], B.H. Hooberman[173], W.H. Hopkins[6], Y. Horii[117], P. Horn[48], L.A. Horyn[37], S. Hou[158], A. Hoummada[35a], J. Howarth[101], J. Hoya[89], M. Hrabovsky[131], J. Hrdinka[77], I. Hristova[19], J. Hrivnac[65], A. Hrynevich[109], T. Hryn'ova[5], P.J. Hsu[64], S.-C. Hsu[148], Q. Hu[29], S. Hu[60c], Y.F. Hu[15a,15d], D.P. Huang[95], Y. Huang[60a], Y. Huang[15a], Z. Hubacek[142], F. Hubaut[102], M. Huebner[24], F. Huegging[24], T.B. Huffman[135], M. Huhtinen[36],

R.F.H. Hunter[34], P. Huo[155], N. Huseynov[80,af], J. Huston[107], J. Huth[59], R. Hyneman[106], S. Hyrych[28a],
G. Iacobucci[54], G. Iakovidis[29], I. Ibragimov[151], L. Iconomidou-Fayard[65], P. Iengo[36], R. Ignazzi[40],
O. Igonkina[120,ab,*], R. Iguchi[163], T. Iizawa[54], Y. Ikegami[82], M. Ikeno[82], D. Iliadis[162], N. Ilic[119,167,ae],
F. Iltzsche[48], G. Introzzi[71a,71b], M. Iodice[75a], K. Iordanidou[168a], V. Ippolito[73a,73b], M.F. Isacson[172],
M. Ishino[163], W. Islam[130], C. Issever[19,46], S. Istin[160], F. Ito[169], J.M. Iturbe Ponce[63a], R. Iuppa[76a,76b],
A. Ivina[180], H. Iwasaki[82], J.M. Izen[43], V. Izzo[70a], P. Jacka[141], P. Jackson[1], R.M. Jacobs[24], B.P. Jaeger[152],
V. Jain[2], G. Jäkel[182], K.B. Jakobi[100], K. Jakobs[52], T. Jakoubek[141], J. Jamieson[57], K.W. Janas[84a],
R. Jansky[54], J. Janssen[24], M. Janus[53], P.A. Janus[84a], G. Jarlskog[97], N. Javadov[80,af], T. Javůrek[36],
M. Javurkova[103], F. Jeanneau[145], L. Jeanty[132], J. Jejelava[159a], A. Jelinskas[178], P. Jenni[52,b], N. Jeong[46],
S. Jézéquel[5], H. Ji[181], J. Jia[155], H. Jiang[79], Y. Jiang[60a], Z. Jiang[153,p], S. Jiggins[52], F.A. Jimenez Morales[38],
J. Jimenez Pena[115], S. Jin[15c], A. Jinaru[27b], O. Jinnouchi[165], H. Jivan[33d], P. Johansson[149], K.A. Johns[7],
C.A. Johnson[66], R.W.L. Jones[90], S.D. Jones[156], S. Jones[7], T.J. Jones[91], J. Jongmanns[61a], P.M. Jorge[140a],
J. Jovicevic[36], X. Ju[18], J.J. Junggeburth[115], A. Juste Rozas[14,z], A. Kaczmarska[85], M. Kado[73a,73b],
H. Kagan[127], M. Kagan[153], A. Kahn[39], C. Kahra[100], T. Kaji[179], E. Kajomovitz[160], C.W. Kalderon[97],
A. Kaluza[100], A. Kamenshchikov[123], M. Kaneda[163], N.J. Kang[146], S. Kang[79], L. Kanjir[92], Y. Kano[117],
V.A. Kantserov[112], J. Kanzaki[82], L.S. Kaplan[181], D. Kar[33d], K. Karava[135], M.J. Kareem[168b],
S.N. Karpov[80], Z.M. Karpova[80], V. Kartvelishvili[90], A.N. Karyukhin[123], L. Kashif[181], R.D. Kass[127],
A. Kastanas[45a,45b], C. Kato[60d,60c], J. Katzy[46], K. Kawade[150], K. Kawagoe[88], T. Kawaguchi[117],
T. Kawamoto[145], G. Kawamura[53], E.F. Kay[176], V.F. Kazanin[122b,122a], R. Keeler[176], R. Kehoe[42],
J.S. Keller[34], E. Kellermann[97], D. Kelsey[156], J.J. Kempster[21], J. Kendrick[21], K.E. Kennedy[39], O. Kepka[141],
S. Kersten[182], B.P. Kerševan[92], S. Ketabchi Haghighat[167], M. Khader[173], F. Khalil-Zada[13],
M. Khandoga[145], A. Khanov[130], A.G. Kharlamov[122b,122a], T. Kharlamova[122b,122a], E.E. Khoda[175],
A. Khodinov[166], T.J. Khoo[54], E. Khramov[80], J. Khubua[159b], S. Kido[83], M. Kiehn[54], C.R. Kilby[94],
E. Kim[165], Y.K. Kim[37], N. Kimura[95], O.M. Kind[19], B.T. King[91,*], M. Kirchmeier[48], J. Kirk[144],
A.E. Kiryunin[115], T. Kishimoto[163], D.P. Kisliuk[167], V. Kitali[46], O. Kivernyk[5], T. Klapdor-Kleingrothaus[52],
M. Klassen[61a], C. Klein[32], M.H. Klein[106], M. Klein[91], U. Klein[91], K. Kleinknecht[100], P. Klimek[121],
A. Klimentov[29], T. Klingl[24], T. Klioutchnikova[36], F.F. Klitzner[114], P. Kluit[120], S. Kluth[115], E. Kneringer[77],
E.B.F.G. Knoops[102], A. Knue[52], D. Kobayashi[88], T. Kobayashi[163], M. Kobel[48], M. Kocian[153],
T. Kodama[163], P. Kodys[143], P.T. Koenig[24], T. Koffas[34], N.M. Köhler[36], T. Koi[153], M. Kolb[145], I. Koletsou[5],
T. Komarek[131], T. Kondo[82], K. Köneke[52], A.X.Y. Kong[1], A.C. König[119], T. Kono[126], R. Konoplich[125,aj],
V. Konstantinides[95], N. Konstantinidis[95], B. Konya[97], R. Kopeliansky[66], S. Koperny[84a], K. Korcyl[85],
K. Kordas[162], G. Koren[161], A. Korn[95], I. Korolkov[14], E.V. Korolkova[149], N. Korotkova[113], O. Kortner[115],
S. Kortner[115], T. Kosek[143], V.V. Kostyukhin[149,166], A. Kotsokechagia[65], A. Kotwal[49], A. Koulouris[10],
A. Kourkoumeli-Charalampidi[71a,71b], C. Kourkoumelis[9], E. Kourlitis[149], V. Kouskoura[29],
A.B. Kowalewska[85], R. Kowalewski[176], W. Kozanecki[145], A.S. Kozhin[123], V.A. Kramarenko[113],
G. Kramberger[92], D. Krasnopevtsev[60a], M.W. Krasny[136], A. Krasznahorkay[36], D. Krauss[115],
J.A. Kremer[84a], J. Kretzschmar[91], P. Krieger[167], F. Krieter[114], A. Krishnan[61b], K. Krizka[18],
K. Kroeninger[47], H. Kroha[115], J. Kroll[141], J. Kroll[137], K.S. Krowpman[107], J. Krstic[16], U. Kruchonak[80],
H. Krüger[24], N. Krumnack[79], M.C. Kruse[49], J.A. Krzysiak[85], T. Kubota[105], O. Kuchinskaia[166],
S. Kuday[4b], J.T. Kuechler[46], S. Kuehn[36], A. Kugel[61a], T. Kuhl[46], V. Kukhtin[80], R. Kukla[102],
Y. Kulchitsky[108,ah], S. Kuleshov[147c], Y.P. Kulinich[173], M. Kuna[58], T. Kunigo[86], A. Kupco[141], T. Kupfer[47],
O. Kuprash[52], H. Kurashige[83], L.L. Kurchaninov[168a], Y.A. Kurochkin[108], A. Kurova[112], M.G. Kurth[15a,15d],
E.S. Kuwertz[36], M. Kuze[165], A.K. Kvam[148], J. Kvita[131], T. Kwan[104], A. La Rosa[115], L. La Rotonda[41b,41a],
F. La Ruffa[41b,41a], C. Lacasta[174], F. Lacava[73a,73b], D.P.J. Lack[101], H. Lacker[19], D. Lacour[136], E. Ladygin[80],
R. Lafaye[5], B. Laforge[136], T. Lagouri[33d], I.K. Lakomiec[84a], S. Lammers[66], W. Lampl[7],
C. Lampoudis[162], E. Lançon[29], U. Landgraf[52], M.P.J. Landon[93], M.C. Lanfermann[54], V.S. Lang[46],
J.C. Lange[53], R.J. Langenberg[103], A.J. Lankford[171], F. Lanni[29], K. Lantzsch[24], A. Lanza[71a],

A. Lapertosa[55b,55a], S. Laplace[136], J.F. Laporte[145], T. Lari[69a], F. Lasagni Manghi[23b,23a], M. Lassnig[36],
T.S. Lau[63a], A. Laudrain[65], A. Laurier[34], M. Lavorgna[70a,70b], S.D. Lawlor[94], M. Lazzaroni[69a,69b], B. Le[105],
E. Le Guirriec[102], M. LeBlanc[7], T. LeCompte[6], F. Ledroit-Guillon[58], A.C.A. Lee[95], C.A. Lee[29],
G.R. Lee[17], L. Lee[59], S.C. Lee[158], S.J. Lee[34], S. Lee[79], B. Lefebvre[168a], H.P. Lefebvre[94], M. Lefebvre[176],
C. Leggett[18], K. Lehmann[152], N. Lehmann[182], G. Lehmann Miotto[36], W.A. Leight[46], A. Leisos[162,x],
M.A.L. Leite[81d], C.E. Leitgeb[114], R. Leitner[143], D. Lellouch[180,*], K.J.C. Leney[42], T. Lenz[24], R. Leone[7],
S. Leone[72a], C. Leonidopoulos[50], A. Leopold[136], C. Leroy[110], R. Les[167], C.G. Lester[32], M. Levchenko[138],
J. Levêque[5], D. Levin[106], L.J. Levinson[180], D.J. Lewis[21], B. Li[15b], B. Li[106], C-Q. Li[60a], F. Li[60c], H. Li[60a],
H. Li[60b], J. Li[60c], K. Li[148], L. Li[60c], M. Li[15a,15d], Q. Li[15a,15d], Q.Y. Li[60a], S. Li[60d,60c], X. Li[46], Y. Li[46],
Z. Li[60b], Z. Liang[15a], B. Liberti[74a], A. Liblong[167], K. Lie[63c], S. Lim[29], C.Y. Lin[32], K. Lin[107], T.H. Lin[100],
R.A. Linck[66], J.H. Lindon[21], A.L. Lionti[54], E. Lipeles[137], A. Lipniacka[17], T.M. Liss[173,ap], A. Lister[175],
J.D. Little[8], B. Liu[79], B.L. Liu[6], H.B. Liu[29], H. Liu[106], J.B. Liu[60a], J.K.K. Liu[37], K. Liu[136], M. Liu[60a],
P. Liu[18], Y. Liu[15a,15d], Y.L. Liu[106], Y.W. Liu[60a], M. Livan[71a,71b], A. Lleres[58], J. Llorente Merino[152],
S.L. Lloyd[93], C.Y. Lo[63b], F. Lo Sterzo[42], E.M. Lobodzinska[46], P. Loch[7], S. Loffredo[74a,74b], T. Lohse[19],
K. Lohwasser[149], M. Lokajicek[141], J.D. Long[173], R.E. Long[90], L. Longo[36], K.A. Looper[127],
J.A. Lopez[147c], I. Lopez Paz[101], A. Lopez Solis[149], J. Lorenz[114], N. Lorenzo Martinez[5], A.M. Lory[114],
M. Losada[22], P.J. Lösel[114], A. Lösle[52], X. Lou[46], X. Lou[15a], A. Lounis[65], J. Love[6], P.A. Love[90],
J.J. Lozano Bahilo[174], M. Lu[60a], Y.J. Lu[64], H.J. Lubatti[148], C. Luci[73a,73b], A. Lucotte[58], C. Luedtke[52],
F. Luehring[66], I. Luise[136], L. Luminari[73a], B. Lund-Jensen[154], M.S. Lutz[103], D. Lynn[29], H. Lyons[91],
R. Lysak[141], E. Lytken[97], F. Lyu[15a], V. Lyubushkin[80], T. Lyubushkina[80], H. Ma[29], L.L. Ma[60b], Y. Ma[60b],
G. Maccarrone[51], A. Macchiolo[115], C.M. Macdonald[149], J. Machado Miguens[137], D. Madaffari[174],
R. Madar[38], W.F. Mader[48], M. Madugoda Ralalage Don[130], N. Madysa[48], J. Maeda[83], T. Maeno[29],
M. Maerker[48], A.S. Maevskiy[113], V. Magerl[52], N. Magini[79], D.J. Mahon[39], C. Maidantchik[81b], T. Maier[114],
A. Maio[140a,140b,140d], K. Maj[84a], O. Majersky[28a], S. Majewski[132], Y. Makida[82], N. Makovec[65],
B. Malaescu[136], Pa. Malecki[85], V.P. Maleev[138], F. Malek[58], U. Mallik[78], D. Malon[6], C. Malone[32],
S. Maltezos[10], S. Malyukov[80], J. Mamuzic[174], G. Mancini[51], I. Mandić[92], L. Manhaes de Andrade Filho[81a],
I.M. Maniatis[162], J. Manjarres Ramos[48], K.H. Mankinen[97], A. Mann[114], A. Manousos[77], B. Mansoulie[145],
I. Manthos[162], S. Manzoni[120], A. Marantis[162], G. Marceca[30], L. Marchese[135], G. Marchiori[136],
M. Marcisovsky[141], L. Marcoccia[74a,74b], C. Marcon[97], C.A. Marin Tobon[36], M. Marjanovic[129],
Z. Marshall[18], M.U.F. Martensson[172], S. Marti-Garcia[174], C.B. Martin[127], T.A. Martin[178], V.J. Martin[50],
B. Martin dit Latour[17], L. Martinelli[75a,75b], M. Martinez[14,z], V.I. Martinez Outschoorn[103],
S. Martin-Haugh[144], V.S. Martoiu[27b], A.C. Martyniuk[95], A. Marzin[36], S.R. Maschek[115], L. Masetti[100],
T. Mashimo[163], R. Mashinistov[111], J. Masik[101], A.L. Maslennikov[122b,122a], L. Massa[74a,74b],
P. Massarotti[70a,70b], P. Mastrandrea[72a,72b], A. Mastroberardino[41b,41a], T. Masubuchi[163], D. Matakias[10],
A. Matic[114], N. Matsuzawa[163], P. Mättig[24], J. Maurer[27b], B. Maček[92], D.A. Maximov[122b,122a],
R. Mazini[158], I. Maznas[162], S.M. Mazza[146], S.P. Mc Kee[106], T.G. McCarthy[115], W.P. McCormack[18],
E.F. McDonald[105], J.A. Mcfayden[36], G. Mchedlidze[159b], M.A. McKay[42], K.D. McLean[176],
S.J. McMahon[144], P.C. McNamara[105], C.J. McNicol[178], R.A. McPherson[176,ae], J.E. Mdhluli[33d],
Z.A. Meadows[103], S. Meehan[36], T. Megy[52], S. Mehlhase[114], A. Mehta[91], T. Meideck[58], B. Meirose[43],
D. Melini[160], B.R. Mellado Garcia[33d], J.D. Mellenthin[53], M. Melo[28a], F. Meloni[46], A. Melzer[24],
S.B. Menary[101], E.D. Mendes Gouveia[140a,140e], L. Meng[36], X.T. Meng[106], S. Menke[115], E. Meoni[41b,41a],
S. Mergelmeyer[19], S.A.M. Merkt[139], C. Merlassino[135], P. Mermod[54], L. Merola[70a,70b], C. Meroni[69a],
G. Merz[106], O. Meshkov[113,111], J.K.R. Meshreki[151], A. Messina[73a,73b], J. Metcalfe[6], A.S. Mete[6],
C. Meyer[66], J-P. Meyer[145], H. Meyer Zu Theenhausen[61a], F. Miano[156], M. Michetti[19], R.P. Middleton[144],
L. Mijović[50], G. Mikenberg[180], M. Mikestikova[141], M. Mikuž[92], H. Mildner[149], M. Milesi[105], A. Milic[167],
D.A. Millar[93], D.W. Miller[37], A. Milov[180], D.A. Milstead[45a,45b], R.A. Mina[153], A.A. Minaenko[123],
M. Miñano Moya[174], I.A. Minashvili[159b], A.I. Mincer[125], B. Mindur[84a], M. Mineev[80], Y. Minegishi[163],

42

L.M. Mir[14], A. Mirto[68a,68b], K.P. Mistry[137], T. Mitani[179], J. Mitrevski[114], V.A. Mitsou[174], M. Mittal[60c], O. Miu[167], A. Miucci[20], P.S. Miyagawa[149], A. Mizukami[82], J.U. Mjörnmark[97], T. Mkrtchyan[61a], M. Mlynarikova[143], T. Moa[45a,45b], K. Mochizuki[110], P. Mogg[52], S. Mohapatra[39], R. Moles-Valls[24], M.C. Mondragon[107], K. Mönig[46], J. Monk[40], E. Monnier[102], A. Montalbano[152], J. Montejo Berlingen[36], M. Montella[95], F. Monticelli[89], S. Monzani[69a], N. Morange[65], D. Moreno[22], M. Moreno Llácer[174], C. Moreno Martinez[14], P. Morettini[55b], M. Morgenstern[120], S. Morgenstern[48], D. Mori[152], M. Morii[59], M. Morinaga[179], V. Morisbak[134], A.K. Morley[36], G. Mornacchi[36], A.P. Morris[95], L. Morvaj[155], P. Moschovakos[36], B. Moser[120], M. Mosidze[159b], T. Moskalets[145], H.J. Moss[149], J. Moss[31,m], E.J.W. Moyse[103], S. Muanza[102], J. Mueller[139], R.S.P. Mueller[114], D. Muenstermann[90], G.A. Mullier[97], D.P. Mungo[69a,69b], J.L. Munoz Martinez[14], F.J. Munoz Sanchez[101], P. Murin[28b], W.J. Murray[178,144], A. Murrone[69a,69b], M. Muškinja[18], C. Mwewa[33a], A.G. Myagkov[123,ak], A.A. Myers[139], J. Myers[132], M. Myska[142], B.P. Nachman[18], O. Nackenhorst[47], A.Nag Nag[48], K. Nagai[135], K. Nagano[82], Y. Nagasaka[62], J.L. Nagle[29], E. Nagy[102], A.M. Nairz[36], Y. Nakahama[117], K. Nakamura[82], T. Nakamura[163], I. Nakano[128], H. Nanjo[133], F. Napolitano[61a], R.F. Naranjo Garcia[46], R. Narayan[42], I. Naryshkin[138], T. Naumann[46], G. Navarro[22], P.Y. Nechaeva[111], F. Nechansky[46], T.J. Neep[21], A. Negri[71a,71b], M. Negrini[23b], C. Nellist[53], M.E. Nelson[45a,45b], S. Nemecek[141], P. Nemethy[125], M. Nessi[36,d], M.S. Neubauer[173], F. Neuhaus[100], M. Neumann[182], R. Newhouse[175], P.R. Newman[21], C.W. Ng[139], Y.S. Ng[19], Y.W.Y. Ng[171], B. Ngair[35e], H.D.N. Nguyen[102], T. Nguyen Manh[110], E. Nibigira[38], R.B. Nickerson[135], R. Nicolaidou[145], D.S. Nielsen[40], J. Nielsen[146], N. Nikiforou[11], V. Nikolaenko[123,ak], I. Nikolic-Audit[136], K. Nikolopoulos[21], P. Nilsson[29], H.R. Nindhito[54], Y. Ninomiya[82], A. Nisati[73a], N. Nishu[60c], R. Nisius[115], I. Nitsche[47], T. Nitta[179], T. Nobe[163], Y. Noguchi[86], I. Nomidis[136], M.A. Nomura[29], M. Nordberg[36], N. Norjoharuddeen[135], T. Novak[92], O. Novgorodova[48], R. Novotny[142], L. Nozka[131], K. Ntekas[171], E. Nurse[95], F.G. Oakham[34,ar], H. Oberlack[115], J. Ocariz[136], A. Ochi[83], I. Ochoa[39], J.P. Ochoa-Ricoux[147a], K. O'Connor[26], S. Oda[88], S. Odaka[82], S. Oerdek[53], A. Ogrodnik[84a], A. Oh[101], S.H. Oh[49], C.C. Ohm[154], H. Oide[165], M.L. Ojeda[167], H. Okawa[169], Y. Okazaki[86], M.W. O'Keefe[91], Y. Okumura[163], T. Okuyama[82], A. Olariu[27b], L.F. Oleiro Seabra[140a], S.A. Olivares Pino[147a], D. Oliveira Damazio[29], J.L. Oliver[1], M.J.R. Olsson[171], A. Olszewski[85], J. Olszowska[85], D.C. O'Neil[152], A.P. O'neill[135], A. Onofre[140a,140e], P.U.E. Onyisi[11], H. Oppen[134], M.J. Oreglia[37], G.E. Orellana[89], D. Orestano[75a,75b], N. Orlando[14], R.S. Orr[167], V. O'Shea[57], R. Ospanov[60a], G. Otero y Garzon[30], H. Otono[88], P.S. Ott[61a], M. Ouchrif[35d], J. Ouellette[29], F. Ould-Saada[134], A. Ouraou[145], Q. Ouyang[15a], M. Owen[57], R.E. Owen[21], V.E. Ozcan[12c], N. Ozturk[8], J. Pacalt[131], H.A. Pacey[32], K. Pachal[49], A. Pacheco Pages[14], C. Padilla Aranda[14], S. Pagan Griso[18], M. Paganini[183], G. Palacino[66], S. Palazzo[50], S. Palestini[36], M. Palka[84b], D. Pallin[38], I. Panagoulias[10], C.E. Pandini[36], J.G. Panduro Vazquez[94], P. Pani[46], G. Panizzo[67a,67c], L. Paolozzi[54], C. Papadatos[110], K. Papageorgiou[9,g], S. Parajuli[42], A. Paramonov[6], D. Paredes Hernandez[63b], S.R. Paredes Saenz[135], B. Parida[166], T.H. Park[167], A.J. Parker[31], M.A. Parker[32], F. Parodi[55b,55a], E.W. Parrish[121], J.A. Parsons[39], U. Parzefall[52], L. Pascual Dominguez[136], V.R. Pascuzzi[167], J.M.P. Pasner[146], F. Pasquali[120], E. Pasqualucci[73a], S. Passaggio[55b], F. Pastore[94], P. Pasuwan[45a,45b], S. Pataraia[100], J.R. Pater[101], A. Pathak[181,i], J. Patton[91], T. Pauly[36], J. Pearkes[153], B. Pearson[115], M. Pedersen[134], L. Pedraza Diaz[119], R. Pedro[140a], T. Peiffer[53], S.V. Peleganchuk[122b,122a], O. Penc[141], H. Peng[60a], B.S. Peralva[81a], M.M. Perego[65], A.P. Pereira Peixoto[140a], D.V. Perepelitsa[29], F. Peri[19], L. Perini[69a,69b], H. Pernegger[36], S. Perrella[140a], A. Perrevoort[120], K. Peters[46], R.F.Y. Peters[101], B.A. Petersen[36], T.C. Petersen[40], E. Petit[102], A. Petridis[1], C. Petridou[162], P. Petroff[65], M. Petrov[135], F. Petrucci[75a,75b], M. Pettee[183], N.E. Pettersson[103], K. Petukhova[143], A. Peyaud[145], R. Pezoa[147c], L. Pezzotti[71a,71b], T. Pham[105], F.H. Phillips[107], P.W. Phillips[144], M.W. Phipps[173], G. Piacquadio[155], E. Pianori[18], A. Picazio[103], R.H. Pickles[101], R. Piegaia[30], D. Pietreanu[27b], J.E. Pilcher[37], A.D. Pilkington[101], M. Pinamonti[67a,67c], J.L. Pinfold[3], M. Pitt[161], L. Pizzimento[74a,74b], M.-A. Pleier[29], V. Pleskot[143], E. Plotnikova[80], P. Podberezko[122b,122a], R. Poettgen[97], R. Poggi[54], L. Poggioli[65],

I. Pogrebnyak[107], D. Pohl[24], I. Pokharel[53], G. Polesello[71a], A. Poley[18], A. Policicchio[73a,73b], R. Polifka[143], A. Polini[23b], C.S. Pollard[46], V. Polychronakos[29], D. Ponomarenko[112], L. Pontecorvo[36], S. Popa[27a], G.A. Popeneciu[27d], L. Portales[5], D.M. Portillo Quintero[58], S. Pospisil[142], K. Potamianos[46], I.N. Potrap[80], C.J. Potter[32], H. Potti[11], T. Poulsen[97], J. Poveda[36], T.D. Powell[149], G. Pownall[46], M.E. Pozo Astigarraga[36], P. Pralavorio[102], S. Prell[79], D. Price[101], M. Primavera[68a], S. Prince[104], M.L. Proffitt[148], N. Proklova[112], K. Prokofiev[63c], F. Prokoshin[80], S. Protopopescu[29], J. Proudfoot[6], M. Przybycien[84a], D. Pudzha[138], A. Puri[173], P. Puzo[65], J. Qian[106], Y. Qin[101], A. Quadt[53], M. Queitsch-Maitland[36], A. Qureshi[1], M. Racko[28a], F. Ragusa[69a,69b], G. Rahal[98], J.A. Raine[54], S. Rajagopalan[29], A. Ramirez Morales[93], K. Ran[15a,15d], T. Rashid[65], S. Raspopov[5], D.M. Rauch[46], F. Rauscher[114], S. Rave[100], B. Ravina[149], I. Ravinovich[180], J.H. Rawling[101], M. Raymond[36], A.L. Read[134], N.P. Readioff[58], M. Reale[68a,68b], D.M. Rebuzzi[71a,71b], A. Redelbach[177], G. Redlinger[29], K. Reeves[43], L. Rehnisch[19], J. Reichert[137], D. Reikher[161], A. Reiss[100], A. Rej[151], C. Rembser[36], A. Renardi[46], M. Renda[27b], M. Rescigno[73a], S. Resconi[69a], E.D. Resseguie[137], S. Rettie[175], B. Reynolds[127], E. Reynolds[21], O.L. Rezanova[122b,122a], P. Reznicek[143], E. Ricci[76a,76b], R. Richter[115], S. Richter[46], E. Richter-Was[84b], O. Ricken[24], M. Ridel[136], P. Rieck[115], O. Rifki[46], M. Rijssenbeek[155], A. Rimoldi[71a,71b], M. Rimoldi[46], L. Rinaldi[23b], G. Ripellino[154], I. Riu[14], J.C. Rivera Vergara[176], F. Rizatdinova[130], E. Rizvi[93], C. Rizzi[36], R.T. Roberts[101], S.H. Robertson[104,ae], M. Robin[46], D. Robinson[32], J.E.M. Robinson[46], C.M. Robles Gajardo[147c], M. Robles Manzano[100], A. Robson[57], A. Rocchi[74a,74b], E. Rocco[100], C. Roda[72a,72b], S. Rodriguez Bosca[174], A. Rodriguez Perez[14], D. Rodriguez Rodriguez[174], A.M. Rodríguez Vera[168b], S. Roe[36], O. Røhne[134], R. Röhrig[115], R.A. Rojas[147c], B. Roland[52], C.P.A. Roland[66], J. Roloff[29], A. Romaniouk[112], M. Romano[23b,23a], N. Rompotis[91], M. Ronzani[125], L. Roos[136], S. Rosati[73a], G. Rosin[103], B.J. Rosser[137], E. Rossi[46], E. Rossi[75a,75b], E. Rossi[70a,70b], L.P. Rossi[55b], L. Rossini[69a,69b], R. Rosten[14], M. Rotaru[27b], J. Rothberg[148], B. Rottler[52], D. Rousseau[65], G. Rovelli[71a,71b], A. Roy[11], D. Roy[33d], A. Rozanov[102], Y. Rozen[160], X. Ruan[33d], F. Rühr[52], A. Ruiz-Martinez[174], A. Rummler[36], Z. Rurikova[52], N.A. Rusakovich[80], H.L. Russell[104], L. Rustige[38,47], J.P. Rutherfoord[7], E.M. Rüttinger[149], M. Rybar[39], G. Rybkin[65], E.B. Rye[134], A. Ryzhov[123], J.A. Sabater Iglesias[46], P. Sabatini[53], G. Sabato[120], S. Sacerdoti[65], H.F-W. Sadrozinski[146], R. Sadykov[80], F. Safai Tehrani[73a], B. Safarzadeh Samani[156], M. Safdari[153], P. Saha[121], S. Saha[104], M. Sahinsoy[61a], A. Sahu[182], M. Saimpert[46], M. Saito[163], T. Saito[163], H. Sakamoto[163], A. Sakharov[125,aj], D. Salamani[54], G. Salamanna[75a,75b], J.E. Salazar Loyola[147c], A. Salnikov[153], J. Salt[174], D. Salvatore[41b,41a], F. Salvatore[156], A. Salvucci[63a,63b,63c], A. Salzburger[36], J. Samarati[36], D. Sammel[52], D. Sampsonidis[162], D. Sampsonidou[162], J. Sánchez[174], A. Sanchez Pineda[67a,36,67c], H. Sandaker[134], C.O. Sander[46], I.G. Sanderswood[90], M. Sandhoff[182], C. Sandoval[22], D.P.C. Sankey[144], M. Sannino[55b,55a], Y. Sano[117], A. Sansoni[51], C. Santoni[38], H. Santos[140a,140b], S.N. Santpur[18], A. Santra[174], A. Sapronov[80], J.G. Saraiva[140a,140d], O. Sasaki[82], K. Sato[169], F. Sauerburger[52], E. Sauvan[5], P. Savard[167,ar], R. Sawada[163], C. Sawyer[144], L. Sawyer[96,ai], C. Sbarra[23b], A. Sbrizzi[23a], T. Scanlon[95], J. Schaarschmidt[148], P. Schacht[115], B.M. Schachtner[114], D. Schaefer[37], L. Schaefer[137], J. Schaeffer[100], S. Schaepe[36], U. Schäfer[100], A.C. Schaffer[65], D. Schaile[114], R.D. Schamberger[155], N. Scharmberg[101], V.A. Schegelsky[138], D. Scheirich[143], F. Schenck[19], M. Schernau[171], C. Schiavi[55b,55a], S. Schier[146], L.K. Schildgen[24], Z.M. Schillaci[26], E.J. Schioppa[36], M. Schioppa[41b,41a], K.E. Schleicher[52], S. Schlenker[36], K.R. Schmidt-Sommerfeld[115], K. Schmieden[36], C. Schmitt[100], S. Schmitt[46], S. Schmitz[100], J.C. Schmoeckel[46], U. Schnoor[52], L. Schoeffel[145], A. Schoening[61b], P.G. Scholer[52], E. Schopf[135], M. Schott[100], J.F.P. Schouwenberg[119], J. Schovancova[36], S. Schramm[54], F. Schroeder[182], A. Schulte[100], H-C. Schultz-Coulon[61a], M. Schumacher[52], B.A. Schumm[146], Ph. Schune[145], A. Schwartzman[153], T.A. Schwarz[106], Ph. Schwemling[145], R. Schwienhorst[107], A. Sciandra[146], G. Sciolla[26], M. Scodeggio[46], M. Scornajenghi[41b,41a], F. Scuri[72a], F. Scutti[105], L.M. Scyboz[115], C.D. Sebastiani[73a,73b], P. Seema[19], S.C. Seidel[118], A. Seiden[146], B.D. Seidlitz[29], T. Seiss[37], J.M. Seixas[81b], G. Sekhniaidze[70a], K. Sekhon[106], S.J. Sekula[42],

N. Semprini-Cesari[23b,23a], S. Sen[49], C. Serfon[77], L. Serin[65], L. Serkin[67a,67b], M. Sessa[60a], H. Severini[129],
S. Sevova[153], T. Šfiligoj[92], F. Sforza[55b,55a], A. Sfyrla[54], E. Shabalina[53], J.D. Shahinian[146],
N.W. Shaikh[45a,45b], D. Shaked Renous[180], L.Y. Shan[15a], J.T. Shank[25], M. Shapiro[18], A. Sharma[135],
A.S. Sharma[1], P.B. Shatalov[124], K. Shaw[156], S.M. Shaw[101], M. Shehade[180], Y. Shen[129], A.D. Sherman[25],
P. Sherwood[95], L. Shi[158], S. Shimizu[82], C.O. Shimmin[183], Y. Shimogama[179], M. Shimojima[116],
I.P.J. Shipsey[135], S. Shirabe[165], M. Shiyakova[80,ac], J. Shlomi[180], A. Shmeleva[111], M.J. Shochet[37],
J. Shojaii[105], D.R. Shope[129], S. Shrestha[127], E.M. Shrif[33d], E. Shulga[180], P. Sicho[141], A.M. Sickles[173],
P.E. Sidebo[154], E. Sideras Haddad[33d], O. Sidiropoulou[36], A. Sidoti[23b,23a], F. Siegert[48], Dj. Sijacki[16],
M.Jr. Silva[181], M.V. Silva Oliveira[81a], S.B. Silverstein[45a], S. Simion[65], R. Simoniello[100], S. Simsek[12b],
P. Sinervo[167], V. Sinetckii[113], N.B. Sinev[132], S. Singh[152], M. Sioli[23b,23a], I. Siral[132], S.Yu. Sivoklokov[113],
J. Sjölin[45a,45b], E. Skorda[97], P. Skubic[129], M. Slawinska[85], K. Sliwa[170], R. Slovak[143], V. Smakhtin[180],
B.H. Smart[144], J. Smiesko[28a], N. Smirnov[112], S.Yu. Smirnov[112], Y. Smirnov[112], L.N. Smirnova[113,u],
O. Smirnova[97], J.W. Smith[53], M. Smizanska[90], K. Smolek[142], A. Smykiewicz[85], A.A. Snesarev[111],
H.L. Snoek[120], I.M. Snyder[132], S. Snyder[29], R. Sobie[176,ae], A. Soffer[161], A. Søgaard[50], F. Sohns[53],
C.A. Solans Sanchez[36], E.Yu. Soldatov[112], U. Soldevila[174], A.A. Solodkov[123], A. Soloshenko[80],
O.V. Solovyanov[123], V. Solovyev[138], P. Sommer[149], H. Son[170], W. Song[144], W.Y. Song[168b], A. Sopczak[142],
A.L. Sopio[95], F. Sopkova[28b], C.L. Sotiropoulou[72a,72b], S. Sottocornola[71a,71b], R. Soualah[67a,67c,f],
A.M. Soukharev[122b,122a], D. South[46], S. Spagnolo[68a,68b], M. Spalla[115], M. Spangenberg[178], F. Spanò[94],
D. Sperlich[52], T.M. Spieker[61a], G. Spigo[36], M. Spina[156], D.P. Spiteri[57], M. Spousta[143], A. Stabile[69a,69b],
B.L. Stamas[121], R. Stamen[61a], M. Stamenkovic[120], E. Stanecka[85], B. Stanislaus[135], M.M. Stanitzki[46],
M. Stankaityte[135], B. Stapf[120], E.A. Starchenko[123], G.H. Stark[146], J. Stark[58], P. Staroba[141],
P. Starovoitov[61a], S. Stärz[104], R. Staszewski[85], G. Stavropoulos[44], M. Stegler[46], P. Steinberg[29],
A.L. Steinhebel[132], B. Stelzer[152], H.J. Stelzer[139], O. Stelzer-Chilton[168a], H. Stenzel[56], T.J. Stevenson[156],
G.A. Stewart[36], M.C. Stockton[36], G. Stoicea[27b], M. Stolarski[140a], S. Stonjek[115], A. Straessner[48],
J. Strandberg[154], S. Strandberg[45a,45b], M. Strauss[129], P. Strizenec[28b], R. Ströhmer[177], D.M. Strom[132],
R. Stroynowski[42], A. Strubig[50], S.A. Stucci[29], B. Stugu[17], J. Stupak[129], N.A. Styles[46], D. Su[153], W. Su[60c],
S. Suchek[61a], V.V. Sulin[111], M.J. Sullivan[91], D.M.S. Sultan[54], S. Sultansoy[4c], T. Sumida[86], S. Sun[106],
X. Sun[3], K. Suruliz[156], C.J.E. Suster[157], M.R. Sutton[156], S. Suzuki[82], M. Svatos[141], M. Swiatlowski[37],
S.P. Swift[2], T. Swirski[177], A. Sydorenko[100], I. Sykora[28a], M. Sykora[143], T. Sykora[143], D. Ta[100],
K. Tackmann[46,aa], J. Taenzer[161], A. Taffard[171], R. Tafirout[168a], H. Takai[29], R. Takashima[87], K. Takeda[83],
T. Takeshita[150], E.P. Takeva[50], Y. Takubo[82], M. Talby[102], A.A. Talyshev[122b,122a], N.M. Tamir[161],
J. Tanaka[163], M. Tanaka[165], R. Tanaka[65], S. Tapia Araya[173], S. Tapprogge[100],
A. Tarek Abouelfadl Mohamed[136], S. Tarem[160], K. Tariq[60b], G. Tarna[27b,c], G.F. Tartarelli[69a], P. Tas[143],
M. Tasevsky[141], T. Tashiro[86], E. Tassi[41b,41a], A. Tavares Delgado[140a], Y. Tayalati[35e], A.J. Taylor[50],
G.N. Taylor[105], W. Taylor[168b], A.S. Tee[90], R. Teixeira De Lima[153], P. Teixeira-Dias[94], H. Ten Kate[36],
J.J. Teoh[120], S. Terada[82], K. Terashi[163], J. Terron[99], S. Terzo[14], M. Testa[51], R.J. Teuscher[167,ae],
S.J. Thais[183], T. Theveneaux-Pelzer[46], F. Thiele[40], D.W. Thomas[94], J.O. Thomas[42], J.P. Thomas[21],
P.D. Thompson[21], L.A. Thomsen[183], E. Thomson[137], E.J. Thorpe[93], R.E. Ticse Torres[53],
V.O. Tikhomirov[111,al], Yu.A. Tikhonov[122b,122a], S. Timoshenko[112], P. Tipton[183], S. Tisserant[102],
K. Todome[23b,23a], S. Todorova-Nova[5], S. Todt[48], J. Tojo[88], S. Tokár[28a], K. Tokushuku[82], E. Tolley[127],
K.G. Tomiwa[33d], M. Tomoto[117], L. Tompkins[153,p], B. Tong[59], P. Tornambe[103], E. Torrence[132], H. Torres[48],
E. Torró Pastor[148], C. Tosciri[135], J. Toth[102,ad], D.R. Tovey[149], A. Traeet[17], C.J. Treado[125], T. Trefzger[177],
F. Tresoldi[156], A. Tricoli[29], I.M. Trigger[168a], S. Trincaz-Duvoid[136], D.T. Trischuk[175], W. Trischuk[167],
B. Trocmé[58], A. Trofymov[145], C. Troncon[69a], M. Trovatelli[176], F. Trovato[156], L. Truong[33b],
M. Trzebinski[85], A. Trzupek[85], F. Tsai[46], J.C-L. Tseng[135], P.V. Tsiareshka[108,ah], A. Tsirigotis[162,x],
V. Tsiskaridze[155], E.G. Tskhadadze[159a], M. Tsopoulou[162], I.I. Tsukerman[124], V. Tsulaia[18], S. Tsuno[82],
D. Tsybychev[155], Y. Tu[63b], A. Tudorache[27b], V. Tudorache[27b], T.T. Tulbure[27a], A.N. Tuna[59],

45

S. Turchikhin[80], D. Turgeman[180], I. Turk Cakir[4b,v], R.J. Turner[21], R.T. Turra[69a], P.M. Tuts[39],
S. Tzamarias[162], E. Tzovara[100], G. Ucchielli[47], K. Uchida[163], I. Ueda[82], F. Ukegawa[169], G. Unal[36],
A. Undrus[29], G. Unel[171], F.C. Ungaro[105], Y. Unno[82], K. Uno[163], J. Urban[28b], P. Urquijo[105], G. Usai[8],
Z. Uysal[12d], V. Vacek[142], B. Vachon[104], K.O.H. Vadla[134], A. Vaidya[95], C. Valderanis[114],
E. Valdes Santurio[45a,45b], M. Valente[54], S. Valentinetti[23b,23a], A. Valero[174], L. Valéry[46], R.A. Vallance[21],
A. Vallier[36], J.A. Valls Ferrer[174], T.R. Van Daalen[14], P. Van Gemmeren[6], I. Van Vulpen[120],
M. Vanadia[74a,74b], W. Vandelli[36], M. Vandenbroucke[145], E.R. Vandewall[130], A. Vaniachine[166],
D. Vannicola[73a,73b], R. Vari[73a], E.W. Varnes[7], C. Varni[55b,55a], T. Varol[158], D. Varouchas[65], K.E. Varvell[157],
M.E. Vasile[27b], G.A. Vasquez[176], F. Vazeille[38], D. Vazquez Furelos[14], T. Vazquez Schroeder[36], J. Veatch[53],
V. Vecchio[75a,75b], M.J. Veen[120], L.M. Veloce[167], F. Veloso[140a,140c], S. Veneziano[73a], A. Ventura[68a,68b],
N. Venturi[36], A. Verbytskyi[115], V. Vercesi[71a], M. Verducci[72a,72b], C.M. Vergel Infante[79], C. Vergis[24],
W. Verkerke[120], A.T. Vermeulen[120], J.C. Vermeulen[120], M.C. Vetterli[152,ar], N. Viaux Maira[147c],
M. Vicente Barreto Pinto[54], T. Vickey[149], O.E. Vickey Boeriu[149], G.H.A. Viehhauser[135], L. Vigani[61b],
M. Villa[23b,23a], M. Villaplana Perez[3], E. Vilucchi[51], M.G. Vincter[34], G.S. Virdee[21], A. Vishwakarma[46],
C. Vittori[23b,23a], I. Vivarelli[156], M. Vogel[182], P. Vokac[142], S.E. von Buddenbrock[33d], E. Von Toerne[24],
V. Vorobel[143], K. Vorobev[112], M. Vos[174], J.H. Vossebeld[91], M. Vozak[101], N. Vranjes[16],
M. Vranjes Milosavljevic[16], V. Vrba[142], M. Vreeswijk[120], R. Vuillermet[36], I. Vukotic[37], P. Wagner[24],
W. Wagner[182], J. Wagner-Kuhr[114], S. Wahdan[182], H. Wahlberg[89], V.M. Walbrecht[115], J. Walder[90],
R. Walker[114], S.D. Walker[94], W. Walkowiak[151], V. Wallangen[45a,45b], A.M. Wang[59], A.Z. Wang[181],
C. Wang[60c], F. Wang[181], H. Wang[18], H. Wang[3], J. Wang[63a], J. Wang[61b], P. Wang[42], Q. Wang[129],
R.-J. Wang[100], R. Wang[60a], R. Wang[6], S.M. Wang[158], W.T. Wang[60a], W. Wang[15c], W.X. Wang[60a],
Y. Wang[60a], Z. Wang[60c], C. Wanotayaroj[46], A. Warburton[104], C.P. Ward[32], D.R. Wardrope[95], N. Warrack[57],
A. Washbrook[50], A.T. Watson[21], M.F. Watson[21], G. Watts[148], B.M. Waugh[95], A.F. Webb[11], S. Webb[100],
C. Weber[183], M.S. Weber[20], S.A. Weber[34], S.M. Weber[61a], A.R. Weidberg[135], J. Weingarten[47],
M. Weirich[100], C. Weiser[52], P.S. Wells[36], T. Wenaus[29], T. Wengler[36], S. Wenig[36], N. Wermes[24],
M.D. Werner[79], M. Wessels[61a], T.D. Weston[20], K. Whalen[132], N.L. Whallon[148], A.M. Wharton[90],
A.S. White[106], A. White[8], M.J. White[1], D. Whiteson[171], B.W. Whitmore[90], W. Wiedenmann[181], C. Wiel[48],
M. Wielers[144], N. Wieseotte[100], C. Wiglesworth[40], L.A.M. Wiik-Fuchs[52], H.G. Wilkens[36], L.J. Wilkins[94],
H.H. Williams[137], S. Williams[32], C. Willis[107], S. Willocq[103], J.A. Wilson[21], I. Wingerter-Seez[5],
E. Winkels[156], F. Winklmeier[132], O.J. Winston[156], B.T. Winter[52], M. Wittgen[153], M. Wobisch[96],
A. Wolf[100], T.M.H. Wolf[120], R. Wolff[102], R.W. Wölker[135], J. Wollrath[52], M.W. Wolter[85],
H. Wolters[140a,140c], V.W.S. Wong[175], N.L. Woods[146], S.D. Worm[21], B.K. Wosiek[85], K.W. Woźniak[85],
K. Wraight[57], S.L. Wu[181], X. Wu[54], Y. Wu[60a], T.R. Wyatt[101], B.M. Wynne[50], S. Xella[40], Z. Xi[106],
L. Xia[178], X. Xiao[106], I. Xiotidis[156], D. Xu[15a], H. Xu[60a], H. Xu[60a], L. Xu[29], T. Xu[145], W. Xu[106], Z. Xu[60b],
Z. Xu[153], B. Yabsley[157], S. Yacoob[33a], K. Yajima[133], D.P. Yallup[95], N. Yamaguchi[88], Y. Yamaguchi[165],
A. Yamamoto[82], M. Yamatani[163], T. Yamazaki[163], Y. Yamazaki[83], Z. Yan[25], H.J. Yang[60c,60d], H.T. Yang[18],
S. Yang[60a], T. Yang[63c], X. Yang[60b,58], Y. Yang[163], W-M. Yao[18], Y.C. Yap[46], Y. Yasu[82], E. Yatsenko[60c,60d],
H. Ye[15c], J. Ye[42], S. Ye[29], I. Yeletskikh[80], M.R. Yexley[90], E. Yigitbasi[25], K. Yorita[179], K. Yoshihara[137],
C.J.S. Young[36], C. Young[153], J. Yu[79], R. Yuan[60b,h], X. Yue[61a], S.P.Y. Yuen[24], M. Zaazoua[35e],
B. Zabinski[85], G. Zacharis[10], E. Zaffaroni[54], J. Zahreddine[136], A.M. Zaitsev[123,ak], T. Zakareishvili[159b],
N. Zakharchuk[34], S. Zambito[59], D. Zanzi[36], D.R. Zaripovas[57], S.V. Zeißner[47], C. Zeitnitz[182],
G. Zemaityte[135], J.C. Zeng[173], O. Zenin[123], T. Ženiš[28a], D. Zerwas[65], M. Zgubič[135], B. Zhang[15c],
D.F. Zhang[15b], G. Zhang[15b], H. Zhang[15c], J. Zhang[6], L. Zhang[15c], L. Zhang[60a], M. Zhang[173], R. Zhang[181],
S. Zhang[106], X. Zhang[60b], Y. Zhang[15a,15d], Z. Zhang[63a], Z. Zhang[65], P. Zhao[49], Y. Zhao[60b], Z. Zhao[60a],
A. Zhemchugov[80], Z. Zheng[106], D. Zhong[173], B. Zhou[106], C. Zhou[181], M.S. Zhou[15a,15d], M. Zhou[155],
N. Zhou[60c], Y. Zhou[7], C.G. Zhu[60b], C. Zhu[15a,15d], H.L. Zhu[60a], H. Zhu[15a], J. Zhu[106], Y. Zhu[60a],
X. Zhuang[15a], K. Zhukov[111], V. Zhulanov[122b,122a], D. Zieminska[66], N.I. Zimine[80], S. Zimmermann[52],

Z. Zinonos[115], M. Ziolkowski[151], L. Živković[16], G. Zobernig[181], A. Zoccoli[23b,23a], K. Zoch[53], T.G. Zorbas[149], R. Zou[37], L. Zwalinski[36].

[1]Department of Physics, University of Adelaide, Adelaide; Australia.

[2]Physics Department, SUNY Albany, Albany NY; United States of America.

[3]Department of Physics, University of Alberta, Edmonton AB; Canada.

[4](a)Department of Physics, Ankara University, Ankara;(b)Istanbul Aydin University, Istanbul;(c)Division of Physics, TOBB University of Economics and Technology, Ankara; Turkey.

[5]LAPP, Université Grenoble Alpes, Université Savoie Mont Blanc, CNRS/IN2P3, Annecy; France.

[6]High Energy Physics Division, Argonne National Laboratory, Argonne IL; United States of America.

[7]Department of Physics, University of Arizona, Tucson AZ; United States of America.

[8]Department of Physics, University of Texas at Arlington, Arlington TX; United States of America.

[9]Physics Department, National and Kapodistrian University of Athens, Athens; Greece.

[10]Physics Department, National Technical University of Athens, Zografou; Greece.

[11]Department of Physics, University of Texas at Austin, Austin TX; United States of America.

[12](a)Bahcesehir University, Faculty of Engineering and Natural Sciences, Istanbul;(b)Istanbul Bilgi University, Faculty of Engineering and Natural Sciences, Istanbul;(c)Department of Physics, Bogazici University, Istanbul;(d)Department of Physics Engineering, Gaziantep University, Gaziantep; Turkey.

[13]Institute of Physics, Azerbaijan Academy of Sciences, Baku; Azerbaijan.

[14]Institut de Física d'Altes Energies (IFAE), Barcelona Institute of Science and Technology, Barcelona; Spain.

[15](a)Institute of High Energy Physics, Chinese Academy of Sciences, Beijing;(b)Physics Department, Tsinghua University, Beijing;(c)Department of Physics, Nanjing University, Nanjing;(d)University of Chinese Academy of Science (UCAS), Beijing; China.

[16]Institute of Physics, University of Belgrade, Belgrade; Serbia.

[17]Department for Physics and Technology, University of Bergen, Bergen; Norway.

[18]Physics Division, Lawrence Berkeley National Laboratory and University of California, Berkeley CA; United States of America.

[19]Institut für Physik, Humboldt Universität zu Berlin, Berlin; Germany.

[20]Albert Einstein Center for Fundamental Physics and Laboratory for High Energy Physics, University of Bern, Bern; Switzerland.

[21]School of Physics and Astronomy, University of Birmingham, Birmingham; United Kingdom.

[22]Facultad de Ciencias y Centro de Investigaciónes, Universidad Antonio Nariño, Bogota; Colombia.

[23](a)INFN Bologna and Universita' di Bologna, Dipartimento di Fisica;(b)INFN Sezione di Bologna; Italy.

[24]Physikalisches Institut, Universität Bonn, Bonn; Germany.

[25]Department of Physics, Boston University, Boston MA; United States of America.

[26]Department of Physics, Brandeis University, Waltham MA; United States of America.

[27](a)Transilvania University of Brasov, Brasov;(b)Horia Hulubei National Institute of Physics and Nuclear Engineering, Bucharest;(c)Department of Physics, Alexandru Ioan Cuza University of Iasi, Iasi;(d)National Institute for Research and Development of Isotopic and Molecular Technologies, Physics Department, Cluj-Napoca;(e)University Politehnica Bucharest, Bucharest;(f)West University in Timisoara, Timisoara; Romania.

[28](a)Faculty of Mathematics, Physics and Informatics, Comenius University, Bratislava;(b)Department of Subnuclear Physics, Institute of Experimental Physics of the Slovak Academy of Sciences, Kosice; Slovak Republic.

[29]Physics Department, Brookhaven National Laboratory, Upton NY; United States of America.

[30]Departamento de Física, Universidad de Buenos Aires, Buenos Aires; Argentina.

[31]California State University, CA; United States of America.

[32]Cavendish Laboratory, University of Cambridge, Cambridge; United Kingdom.

[33][a]Department of Physics, University of Cape Town, Cape Town;[b]Department of Mechanical Engineering Science, University of Johannesburg, Johannesburg;[c]University of South Africa, Department of Physics, Pretoria;[d]School of Physics, University of the Witwatersrand, Johannesburg; South Africa.

[34]Department of Physics, Carleton University, Ottawa ON; Canada.

[35][a]Faculté des Sciences Ain Chock, Réseau Universitaire de Physique des Hautes Energies - Université Hassan II, Casablanca;[b]Faculté des Sciences, Université Ibn-Tofail, Kénitra;[c]Faculté des Sciences Semlalia, Université Cadi Ayyad, LPHEA-Marrakech;[d]Faculté des Sciences, Université Mohamed Premier and LPTPM, Oujda;[e]Faculté des sciences, Université Mohammed V, Rabat; Morocco.

[36]CERN, Geneva; Switzerland.

[37]Enrico Fermi Institute, University of Chicago, Chicago IL; United States of America.

[38]LPC, Université Clermont Auvergne, CNRS/IN2P3, Clermont-Ferrand; France.

[39]Nevis Laboratory, Columbia University, Irvington NY; United States of America.

[40]Niels Bohr Institute, University of Copenhagen, Copenhagen; Denmark.

[41][a]Dipartimento di Fisica, Università della Calabria, Rende;[b]INFN Gruppo Collegato di Cosenza, Laboratori Nazionali di Frascati; Italy.

[42]Physics Department, Southern Methodist University, Dallas TX; United States of America.

[43]Physics Department, University of Texas at Dallas, Richardson TX; United States of America.

[44]National Centre for Scientific Research "Demokritos", Agia Paraskevi; Greece.

[45][a]Department of Physics, Stockholm University;[b]Oskar Klein Centre, Stockholm; Sweden.

[46]Deutsches Elektronen-Synchrotron DESY, Hamburg and Zeuthen; Germany.

[47]Lehrstuhl für Experimentelle Physik IV, Technische Universität Dortmund, Dortmund; Germany.

[48]Institut für Kern- und Teilchenphysik, Technische Universität Dresden, Dresden; Germany.

[49]Department of Physics, Duke University, Durham NC; United States of America.

[50]SUPA - School of Physics and Astronomy, University of Edinburgh, Edinburgh; United Kingdom.

[51]INFN e Laboratori Nazionali di Frascati, Frascati; Italy.

[52]Physikalisches Institut, Albert-Ludwigs-Universität Freiburg, Freiburg; Germany.

[53]II. Physikalisches Institut, Georg-August-Universität Göttingen, Göttingen; Germany.

[54]Département de Physique Nucléaire et Corpusculaire, Université de Genève, Genève; Switzerland.

[55][a]Dipartimento di Fisica, Università di Genova, Genova;[b]INFN Sezione di Genova; Italy.

[56]II. Physikalisches Institut, Justus-Liebig-Universität Giessen, Giessen; Germany.

[57]SUPA - School of Physics and Astronomy, University of Glasgow, Glasgow; United Kingdom.

[58]LPSC, Université Grenoble Alpes, CNRS/IN2P3, Grenoble INP, Grenoble; France.

[59]Laboratory for Particle Physics and Cosmology, Harvard University, Cambridge MA; United States of America.

[60][a]Department of Modern Physics and State Key Laboratory of Particle Detection and Electronics, University of Science and Technology of China, Hefei;[b]Institute of Frontier and Interdisciplinary Science and Key Laboratory of Particle Physics and Particle Irradiation (MOE), Shandong University, Qingdao;[c]School of Physics and Astronomy, Shanghai Jiao Tong University, KLPPAC-MoE, SKLPPC, Shanghai;[d]Tsung-Dao Lee Institute, Shanghai; China.

[61][a]Kirchhoff-Institut für Physik, Ruprecht-Karls-Universität Heidelberg, Heidelberg;[b]Physikalisches Institut, Ruprecht-Karls-Universität Heidelberg, Heidelberg; Germany.

[62]Faculty of Applied Information Science, Hiroshima Institute of Technology, Hiroshima; Japan.

[63][a]Department of Physics, Chinese University of Hong Kong, Shatin, N.T., Hong Kong;[b]Department of Physics, University of Hong Kong, Hong Kong;[c]Department of Physics and Institute for Advanced Study, Hong Kong University of Science and Technology, Clear Water Bay, Kowloon, Hong Kong; China.

[64]Department of Physics, National Tsing Hua University, Hsinchu; Taiwan.

[65]IJCLab, Université Paris-Saclay, CNRS/IN2P3, 91405, Orsay; France.

[66]Department of Physics, Indiana University, Bloomington IN; United States of America.

[67][a]INFN Gruppo Collegato di Udine, Sezione di Trieste, Udine;[b]ICTP, Trieste;[c]Dipartimento Politecnico di Ingegneria e Architettura, Università di Udine, Udine; Italy.

[68][a]INFN Sezione di Lecce;[b]Dipartimento di Matematica e Fisica, Università del Salento, Lecce; Italy.

[69][a]INFN Sezione di Milano;[b]Dipartimento di Fisica, Università di Milano, Milano; Italy.

[70][a]INFN Sezione di Napoli;[b]Dipartimento di Fisica, Università di Napoli, Napoli; Italy.

[71][a]INFN Sezione di Pavia;[b]Dipartimento di Fisica, Università di Pavia, Pavia; Italy.

[72][a]INFN Sezione di Pisa;[b]Dipartimento di Fisica E. Fermi, Università di Pisa, Pisa; Italy.

[73][a]INFN Sezione di Roma;[b]Dipartimento di Fisica, Sapienza Università di Roma, Roma; Italy.

[74][a]INFN Sezione di Roma Tor Vergata;[b]Dipartimento di Fisica, Università di Roma Tor Vergata, Roma; Italy.

[75][a]INFN Sezione di Roma Tre;[b]Dipartimento di Matematica e Fisica, Università Roma Tre, Roma; Italy.

[76][a]INFN-TIFPA;[b]Università degli Studi di Trento, Trento; Italy.

[77]Institut für Astro- und Teilchenphysik, Leopold-Franzens-Universität, Innsbruck; Austria.

[78]University of Iowa, Iowa City IA; United States of America.

[79]Department of Physics and Astronomy, Iowa State University, Ames IA; United States of America.

[80]Joint Institute for Nuclear Research, Dubna; Russia.

[81][a]Departamento de Engenharia Elétrica, Universidade Federal de Juiz de Fora (UFJF), Juiz de Fora;[b]Universidade Federal do Rio De Janeiro COPPE/EE/IF, Rio de Janeiro;[c]Universidade Federal de São João del Rei (UFSJ), São João del Rei;[d]Instituto de Física, Universidade de São Paulo, São Paulo; Brazil.

[82]KEK, High Energy Accelerator Research Organization, Tsukuba; Japan.

[83]Graduate School of Science, Kobe University, Kobe; Japan.

[84][a]AGH University of Science and Technology, Faculty of Physics and Applied Computer Science, Krakow;[b]Marian Smoluchowski Institute of Physics, Jagiellonian University, Krakow; Poland.

[85]Institute of Nuclear Physics Polish Academy of Sciences, Krakow; Poland.

[86]Faculty of Science, Kyoto University, Kyoto; Japan.

[87]Kyoto University of Education, Kyoto; Japan.

[88]Research Center for Advanced Particle Physics and Department of Physics, Kyushu University, Fukuoka ; Japan.

[89]Instituto de Física La Plata, Universidad Nacional de La Plata and CONICET, La Plata; Argentina.

[90]Physics Department, Lancaster University, Lancaster; United Kingdom.

[91]Oliver Lodge Laboratory, University of Liverpool, Liverpool; United Kingdom.

[92]Department of Experimental Particle Physics, Jožef Stefan Institute and Department of Physics, University of Ljubljana, Ljubljana; Slovenia.

[93]School of Physics and Astronomy, Queen Mary University of London, London; United Kingdom.

[94]Department of Physics, Royal Holloway University of London, Egham; United Kingdom.

[95]Department of Physics and Astronomy, University College London, London; United Kingdom.

[96]Louisiana Tech University, Ruston LA; United States of America.

[97]Fysiska institutionen, Lunds universitet, Lund; Sweden.

[98]Centre de Calcul de l'Institut National de Physique Nucléaire et de Physique des Particules (IN2P3), Villeurbanne; France.

[99]Departamento de Física Teorica C-15 and CIAFF, Universidad Autónoma de Madrid, Madrid; Spain.

[100]Institut für Physik, Universität Mainz, Mainz; Germany.

[101]School of Physics and Astronomy, University of Manchester, Manchester; United Kingdom.

[102]CPPM, Aix-Marseille Université, CNRS/IN2P3, Marseille; France.

[103]Department of Physics, University of Massachusetts, Amherst MA; United States of America.

[104]Department of Physics, McGill University, Montreal QC; Canada.

[105]School of Physics, University of Melbourne, Victoria; Australia.

[106]Department of Physics, University of Michigan, Ann Arbor MI; United States of America.

[107]Department of Physics and Astronomy, Michigan State University, East Lansing MI; United States of America.

[108]B.I. Stepanov Institute of Physics, National Academy of Sciences of Belarus, Minsk; Belarus.

[109]Research Institute for Nuclear Problems of Byelorussian State University, Minsk; Belarus.

[110]Group of Particle Physics, University of Montreal, Montreal QC; Canada.

[111]P.N. Lebedev Physical Institute of the Russian Academy of Sciences, Moscow; Russia.

[112]National Research Nuclear University MEPhI, Moscow; Russia.

[113]D.V. Skobeltsyn Institute of Nuclear Physics, M.V. Lomonosov Moscow State University, Moscow; Russia.

[114]Fakultät für Physik, Ludwig-Maximilians-Universität München, München; Germany.

[115]Max-Planck-Institut für Physik (Werner-Heisenberg-Institut), München; Germany.

[116]Nagasaki Institute of Applied Science, Nagasaki; Japan.

[117]Graduate School of Science and Kobayashi-Maskawa Institute, Nagoya University, Nagoya; Japan.

[118]Department of Physics and Astronomy, University of New Mexico, Albuquerque NM; United States of America.

[119]Institute for Mathematics, Astrophysics and Particle Physics, Radboud University Nijmegen/Nikhef, Nijmegen; Netherlands.

[120]Nikhef National Institute for Subatomic Physics and University of Amsterdam, Amsterdam; Netherlands.

[121]Department of Physics, Northern Illinois University, DeKalb IL; United States of America.

[122](a)Budker Institute of Nuclear Physics and NSU, SB RAS, Novosibirsk;(b)Novosibirsk State University Novosibirsk; Russia.

[123]Institute for High Energy Physics of the National Research Centre Kurchatov Institute, Protvino; Russia.

[124]Institute for Theoretical and Experimental Physics named by A.I. Alikhanov of National Research Centre "Kurchatov Institute", Moscow; Russia.

[125]Department of Physics, New York University, New York NY; United States of America.

[126]Ochanomizu University, Otsuka, Bunkyo-ku, Tokyo; Japan.

[127]Ohio State University, Columbus OH; United States of America.

[128]Faculty of Science, Okayama University, Okayama; Japan.

[129]Homer L. Dodge Department of Physics and Astronomy, University of Oklahoma, Norman OK; United States of America.

[130]Department of Physics, Oklahoma State University, Stillwater OK; United States of America.

[131]Palacký University, RCPTM, Joint Laboratory of Optics, Olomouc; Czech Republic.

[132]Center for High Energy Physics, University of Oregon, Eugene OR; United States of America.

[133]Graduate School of Science, Osaka University, Osaka; Japan.

[134]Department of Physics, University of Oslo, Oslo; Norway.

[135]Department of Physics, Oxford University, Oxford; United Kingdom.

[136]LPNHE, Sorbonne Université, Université de Paris, CNRS/IN2P3, Paris; France.

[137]Department of Physics, University of Pennsylvania, Philadelphia PA; United States of America.

[138]Konstantinov Nuclear Physics Institute of National Research Centre "Kurchatov Institute", PNPI, St. Petersburg; Russia.

[139]Department of Physics and Astronomy, University of Pittsburgh, Pittsburgh PA; United States of

America.

[140] (a)Laboratório de Instrumentação e Física Experimental de Partículas - LIP, Lisboa;(b)Departamento de Física, Faculdade de Ciências, Universidade de Lisboa, Lisboa;(c)Departamento de Física, Universidade de Coimbra, Coimbra;(d)Centro de Física Nuclear da Universidade de Lisboa, Lisboa;(e)Departamento de Física, Universidade do Minho, Braga;(f)Departamento de Física Teórica y del Cosmos, Universidad de Granada, Granada (Spain);(g)Dep Física and CEFITEC of Faculdade de Ciências e Tecnologia, Universidade Nova de Lisboa, Caparica;(h)Instituto Superior Técnico, Universidade de Lisboa, Lisboa; Portugal.

[141] Institute of Physics of the Czech Academy of Sciences, Prague; Czech Republic.

[142] Czech Technical University in Prague, Prague; Czech Republic.

[143] Charles University, Faculty of Mathematics and Physics, Prague; Czech Republic.

[144] Particle Physics Department, Rutherford Appleton Laboratory, Didcot; United Kingdom.

[145] IRFU, CEA, Université Paris-Saclay, Gif-sur-Yvette; France.

[146] Santa Cruz Institute for Particle Physics, University of California Santa Cruz, Santa Cruz CA; United States of America.

[147] (a)Departamento de Física, Pontificia Universidad Católica de Chile, Santiago;(b)Universidad Andres Bello, Department of Physics, Santiago;(c)Departamento de Física, Universidad Técnica Federico Santa María, Valparaíso; Chile.

[148] Department of Physics, University of Washington, Seattle WA; United States of America.

[149] Department of Physics and Astronomy, University of Sheffield, Sheffield; United Kingdom.

[150] Department of Physics, Shinshu University, Nagano; Japan.

[151] Department Physik, Universität Siegen, Siegen; Germany.

[152] Department of Physics, Simon Fraser University, Burnaby BC; Canada.

[153] SLAC National Accelerator Laboratory, Stanford CA; United States of America.

[154] Physics Department, Royal Institute of Technology, Stockholm; Sweden.

[155] Departments of Physics and Astronomy, Stony Brook University, Stony Brook NY; United States of America.

[156] Department of Physics and Astronomy, University of Sussex, Brighton; United Kingdom.

[157] School of Physics, University of Sydney, Sydney; Australia.

[158] Institute of Physics, Academia Sinica, Taipei; Taiwan.

[159] (a)E. Andronikashvili Institute of Physics, Iv. Javakhishvili Tbilisi State University, Tbilisi;(b)High Energy Physics Institute, Tbilisi State University, Tbilisi; Georgia.

[160] Department of Physics, Technion, Israel Institute of Technology, Haifa; Israel.

[161] Raymond and Beverly Sackler School of Physics and Astronomy, Tel Aviv University, Tel Aviv; Israel.

[162] Department of Physics, Aristotle University of Thessaloniki, Thessaloniki; Greece.

[163] International Center for Elementary Particle Physics and Department of Physics, University of Tokyo, Tokyo; Japan.

[164] Graduate School of Science and Technology, Tokyo Metropolitan University, Tokyo; Japan.

[165] Department of Physics, Tokyo Institute of Technology, Tokyo; Japan.

[166] Tomsk State University, Tomsk; Russia.

[167] Department of Physics, University of Toronto, Toronto ON; Canada.

[168] (a)TRIUMF, Vancouver BC;(b)Department of Physics and Astronomy, York University, Toronto ON; Canada.

[169] Division of Physics and Tomonaga Center for the History of the Universe, Faculty of Pure and Applied Sciences, University of Tsukuba, Tsukuba; Japan.

[170] Department of Physics and Astronomy, Tufts University, Medford MA; United States of America.

[171] Department of Physics and Astronomy, University of California Irvine, Irvine CA; United States of

America.

[172]Department of Physics and Astronomy, University of Uppsala, Uppsala; Sweden.

[173]Department of Physics, University of Illinois, Urbana IL; United States of America.

[174]Instituto de Física Corpuscular (IFIC), Centro Mixto Universidad de Valencia - CSIC, Valencia; Spain.

[175]Department of Physics, University of British Columbia, Vancouver BC; Canada.

[176]Department of Physics and Astronomy, University of Victoria, Victoria BC; Canada.

[177]Fakultät für Physik und Astronomie, Julius-Maximilians-Universität Würzburg, Würzburg; Germany.

[178]Department of Physics, University of Warwick, Coventry; United Kingdom.

[179]Waseda University, Tokyo; Japan.

[180]Department of Particle Physics, Weizmann Institute of Science, Rehovot; Israel.

[181]Department of Physics, University of Wisconsin, Madison WI; United States of America.

[182]Fakultät für Mathematik und Naturwissenschaften, Fachgruppe Physik, Bergische Universität Wuppertal, Wuppertal; Germany.

[183]Department of Physics, Yale University, New Haven CT; United States of America.

[a] Also at Borough of Manhattan Community College, City University of New York, New York NY; United States of America.

[b] Also at CERN, Geneva; Switzerland.

[c] Also at CPPM, Aix-Marseille Université, CNRS/IN2P3, Marseille; France.

[d] Also at Département de Physique Nucléaire et Corpusculaire, Université de Genève, Genève; Switzerland.

[e] Also at Departament de Fisica de la Universitat Autonoma de Barcelona, Barcelona; Spain.

[f] Also at Department of Applied Physics and Astronomy, University of Sharjah, Sharjah; United Arab Emirates.

[g] Also at Department of Financial and Management Engineering, University of the Aegean, Chios; Greece.

[h] Also at Department of Physics and Astronomy, Michigan State University, East Lansing MI; United States of America.

[i] Also at Department of Physics and Astronomy, University of Louisville, Louisville, KY; United States of America.

[j] Also at Department of Physics, Ben Gurion University of the Negev, Beer Sheva; Israel.

[k] Also at Department of Physics, California State University, East Bay; United States of America.

[l] Also at Department of Physics, California State University, Fresno; United States of America.

[m] Also at Department of Physics, California State University, Sacramento; United States of America.

[n] Also at Department of Physics, King's College London, London; United Kingdom.

[o] Also at Department of Physics, St. Petersburg State Polytechnical University, St. Petersburg; Russia.

[p] Also at Department of Physics, Stanford University, Stanford CA; United States of America.

[q] Also at Department of Physics, University of Adelaide, Adelaide; Australia.

[r] Also at Department of Physics, University of Fribourg, Fribourg; Switzerland.

[s] Also at Department of Physics, University of Michigan, Ann Arbor MI; United States of America.

[t] Also at Dipartimento di Matematica, Informatica e Fisica, Università di Udine, Udine; Italy.

[u] Also at Faculty of Physics, M.V. Lomonosov Moscow State University, Moscow; Russia.

[v] Also at Giresun University, Faculty of Engineering, Giresun; Turkey.

[w] Also at Graduate School of Science, Osaka University, Osaka; Japan.

[x] Also at Hellenic Open University, Patras; Greece.

[y] Also at IJCLab, Université Paris-Saclay, CNRS/IN2P3, 91405, Orsay; France.

[z] Also at Institucio Catalana de Recerca i Estudis Avancats, ICREA, Barcelona; Spain.

[aa] Also at Institut für Experimentalphysik, Universität Hamburg, Hamburg; Germany.

[ab] Also at Institute for Mathematics, Astrophysics and Particle Physics, Radboud University

Nijmegen/Nikhef, Nijmegen; Netherlands.

[ac] Also at Institute for Nuclear Research and Nuclear Energy (INRNE) of the Bulgarian Academy of Sciences, Sofia; Bulgaria.

[ad] Also at Institute for Particle and Nuclear Physics, Wigner Research Centre for Physics, Budapest; Hungary.

[ae] Also at Institute of Particle Physics (IPP), Vancouver; Canada.

[af] Also at Institute of Physics, Azerbaijan Academy of Sciences, Baku; Azerbaijan.

[ag] Also at Instituto de Fisica Teorica, IFT-UAM/CSIC, Madrid; Spain.

[ah] Also at Joint Institute for Nuclear Research, Dubna; Russia.

[ai] Also at Louisiana Tech University, Ruston LA; United States of America.

[aj] Also at Manhattan College, New York NY; United States of America.

[ak] Also at Moscow Institute of Physics and Technology State University, Dolgoprudny; Russia.

[al] Also at National Research Nuclear University MEPhI, Moscow; Russia.

[am] Also at Physics Department, An-Najah National University, Nablus; Palestine.

[an] Also at Physics Dept, University of South Africa, Pretoria; South Africa.

[ao] Also at Physikalisches Institut, Albert-Ludwigs-Universität Freiburg, Freiburg; Germany.

[ap] Also at The City College of New York, New York NY; United States of America.

[aq] Also at Tomsk State University, Tomsk, and Moscow Institute of Physics and Technology State University, Dolgoprudny; Russia.

[ar] Also at TRIUMF, Vancouver BC; Canada.

[as] Also at Universita di Napoli Parthenope, Napoli; Italy.

* Deceased